Norwegian University of Life Sciences

Master's Thesis 2022 60 ECTS

Faculty of Environmental Science and Natural Resource Management

Long-range pollution and historic climate and element trends in an 1100-year lake sediment record from the remote lake Sarsvatnet, Svalbard

Karoline Kristin Vognild

Environment and Natural Resources

This page intentionally left blank

Preface

This thesis concludes my master's degree in Environmental Sciences at the Norwegian University of Life Sciences (NMBU). The process of planning, applying for grant applications, implementing the field campaign, participating in Svalbard Science Conference 2021, processing the obtained data, and writing a reasonable thesis has been challenging, developing, frustrating, but fun and rewarding. I want to express my gratitude to the people that made this thesis possible.

Firstly, a huge thanks to my supervisors; supervisor Dr. Thomas Rohrlack (NMBU), co-supervisor Dr. Gunnhild Riise (NMBU), and co-supervisor Dr. Øyvind Mikkelsen (Norwegian University of Science and Technology (NTNU)). Thanks for constructive feedback and help during fieldwork and in the laboratory. An extra shout out to Dr. Øyvind Mikkelsen for giving me the opportunity to travel to Svalbard and experience the research hub in Ny-Ålesund. Thanks for fulfilling my dream of writing about an Arctic related topic!

Thanks to Tore Krogstad and Irene E. Eriksen Dahl at the Laboratory for soil and water chemistry and soil physics at NMBU. Without your help, there would be no Loss On Ignition data. Also, a huge thanks to Tore Krogstad, Solfrid Lohne, and Karl Andreas Jensen for your support and patient feedback during my outburst of frustration. Thanks to Kyyas Seyitmuhammedov and Anica Simic at NTNU for analysing my samples and for your feedback on bombarding questions.

Thanks to the Norwegian Polar Institute and Kings Bay in Ny-Ålesund for making the fieldwork feasible. Thanks to the Research Council of Norway for the economic support through Arctic Field Grand. Thanks to Vannforeningen for your economic support in buying the inflatable boat.

A huge thanks to Team Mikkelsen (Lill Katrin Gorseth, Sunniva Kvamme, Mathilde Syvertsen, Nicola Messinger, and Thomas Walmsley) for a fun trip to Svalbard and for your help during the field work!

Thanks to Kylie Compe and Darcy Roeger for proofreading this thesis!

Lastly, thanks to my family for the endless support! Thanks to my roomies at Heimen and all the amazing people I have crossed paths with the last years!

I am grateful!

Oppdal, July 2022,
Karoline Kristin Vognild

This page intentionally left blank

Abstract

Although remote, the Arctic is influenced by long-range pollution from lower latitudes. Lake sediments are sensitive to minor environmental changes, and thus accumulated heavy metals and organic substitutes can represent the concentration trends through time and as a climate proxy. To assess the extent of long-range pollution influence in Lake Sarsvatnet, Svalbard, and the different forcing mechanisms in the catchment, chlorophyll *a*, Loss on Ignition (LOI), and selected heavy metals were analysed from a sediment core. Selected elements are aluminium (Al), arsenic (As), cadmium (Cd), calcium (Ca), chromium (Cr), copper (Cu), iron (Fe), lead (Pb), magnesium (Mg), manganese (Mn), nickel (Ni), phosphorus (P), potassium (K), sodium (Na), sulphur (S), titanium (Ti), and zinc (Zn). Results indicate that Cd in the sediment surface is derived from bird guano and atmospheric deposition from long-range pollution. A contribution of Pb concentrations in the sediment surface may originate from atmospheric deposition, however, more research is needed as geological processes likely contribute most of the Pb content in Sarsvatnet.

Climate proxies (LOI and Chlorophyll *a*) demonstrated historical periods e.g., the Little Ice Age and Medieval Climate Anomaly. Although variations over the last 1100 years, increased primary production and elemental concentrations in the last century are major findings identified in this thesis. With rising temperatures, precipitation, and bedrock weathering, it is fair to expect an alternation of elements, primary production residues, and soil organic matter in the Sarsvatnet catchment in the future. In other words, climate change has a more significant impact on the composition of the sediments in Sarsvatnet than long-range pollution.

This master's thesis provides an updated evaluation of the status quo in Sarsvatnet catchment and could be relevant to further investigations at Ossian Sars.

This page intentionally left blank

Sammendrag

Til tross for at arktiske områder er avsidesliggende, er Arktis påvirket av langtransportert forurensning fra lavere breddegrad. Innsjøsedimenter er sensitiv for små miljøforandringer, dermed kan akkumulerte grunnstoff og organiske substanser benyttes til å vurdere konsentrasjonstrender gjennom tiden og for å indikere tidligere klima. Klorofyll *a*, glødetap (LOI) og valgte grunnstoff fra en sedimentkjerne ble anvendt for å vurdere grad av langtransportert forurensning i Sarsvatnet, Svalbard, samt naturlige mekanismer i nedbørsfeltet. Valgte grunnstoff er aluminium (Al), arsen (As), bly (Pb), fosfor (P), jern (Fe), kadmium (Cd), kalium (K), kalsium (Ca), kobber (Cu), krom (Cr), magnesium (Mg), mangan (Mn), natrium (Na), nikkel (Ni), sink (Zn), svovel (S), og titan (Ti). Resultatene indikerer at fugleekskrementer og atmosfærisk avsetting fra langtransportert forurensning kan være kilder til oppkonsentrert kadmium i det øverste sedimentlaget. En del av blykonsentrasjonen i det øverste sedimentlaget kan stamme fra atmosfærisk avsetting. Mer forskning er nødvendig, siden geologiske prosesser bidrar med mesteparten av blykonsentrasjonen i Sarsvatnet.

Klimaindikatorer (klorofyll *a* og glødetap) har identifisert historiske perioder, som Den lille istid og den Middelalderske varmeperioden. Et av hovedfunnene var økt primærproduksjon og økte grunnstoffkonsentrasjoner det siste århundre til tross for varierende konsentrasjoner de siste 1100 årene. Likevel antyder resultatene en endring i bakgrunnsverdier grunnet økt nedbør og forvitring av lokal berggrunn i det siste århundret. Klimaendringer har dermed større påvirkning på grunnstoffkonsentrasjonen enn langtransportert forurensning i innsjøsedimenter i Sarsvatnet.

Denne masteroppgaven gir oppdatert vurdering av status quo i Sarsvatnet, og kan være relevant ved videre arbeid på Ossian Sars.

This page intentionally left blank

Table of Content

Table of Figures, Tables, Equations, and Appendix figures

1 Introduction

The Arctic environment is sensitive to changes, and so are lake sediments. Although remote, the assumption of Svalbard (74-81°N) being "pristine" and "stable" (Birks et al., 2004a) is disputable. The Arctic has experienced a temperature rise twice the global average (Isaksen et al., 2016). This "Arctic amplification" has caused changes in the Arctic environment, producing physical, chemical, and biological stressors observed in the atmosphere, water, soil, sediments, and biota (Luoto et al., 2016; Noyes et al., 2009). Furthermore, increased temperatures and precipitation largely influence the distribution of toxic chemicals (AMAP, 2016; Macdonald et al., 2005; Noyes et al., 2009). Lake sediments are the major recipient of contaminants associated with particles and colloids (Sagar et al., 2021) and primary production residues (Boldt et al., 2015) in the limnologic environment. Minor changes are therefore more apparent in the accumulated organic substitutes in the sediment. Applied as climate proxies, these accumulated organic substitutes represents historical climate trends (Boldt et al., 2015). Moreover, Arctic paleolimnology has been crucial in identifying pathways, trajectories, and effects of long-range contaminants (Smol, 2016).

Although metals occur naturally in the environment and cycled through biogeochemical processes unaided, metals also reach and re-distribute to the Arctic as pollutants through atmospheric, freshwater, oceanic, ice, sediment, and biotic transport mechanisms (Macdonald et al., 2003). Atmospheric circulation is the quickest transportation route for pollutants, however, it differs with seasons (Willis et al., 2018). The atmospheric circulation is controlled by swings in the North Atlantic Oscillation (NAO), which generate wind through fluctuations in the different atmospheric pressures at sea level (Eckhardt et al., 2003). The tropospheric circulation, and thus the transportation of winds, is generally higher during the winter and elevated during cyclonic swings (AO^+) compared to anticyclonic swings (AO^-). In contrast, the air mass inflow to the Arctic in the summer months is reduced as oceanic low-pressure cells weaken and the continental high-pressure cells disappear (Macdonald et al., 2005). Spring and autumn are transition periods (Bottenheim et al., 2004). Consequently, the input of long-range pollution to the Arctic is greater in the winter compared to the summer. Transportation through ocean currents and biota, e.g., migrating birds, are significant yet slower pathways (Yang et al., 2020, and the references therein).

Pollution in the Arctic is marginally and contributes less than southern originated contaminants (Law & Stohl, 2007). However, due to increased population and increased industrial activity projected in the Arctic, Arctic emissions are expected to rise (Schmale et al., 2018). Nevertheless, two-thirds of the heavy metals measured in the Arctic are thought to have

originated from lower latitudes. Asia contributes more pollution compared to emissions from North America, Europe, and Russia combined (Pacyna & Pacyna, 2001; Stohl, 2006), and thus contributes the most to the global environment. Major sources of heavy metal emissions are fossil fuel combustion, non-ferrous metal production, and waste incineration (Macdonald et al., 2003).

Fossil fuel combustion is the primary source of atmospheric emissions, contributing with chromium (Cr), mercury (Hg), manganese (Mn), antimony (Sb), selenium (Se), tin (Sn), thallium (Tl), lead (Pb), nickel, (Ni), and vanadium (V) (Macdonald et al., 2003; Pacyna & Pacyna, 2001). Non-ferrous metal production is another major source of atmospheric emission, however the production decreased from the early 1980s to the mid-1990s. Contributing elements are arsenic (As), cadmium (Cd), copper (Cu), indium (In), and zinc (Zn). Waste incineration is also a noteworthy contributor to heavy metal likely underestimated due to a lack of emission information (Macdonald et al., 2003). The sources of contaminants are varied, and special attention to the fragile Arctic environment is needed.

While several elements are emitted and introduced to the Arctic environment, Cd, Pb, and Hg are elements with greater concerns due to their bioaccumulation and biomagnification properties, and lack of biological functions (AMAP, 2016). Limiting the emissions of these elements is the primary objective of the Convention on Long-Range Transboundary Air Pollution (LRTAP Convention; Macdonald et al., 2003). The worldwide reduction of Pb in leaded gasoline since the 1970s is evident in sediment samples in the Northern Hemisphere and in the Arctic (Liu et al., 2012; Sun et al., 2006). However, Pb concentrations from anthropogenic sources are still significant in natural samples. In contrary, Pb emissions increases in the Southern Hemisphere (Marx et al., 2016). Despite international interest in reducing emission, climate change will present challenges in respect of toxic elements.

Climate change is now a consensus. Metals occur naturally in the environment and cannot be broken down into less toxic substances. However, rising temperature and associated processes will impact the distribution and remobilisation of elements in the Arctic (AMAP, 2016; Førland et al., 2011; Macdonald et al., 2005). For instance, climatic change is influencing the characteristics of NAO, increasing cyclone activity poleward, transporting heat and contaminants toward the Arctic (Macdonald et al., 2005). Rising temperatures (Førland et al., 2020) will result in increased primary production, accelerated permafrost thawing, increased humidity and precipitation. This will enhance the local bedrock's mechanical and chemical weathering rate, releasing dissolved solids, elements, and nutrients in the catchment (Liu et al.,

2012). Increased precipitation in the Arctic will also enhance deposition of atmospheric contaminants to the surface (Macdonald et al., 2005).

Changes in the environment are prominent in lake sediments. Therefore, by investigating historically accumulated chlorophyll *a* and contaminants trends in a sediment core, it is possible to indicate climatic processes and mechanisms enhancing element accumulation. This is particularly important as Svalbard acts as a pollution reservoir (Bottenheim et al., 2004), contributing to our understanding of contaminant distributions and their effects on the environment and biota. Furthermore, understanding the Arctic environment is crucial to recognise future climatic and pollution scenarios.

The objective is to assess the extent of influence from long-range pollution in Lake Sarsvatnet, Svalbard, and to discuss different forcing mechanisms of climatic and element trends over the last 1100 years from a sediment core obtained from a remote lake.

This thesis is partly in collaboration with master's student Lill Katrin Gorseth (2022). Her thesis focuses on factors affecting the water chemistry of Lake Sarsvatnet and its inlet and outlet streams. The two theses will give valuable information about processes within the Sarsvatnet catchment and update impact evaluations for long-range pollutants on Ossian Sars.

There are some previous publications from Sarsvatnet. The Journal of Paleolimnology, volume 31, issue 4, May 2004, published a series of interdisciplinary work working on Recent *Environmental Change and Atmospheric Contamination on Svalbard as Recorded in Lake Sediments*. Lake Sarsvatnet was one of 23 Arctic lakes studied for sediment accumulation rates, organic matter accumulation rates, atmospheric contaminants, inorganic geochemistry, and biological assemblages (Birks et al., 2004a). Eight lakes were dated radiometrically using naturally (^{210}Pb) and artificial (^{137}Cs and ^{241}Am) fallout radionuclides (Appleby, 2004) to assess the sediment accumulation rate. As the field campaign ended in 1995, an updated evaluation of possible changes is helpful for contamination and climate trend assessments over the last 26 years. The most recent work was published as master's theses; based on sediment samples from Sarsvatnet, (Bjerkås, 2019) performed a Holocene reconstruction of Kongsbreen, whereas (Decorte, 2020) reconstructed past changes in primary production and the eukaryotic community structure of Sarsvatnet catchment. This thesis will contribute confirmatory findings from a region with limited research applying modernised and sensitive analytical instruments. Using modern analytical instruments is beneficial to increase the accuracy of the data, especially when quantifying and assessing trace elements in parts per million. This increased accuracy is also advantageous when comparing with older research materials. This thesis

therefore gives an updated and valuable understanding of the biogeochemical processes within the Sarsvatnet catchment.

2 Materials and Methods

2.1 Study area

Lake Sarsvatnet (Figure 1) is situated 100 m.a.s.l. at Ossian Sars Nature Reserve (11.4 km^2) (Forskrift om Ossian Sars naturreservat, 2003). The nature reserve located in Kongsfjorden, northwest of Spitsbergen, Svalbard. Ny-Ålesund and the previously used mining fields located approximately 12.5 km southeast of Sarsvatnet (Hanoa, 2016; Kern et al., 2019). Five tide water glaciers calve into Kongsfjorden: Blomstrandbreen, Conwaybreen, Kongsbreen, Kronebreen, and Kongsvegen. Ossian Sars separates the two branches of Kongsbreen, which calves into Kongsfjorden on the northern and southern sides of the nature reserve (Bennet et al., 1998; Lindbäck et al., 2018).

The catchment area is approximately 1.3 km^2, whereas the lake has an area of 0.22 km^2 (Pearce et al., 2007). Sarsvatnet is a deep meltwater lake (Lindström & Leskinen, 2002), with record depths ranging from 22 meters (Bjerkås, 2019) to 26 meters (Birks et al., 2004c). Round and bare but steep mountains raise on the northern and eastern sides of the lake. In contrast, the southern side of the lake has less-steep slopes with a series of fresh glacier moraine ridges (Birks et al., 2004c). Water drains from the outlet on the lake's western side toward Kongsfjorden. The lake has six gullies formed by melt waters, rivers, and stream runs. Additionally, excessive melt water from Kongsbreen may pass through the pass-point at approximately 150 m.a.s.l. on the lake's western side (Bjerkås, 2019). Normally, when little discharge, water seeps through the wetlands toward the lake on the southern side of the lake.

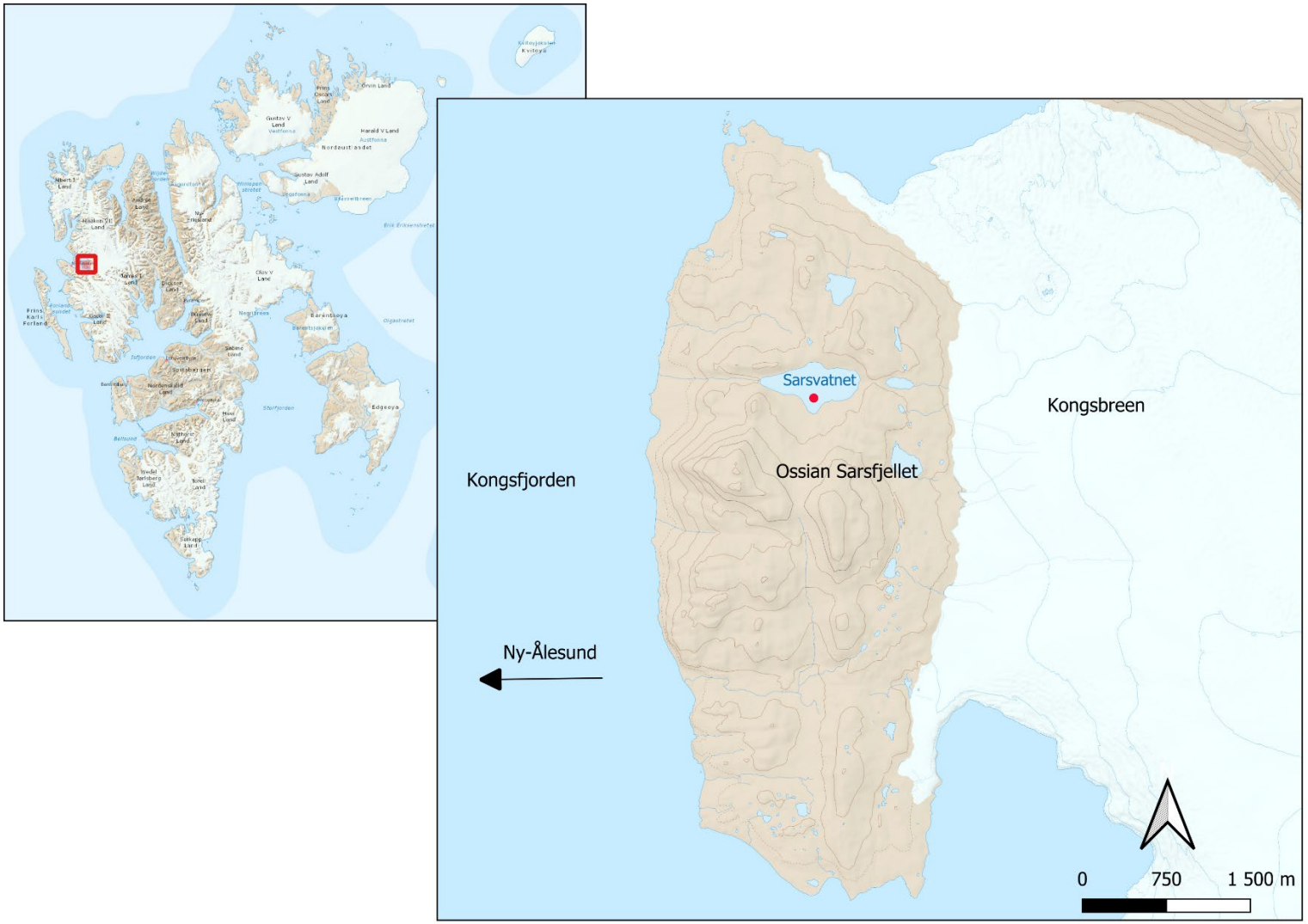

Figure 1 Topographic map of Svalbard and Ossian Sars. The red dot in lake Sarsvatnet illustrates the retrieval point of the sediment core at N 78° 56.9818' E 012° 29.9275'. The map is based on the Norwegian Polar Institute's base map (Skoglund, not released).

Sarsvatnet was defined as an ultra-oligotrophic lake with a sparse vegetation cover by (Lindström & Leskinen, 2002). However, Ossian Sars is a middle arctic-tundra zone (MATZ; (Birks et al., 2004c; Elvebakk, 1997), recognised for its floral and faunal diversity (Birks et al., 2004c; Shears et al., 1998). Identified flora include smooth cliff fern (*Woodsia glabella)*, net-leaved willow (*Salix reticulata),* crowberry *(Empetrum nigrum),* brittle bladder fern *(Cystopteris fragilis),* and monocot *(Carex nardina)* (Birks et al., 2004c; Lee, 2020). One of the largest bird cliffs in Kongsfjorden is located on Ossian Sars (Shears et al., 1998), being a nesting spot for black-legged kittiwake (*Rissa tridactyla)*, fulmars (*Fulmarus glacialis*), Brünnich's guillemots (*Uria lomvia*), puffins (*Fratercula arctica*), little auks (*Alle alle*), black guillemots (*Cepphus grylle*), and glaucous gulls (*Larus hyperboreus*) (Shears et al., 1998), common eiders (*Somateria mollissima*), and barnacle goose (*Branta leucopsis*) (Referred in Syvertsen, 2022). During the bird nesting season, entry to Ossian Sars requires permission from the Governor of Svalbard (Forskrift om Ossian Sars naturreservat, 2003; Shears et al., 1998).

Svalbard archipelago encompasses a variety of rock types and formations throughout the geological times and is known as "a geological picture book" (Dallmann, 2015; Hjelle, 1993). The basement rock of Ossian Sars is part of the Signehamna Formation and Generalfjella formation (Dallmann, 2015), which was folded during the Silurian times (Grant, 2016; Hjelle, 1993). Phyllites, mica schists, quartzite, and other metasedimentary rocks are observed near the fjord, grading east into limestone and marble, eventually to the moraine, unconsolidated materials deposited of the Kongsbreen glacier (Figure 2) (Dallmann, 2015; Hjelle, 1993). Kern et al. (2019) analysed catena soil samples, finding the Sarsvatnet catchment's mineralogy. Quartz and dolomite/ ankerite were the first and second, respectively, most abundant minerals in the catchment. Na-plagioclase had medium concentrations whereas calcite, muscovite, and biotite were found in medium-low concentrations. Chlorite and K-feldspar had low values in the Sarsvatnet catchment.

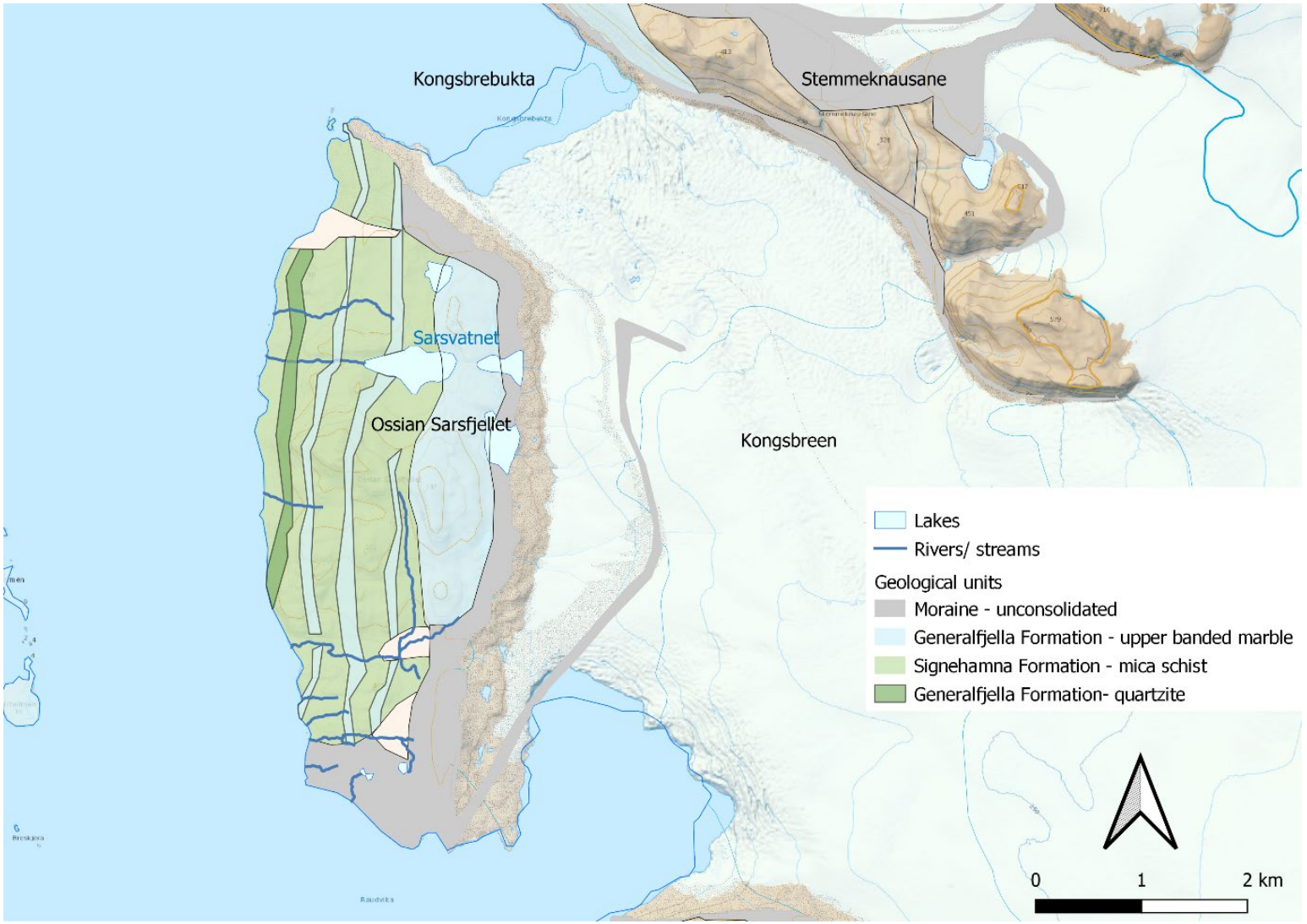

Figure 2 Bedrock map of Ossian Sars. Ossian Sars consists of a layer of mica schists with interlayered quartzite and carbonate rocks, grading east to upper banded marble. The map is modified after (Norwegian Polar Institute, 2016) and (Hjelle, 1993).

Th Svalbard archipelago is characterised by a maritime tundra climate, while Kongsfjorden is characterised as a polar semi-desert (Muraoka et al., 2002; Thusen, 2021). Several papers, e.g., Isaksen et al. (2016) and Ding et al. (2018), observed increased temperatures in Ny-Ålesund in the period 1971 to 2015. Isaksen et al. (2016) noted an increase in annual mean temperature from -5.7ºC to -3.9ºC during the intervals of 1971-2000 to 2001-2015. Summer and winter mean temperatures during 2001-2015 were recorded to 4.5ºC and -9.1ºC, respectively. This is a change of 0.8ºC and 3.8ºC respectively compared to the 1971-2000 period. Ding et al. (2018) determined the warming rate of the annual mean temperature in Ny-Ålesund to be approximately four times greater than the global average from 1975-2014. Simultaneously, the total annual precipitation in Ny-Ålesund increased from 385 mm in 1961-1990 to 442 mm in 1981-2010 (Førland et al., 2011). Due to lower pressures and warm water from the West-Spitsbergen current, i.e., a branch from the Atlantic current, West-Spitsbergen has a milder climate and little sea ice along the coast compared to eastern and northern Svalbard.

Local anthropogenic activities concerning Ossian Sars are mainly linked to Ny-Ålesund, such as cultural monuments which indicate whaling activity from 1600. The first observations of coal in Kongsfjorden occurred in 1610 and later in the 1860s. Coal mining was implemented periodically from 1910-1962 (Reymert, 2016). However, mining ceased in 1963 after a tragic accident in November 1962 that claimed 21 lives. Today, Ny-Ålesund is a center of international Arctic research and environmental monitoring (Hanoa, 2016). The population varies from an average of 10 people during the winter to about 100 people during the summer. Local pollution sources are attributed to the settlement, include the power station, motor vehicles, aircraft, boats, and ships, and occasionally, construction works (Moroni et al., 2016).

2.2 Data collection and data processing

2.2.1 Sediment samples

Per NS- ISO 5667-12:2017 (Standard Norge, 2017), one bottom sediment core was obtained by a UWITEC sediment corer at N 78º 56.9818’ E 012º 29.9275’, 20.0 m. The deepest point at Sarsvatnet was registered to 20.5 m., using echo-sounding (Plastimo Echotest II Depth Sounder). Due to time limitations on Ossian Sars, only one sediment core was retrieved. This core was transported in a vertical position until the core was divided into 46 layers (S1-S46) approximately three hours after collection in Ny-Ålesund. Nevertheless, the sediment core was transported in a vertical position until slicing.

The core had a length of 39 cm, including organic-rich moss debris on the sediment surface. The 1-11 uppermost layers were divided into layers of 0.5 cm thickness, whereas the rest were

divided into 1.0 cm thickness. Layer S29 was exceptional, with a thickness of 1.5 cm. The samples were stored in a cold environment until further procedure.

Figure 3 Lill Katrin Gorseth and Karoline Kristin Vognild on their way to take sediment and water samples. Credit: Nicola Messinger.

2.2.2 Freeze drying of sediment samples

The samples were freeze dried to preserve the chemical and physical structure of the sediment sample, as per NS- EN 16720:2007 (Standard Norge, 2007). This process consists of three stages: freezing, primary and secondary drying (Shukla, 2011). The freezing process aims to stabilise the structure. Ice crystals grow intertwined with crystalline or amorphous components of either the excipients or the active product (Corver, 2009). In the second step, a vacuum is introduced. The pressure is lowered, and heat is supplied to convert water from ice to vapour (sublimation) without destroying the physical structure. The third step, i.e., secondary drying, aims to remove unfrozen water molecules which were not removed in the primary drying. The remaining water is removed through a temperature increase even above 0ºC. The pressure is also lowered to encourage desorption. After that, the samples are ready for further investigations.

2.2.3 Pigment analysis

High Performance Liquid Chromatography (HPLC) is a commonly applied technique for separating, identifying and quantifying compounds in organic, inorganic, and biological

samples. In short, the principle of HPLC is based on the distribution of the sample solution (analyte) between the mobile phase (eluent, normally non-polar) and a stationary phase (porous particle packed column, typically polar silica particles). A sample containing analytes A and B in the mobile phase are introduced to the column through high pressure and distributed differently through the stationary phase, and elution occurs. The migration of the two analytes in the eluent differs through the stationary phase, i.e., the average migration rate depends on the time fraction they use in that phase. Solutes with lower affinity, i.e., have lower polarity, have decreased adsorption capacity, and hence have a quicker migration time through the column. On the contrary, a solute with increased polarity has increased affinity to the stationary phase and thus has a longer migration rate. At the end of the column, a detector measures the solute concentrations based on the absorption of ultraviolet or visible radiation. These are shown as absorption peaks, which are used to identify the compound in the sample (Chakole et al., 2021; Skoog et al., 2014; Vidushi & Meenakshi, 2017). The advantages of HPLC are short procedure but high sensitivity using a limited sample amount, high resolution, ease to fractionate and purify the sample, and possible to do simultaneous analysis (Chakole et al., 2021). Disadvantages include a lower separation efficiency compared to gas chromatography, it is relatively complex for novices, and the process is time-consuming and expensive. Furthermore, a universal detector is lacking (Dong, 2013).

The methodology of pigment extraction is based on Hagman et al. (2019). 1 mL of 100% acetone was added to 100-400 mg of homogenised and weighted sediment samples in Eppendorf tubes. β-apocarotenal (Sigma-Aldrich, Oslo, Norway), as an internal standard, was added to correct possible degradation during the extraction (Dr. Thomas Rohrlack, pers. commun., 11.10.2021) and to calibrate the system. Then, the samples were vortexed and extracted for 24 hours in the refrigerator. The next day, the samples were centrifuged at 3000 rpm for 10 minutes to remove particles before transferring to High Performance Liquid Chromatography (HPLC) vials. Additional water was added to the supernatant to a final concentration of 20% to improve the separation of polar pigments due to assumable low pigment concentrations in the sediment samples.

The HPLC-Photometric Diode Array (HPLC-PDA) analysis was completed using a Dionex™ UltiMate 3000 HPLC (Thermo Scientific™) with an Acclaim™ C30 column, 3 µm (ThermoScientific). Certified Dansk Hydraulisk Institut (DHI) pigment standards were used to one-point calibrate the HPLC system, whereas Dionex™ Chromeleon™ version 7.2.6 (Thermo Scientific™) was applied for manual pigment identification. The detection limit was set to 0.3 AU (absorption units). Chlorophyll *a* and its derivatives, i.e., ∑ chlorophyll *a*, hereafter referred

to as chlorophyll *a*, were identified and quantified based on retention time and the specific maximum absorption spectrum of standard pigments. The concentration of pigments in parts per million (ppm) in each layer was calculated by using Equation 1 (Dr. Thomas Rohrlack, pers. commun., 11.10.2021):

$$Concentration\ of\ pigment\ in\ sample\ x = DF * \left(\frac{A_1}{A_2} * \frac{\left(\frac{C}{A_3} * A_4\right) * D}{B} \right)$$

Equation 1

Where

A_1 = areal of pure standard [mAU]

A_2 = areal of intern standard in sample [mAU]

A_3 = areal peak standard [mAU]

A_4 = areal peak of pigment in sample x [mAU]

B = extracted sediment [g]

C = concentration of pigment standard [µg/mL]

D = amount of extracted acetone [mL]

DF = dilution factor (no unit).

An example of calculations of concentration of Fucoxanthin in sample 1 (S1), is found in Appendix 3.

2.2.4 Loss on Ignition (LOI)

Loss on Ignition is the percentage sample loss in weight due to combustion in temperatures of 450-550ºC (Bojko & Kabała, 2014). Due to the low cost and simple methodology, LOI is commonly used as an indication of the humus content (Krogstad & Børresen, 2015) in soil and sediments when corrected for clay content, carbonates, volatile salts, aluminium, and chemically bonded water to clay. Correction of clay content is a normal procedure in Norwegian soil to adjust to the real content of organic matter in the sample (Krogstad & Børresen, 2015; Pommeresche et al., 2019). Samples from calcium-rich geology should be tested for the loss of carbonates but can be eliminated by being combusted in temperatures below 500ºC or by treatment with hydrochloric acid prior to combustion (Bojko & Kabała, 2014).

Crucibles and samples of approximately 3.00 g were weighted on a Sartorius 1202 MP 300.00 g scale with an accuracy of ± 0.01 g before and after drying at 110ºC in a Memmert GmbH oven until the next day. Samples were calcinated in the calcinating oven for 3 hours at 550ºC ±

25ºC, then cooled before weighing. The procedure followed NS-EN 15935:2021 (Standard Norge, 2021). Based on the weight differences, Loss on Ignition was calculated as described in Equation 2 (Krogstad & Børresen, 2015):

$$\%\ Loss\ on\ Ignition = \frac{(m_3 - m_4)}{(m_3 - m_1)} * 100\%$$

Equation 2

Where

m_1 = weight of crucible [g]

m_2 = weight of sample before drying [g]

m_3 = weight of crucible with sample after drying [g]

m_4 = weight of crucible and sample after calcination [g]

Correction of Loss on Ignition should be performed in mineral samples to adjust to the clay content (Krogstad & Børresen, 2015). However, it was not performed in these samples. Table 1 refers to what correction figure to choose depending on soil type and clay content.

Table 1 Correction figures to adjust according to the clay content in the sample. The correction figures are average values for each soil type classification. Retrieved from (Krogstad & Børresen, 2015).

Soil type	Clay content	Correction figure
Sand and silt	5-9%	1
Light clay	10-24 %	2
Medium clay	25-39 %	2.5
Stiff clay	40-59 %	3.5
Very stiff clay	> 60 %	4.5

2.2.5 Indirect dating of core based on pigment content

^{210}Pb is a naturally occurring isotope and is one of several of the ^{238}U decay series. ^{210}Pb is present in the sediments as a response to sediment decay (supported ^{210}Pb) or as a supply from atmospheric precipitation (unsupported ^{210}Pb). The deposition gives an elevation of ^{210}Pb on the Earth's surface. ^{210}Pb dating is based on the unsupported fraction (Weckström et al., 2017), and is crucial in studying environmental records in natural archives, e.g., lakes sediments, over the last 100-150 years (Appleby, 2004). It is recognised for its reliability particularly in stable environments (Appleby, 1998). Several methods are applied in ^{210}Pb dating; Constant Initial Concentration (CIC) and Constant Rate Supply (CRS) are the most practiced methods. The latter is commonly applied. However, since the indirect dating of this sediment core is based on the CIC ^{210}Pb dating in Appleby (2004), a short presentation of CIC is presented below.

The CIC model assumes a constant initial unsupported and independent ^{210}Pb activity to any changes in the sedimentation rate (Allen et al., 1993). Therefore, any changes in the flux of sediment particles from the water column indicate the ^{210}Pb amount removed from the water to the sediments. As ^{210}Pb seldom decreases completely monotonically down-core, which thus is required to avoid an age-reversal, a smoothing of the chronology is often needed. The complicated procedure requiring detailed calculations, thus time-consuming, is a disadvantage. Hence, other methods, e.g., the CRS method, are better suited. However, if a constant ^{210}Pb deposition is expected through time irrespective of changes in the sedimentation rate, a CIC method is beneficial (Weckström et al., 2017).

A limitation of applying ^{210}Pb dating is the poor resolution of the last 100-150 years (Weckström et al., 2017). Thus, the dating of previous sediments lacks certainty. If assuming monotonic sedimentation accumulation rate, extrapolation can be applied, as, e.g., Appleby (2004) did. As for indirect dating, the uncertainties are relevant to consider as the interpolation of extrapolated estimates may be a source of errors. Comparison with other data is therefore crucial.

It was possible to do an indirect dating of the sediment core. Based on the sedimentation rate from ^{210}Pb dating using the CIC method, as described in Appleby (2004), and the thickness of each layer of the sediment core, an estimated year of sedimentation was calculated. This is explained in equation 3 (Dr. Thomas Rohrlack, pers. commun., 09.11.2021):

$$current\ year\ [AD\ yr] = previous\ year\ [AD\ yr] - \frac{thickness\ of\ layer\ [cm]}{sedimentation\ rate\ [cm\ y^{-1}]}$$

Equation 3

Appendix 4 shows an example of calculation.

2.2.6 Decomposition and analysis of elements

Decomposition is a standard procedure prior to organic and inorganic samples analysis, e.g., Inductive Coupled Plasma Mass Spectrometry (ICP-MS). Decomposition in a closed vessel is the normal procedure because this procedure can achieve high pressure and high temperature in a shorter time. In a closed vessel, the energy is directly transferred to the molecules of the solution nearly simultaneously without heating the vessel. Hence, boiling temperatures are quickly reached throughout the solution. Time efficiency, due to alternate decomposition mechanisms, is the main advantage compared to decomposition in an open vessel. High temperatures in the chamber are achieved faster with increased pressure (Skoog et al., 2014). The disadvantages include precipitation depending on the concentration of acid applied in the

decomposition process and residue carbon content (RCC). RCC is an insoluble carbon that precipitates after digestion. The precipitation may cause interferences in further analysis (Barnes et al., 2014).

Per ISO 16729:2013 (International Standard, 2013a), the use of nitric acid (HNO_3) is commonly used in environmental studies, e.g., in soil samples. However, digestion with HNO_3 will not thoroughly homogenise the sample, thus a total decomposition of the sample will not necessarily occur. Hence, the recovery of certain elements may appear lower than, for instance, the interval of certified reference materials (CRM) (Arunachalam et al., 1995). As an indicator of the labile fraction and thus results indicate trends of elements, this is sufficient in environmental studies.

ICP-MS is commonly applied in environmental studies (Davison, 1993; e.g., International Standard, 2013b), and is beneficial for analysing multiple elements in a single analyse with a detection limit in ppm, compared to other atomic spectrometry techniques (Wilschefski & Baxter, 2019). The construction of an ICP-MS instrument includes 1) an inlet system for samples, 2) an ion source, 3) a mass analyser, 4) a detector, 5) a signal processor, and 6) a readout. The instrument also requires a vacuum system to maintain low pressure in all compartments. Briefly, the decomposed sample is introduced into the ion source, where the components are converted into positive or negative gaseous ions. The ions are thereafter separated in the mass analyse according to their mass-to-charge ratios (m/z ratio). Ions in a particular mass-to-charge ratios are collected and converted into an electrical signal, which the signal processor process. The signal processor often compares the results with known spectra, tabulation of results, and data storage (Skoog et al., 2014). Table 2 summarises the advantages and the limitations of an ICP-MS (Wilschefski & Baxter, 2019).

Table 2 Summarised advantages and disadvantages of an ICP-MS. Modified after Wilschefski and Baxter (2019).

Advantages	Disadvantages
• Multi-element technique • Large analytical range • High sample throughput • Low sample volume • Low detection limit • Simple sample preparation • High-resolution and tandem mass spectrometry (triple quadrupole) instruments offer a very high level of interference control	• Operating and equipment costs • Multiple high purity gases required • Interferences need to be controlled • High level of staff expertise • Laboratory set up costs (air-conditioning, HEPA filters, pipe work, dust reduction measures)

Samples, certified reference materials (CRM), and blanks were treated with 9 mL 50% nitric acid (HNO_3, v/v; ultrapure grade, distilled by Milestone SubPur unit), then decomposed in a high-pressure microwave digestion reactor (UltraClave, Milestone GmbH, Leutkirch, Germany). The procedure was in accordance with ISO 16729:2013 (International Standard, 2013a) and ISO/TS 16965:2013 (International Standard, 2013b). The CRM used in batch one (including S1-S35) of the digestion process was MODAS-2- Bottom Sediment (M-2 BotSed) No. 0382. MESS-4 Marine Sediments was used as certified reference material in batch two. All samples were diluted with ultrapure water (~18.2 MΩ·cm) prior to element analysis to achieve a final HNO_3 concentration of 0.6 M. A 8800 Triple Quadrupole inductive coupled plasma mass spectrometry (ICP-MS) system (Agilent, USA) was applied for elemental analysis. The ICP-MS was equipped with prepFAST M5 autosampler (ESI, USA). System parameters during analysis are listed up in Table 3. Internal standards used were rhodium (Rh), rhenium (Re), and iridium (Ir). The retrieved element concentrations from ICP-MS analyses were corrected for the blank concentrations and the dilutions. Detection limits for the system are summarised in Appendix 2.

Table 3 General Parameters applied during ICP-MS analysis.

General parameters	
RF Power	1550 W
Nebulizer Gas	0.80 L/min
Makeup Gas	0.38 L/min
Sample Depth	8.0 mm
Ion Lenses	x-lens
H_2 mode	
H_2 Gas Flow	4.5 mL/min
He Gas Flow	1.0 mL/min
O_2 mode	
O_2 Gas Flow	0.525 mL/min

2.2.7 Quality Assurance (QA) & Quality Control (QC)

Quality assurance (QA) and quality control (QC) are essential to control analytical measurement errors at acceptable levels to assure that the analytical data have a high probability of acceptable quality (Keith, 1999). QA refers to all actions, procedures, checks, and decisions undertaken to guarantee the integrity and representativeness of samples, as well as the reliability and accuracy in analytical results. QC consists of actions that monitor and measure the effectiveness of QA (Batley, 1999).

Necessary precautions were taken during fieldwork and in the labs. Equipment used was thoroughly cleaned, e.g., cleaning of Teflon vials with Ultrapure water before adding samples

and solutions, new plastic foil was used on the spatula before weighting samples, and nitrile gloves were used to avoid contamination and mitigate health risks. Standard procedures and ISO routines were applied where relevant. Whereas pigment analysis followed a previously published method. Only high-grade chemicals were used. Standards (internal and injection standards) were applied for calibration curves, quantification, and control of matrix effects, in addition to loss or contamination from extraction and digestion. Certified reference materials were used for quantification and calibration purposes. Limit of Detection was applied to assess values below the detection limit in element analysis.

2.2.8 Data manipulation

Based on a visible greyish colour of the sediments, high Ti concentration, low chlorophyll *a* content and low Loss on Ignition values, the layers were determined to be identified as an episodic accumulation event. Following a literature review and data assessments, the greyish-coloured layers in this upper core (S2-S13) of 1-7.5 cm depth appear to have occurred from an episodic accumulation of sediments between 1890-1910 (Boyle et al., 2004). Similar observations were made in the depth of 38-39 cm (layers of S43 and S44). However, these layers were excluded to visualise the consistency of chlorophyll *a*, LOI, and element trends.

2.2.8.1 Statistical analysis

A Principal Component Analysis (PCA) aimed to reduce the large dataset and evaluate what parameters contribute the most to the total variation in the data frame (Crawley, 2012). This multivariate analytical tool showed what parameters are correlated to each other, what direction sample scores parameters point toward and what contribution they have. A PCA with a scaled parameter was conducted in RStudio Version 2021.09.0, Ghost Orchid. The biplot is visualised using "fviz_pca_biplot()" function from the "factoextra" package, version 1.0.7 (Kassambara & Mundt, 2020). The variables in the biplot are coloured by contribution to the PCA.

A combined non-parametric Mann-Kendall Trend Test and Sen's slope were applied to assess if there is a pattern trend of the variables. Null hypothesis, H_0, propose that the data has randomised variables that are independent and identically distributed. The alternative hypothesis, H_1, propose that the data follow a monotonic trend over time. The significance level was set to $\alpha = 0.05$. A positive or negative trend is assessed on the test statistic Z when $n \geq 10$ from the Mann-Kendall test statistic S; a positive Z value indicate an upward trend, and vice versa (Hipel & McLeod, 1994; Salmi, 2002). If a linear trend is present in the sediment core's time series, a Sen's slope is applied to an existing trend (Salmi, 2002; Tabari & Talaee, 2011). The combination of the Mann-Kendall Trend Test and Sen's slope was performed in RStudio using "sens.slope()" function from the "trend" package, version 1.1.4 (Pohlert, 2020).

A Spearman correlation plot, using the function “corrplot()” in the package “corrplot” version 0.92 (Wei et al., 2021) was used to test the monotonic relationship between the variables. The function “cor.test”, which is part of the “stats” package (R Core Team, 2013), was applied to run a similar test; Spearman Rank Correlation Test but testing two variables (chlorophyll *a* and Loss on Ignition, and Native Chlorophyll (NC) and Chlorophyll Derivatives (CD)) receiving the significance of the correlation. Owned to the nonparametric technique, i.e., unaffected by the distribution of the data, insensitive to outliers, and no obligations to regularly have data collection, it is advantageous to apply Spearman Rank Coefficient to assess the correlation between two parameters. However, this method is not applicable in datasets that are normally distributed. A value Spearman Rank Coefficient, r = 1, between two parameters gives a perfect positive correlation, whereas r = -1 indicates a perfectly negative correlation. A coefficient of 0 indicates no correlation. The significance of the correlation is tested based on a 95% probability level, using $\alpha = 0.05$ (Gauthier, 2001).

2.2.8.2 Maps of Svalbard and study location

Geological and topographic maps of Ossian Sars were modified using QGIS Tisler, version 3.24.0. Maps and layers of geological and topographic maps were retrieved from the Dataset catalogue of the Norwegian Polar Institute (Norwegian Polar Institute, 2016; Skoglund, not released, respectively).

2.2.8.3 Visualisation plots and data manipulation

Visualisation of elements, LOI, and chlorophyl trends were performed in RStudio. Tables and general data manipulation was conducted in Excel version 2203.

3 Results

Trends of elements, Loss on Ignition (LOI), and chlorophyll *a* exclude the episodic accumulation of sediments in the 1-7.5 cm depth and 38-39 cm depth. Criteria for excluding these layers are described in chapter 2.2.8. However, all numeric values are presented in Appendix 1.

3.1 Observations

Figure 4 Obtained sediment core from approximately 20 cm depth at Sarsvatnet. The sediment surface was covered in moss and organic rich debris. Credit: Karoline Kristin Vognild.

Figure 4 shows the sediment core obtained from approximately 20 m depth at Sarsvatnet. The core had a distinct greyish colour in the 1-7.5 cm depth and the 38-39.0 cm depth. The samples alternated between a greenish-brown and a clear brown colour throughout the browner layers. Additionally, some samples had more noticeable structures than others, for instance, bubbles and darker lines or dots on the sliced sediment surfaces.

From the fieldwork, relatively rich vegetation was observed on the southern part of Sarsvatnet. This area was rather swampy and influenced by bird guano. Figure 4 indicates the southerly topography from Sarsvatnet.

It was observed precipitate of sediment samples after the decomposition process. Some samples had a reddish precipitate.

3.2 Chlorophyll *a* and Loss on Ignition

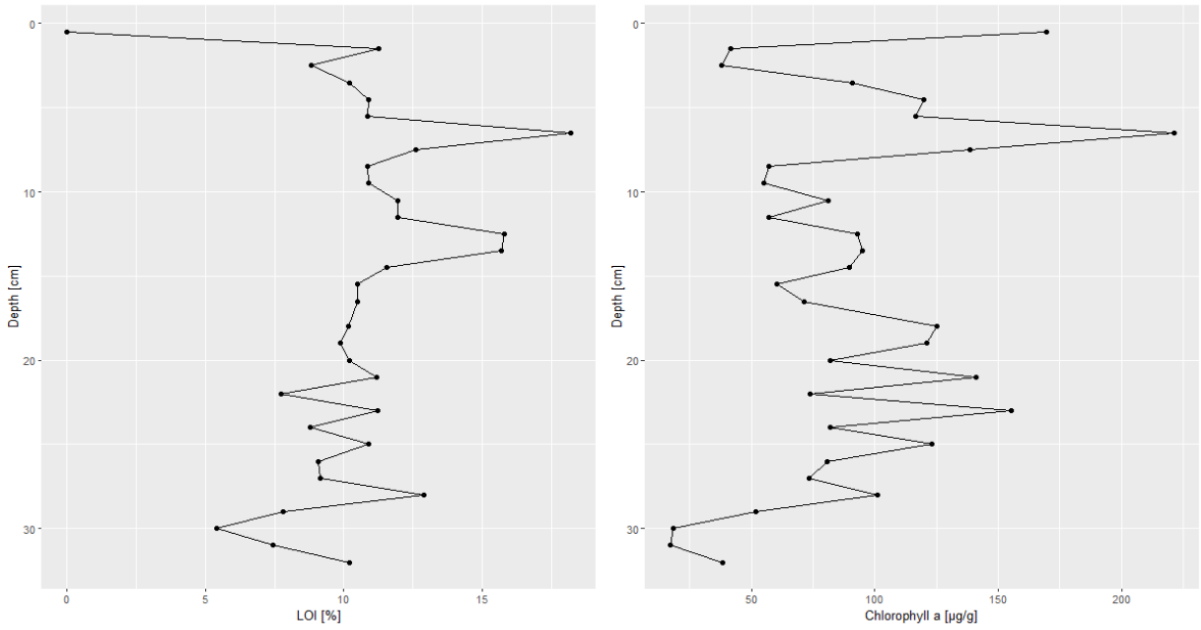

Figure 5 Loss on Ignition [%] and Chlorophyll a [mg/g] data in the sediment core.

Loss on Ignition and chlorophyll *a* have relatively similar trend patterns (figure 5); for instance, peaks at 6.5 cm (the mid-1650s) and troughs at 1.5-2.5 cm and 8.5-9.5 cm (19th century and late 1500, respectively). There is no value of LOI in the 0-0.5 cm of sediments since there was no more sample to use. However, somewhat higher percentage in the first layer is expected as rich moss content was observed in that layer, which also corresponds to findings in (Brooks & Birks, 2004). Although expecting a higher LOI in the first layer, there is still a weak correlation between Chlorophyll *a* and LOI of 38.5%, yet significant ($p = 0.03$); also prominent in the biplot in Figure 15. However, a higher correlation between chlorophyll *a* and Loss on Ignition

is expected if the LOI result of first layer was included. Furthermore, a Mann-Kendall Trend Test (n= 32) reveal a significant LOI trend.

The presented LOI results are not corrected for the clay content since the samples were not analysed for grain size distribution, and thus correction would be difficult and uncertain. However, visual assessment of the sediment colour and sediment texture indicated a clay-rich content in the samples S2-S14 and S43-S44 relative to the remaining samples that contained more organic matter with depth. Therefore, it was suggested to apply correction Figure 1 for LOI values of approximately 10 %, whereas correction Figure 2 for samples having a LOI value of approximately 4-5 % (Table 1; Dr. Tore Krogstad, pers. commun., 08.02.2022). This assumption is reasonable and comparable to Brooks and Birks (2004), who reported a LOI of approximately 5% in the upper 12 cm of the entire core, whereas a higher LOI percentage (10 % - 20 %) with depth. Consequently, there is a greater contrast of organic matter deeper in the core than what the current LOI explains. Bjerkås (2019) reported a higher clay content in the first 0-5 cm of the sediment core, with characteristics such as density increment, especially at the bottom of this layer, and a LOI of 3.9%. Additionally, as Ossian Sars constitutes of marble and thus calcium carbonates, it would be interesting to assess the loss of carbonates that contributed to the LOI.

A Spearman correlation test between Native Chlorophyll and Chlorophyll derivatives gave a significant positive correlation, R^2= 0.575, p = 0.0007.

3.3 Elements

Of 63 elements analysed, only 17 elements are considered here. A complete overview is found in Appendix 1. The 17 elements are aluminium (Al), arsenic (As), cadmium (Cd), calcium (Ca), chromium (Cr), copper (Cu), iron (Fe), lead (Pb), magnesium (Mg), manganese (Mn), nickel (Ni), phosphorus (P), potassium (K), sodium (Na), sulphur (S), titanium (Ti), and zinc (Zn).

The selection of elements is based on the different sources of elements, i.e., elements associated with long-range pollution (e.g., Pb, Cu, Cr, Ni, and Cd), geochemical elements (e.g., K, Ti, As, and Fe), marine elements (e.g., S and Ca), and associated biological elements (e.g., P). It has been necessary not to have too broad or too small selection of elements, as too few elements may fail to show a correlation between important parameters and thus possible biogeochemical processes. Furthermore, these elements are comparable to previous studies, for instance, Birks et al. (2004b).

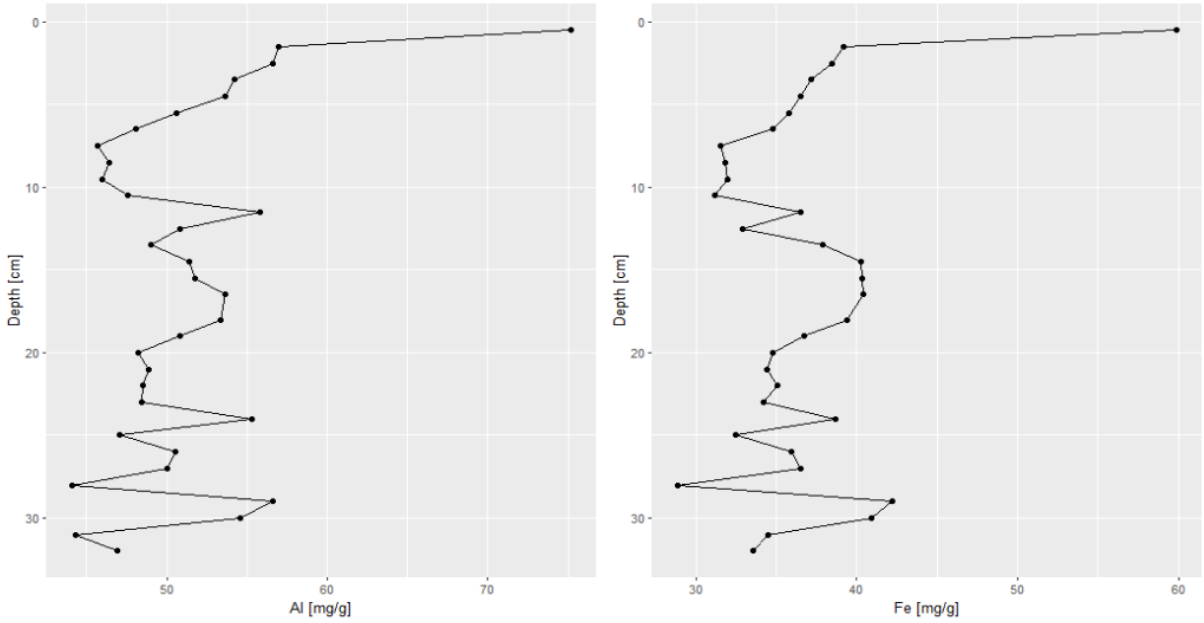

Figure 6 Aluminium and iron concentrations in mg/g from 0-32 cm depth.

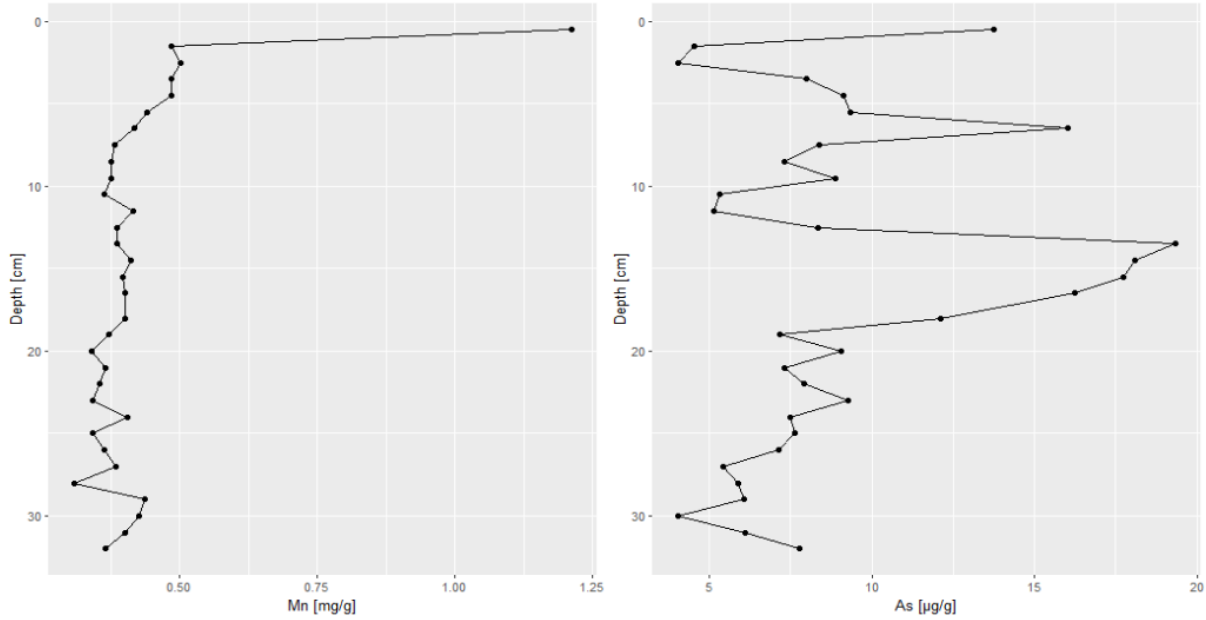

Figure 7 Manganese (mg/g) and arsenic (µg/g) from 0-32 cm depth.

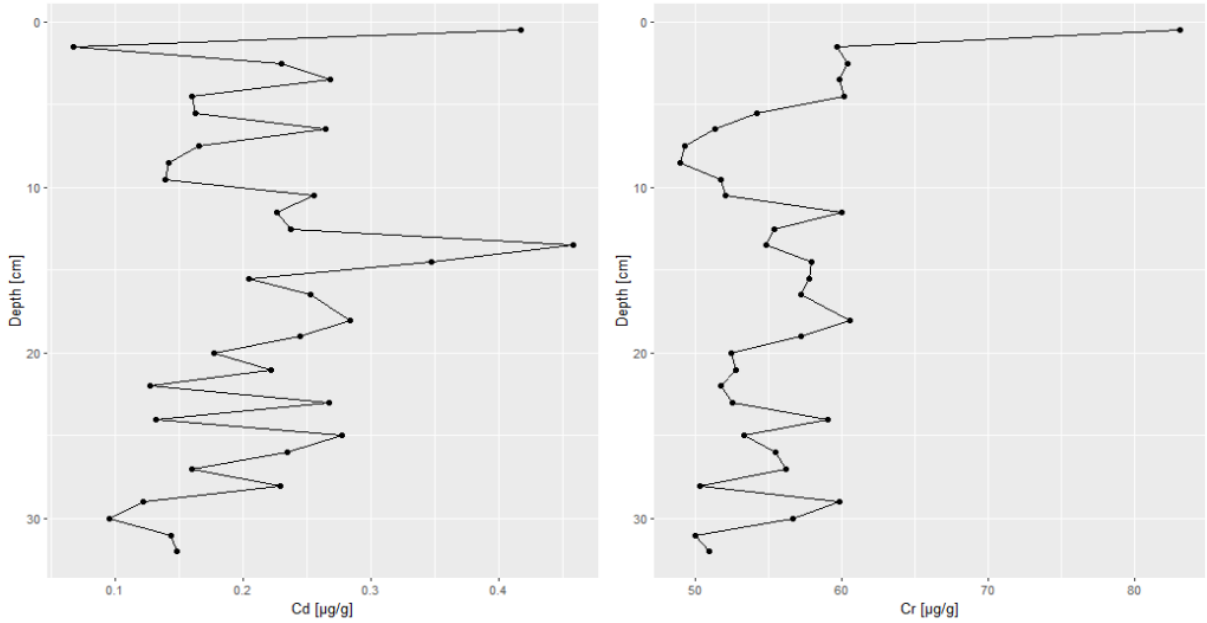

Figure 8 Cadmium and chrome in µg/g from 0-32 cm depth.

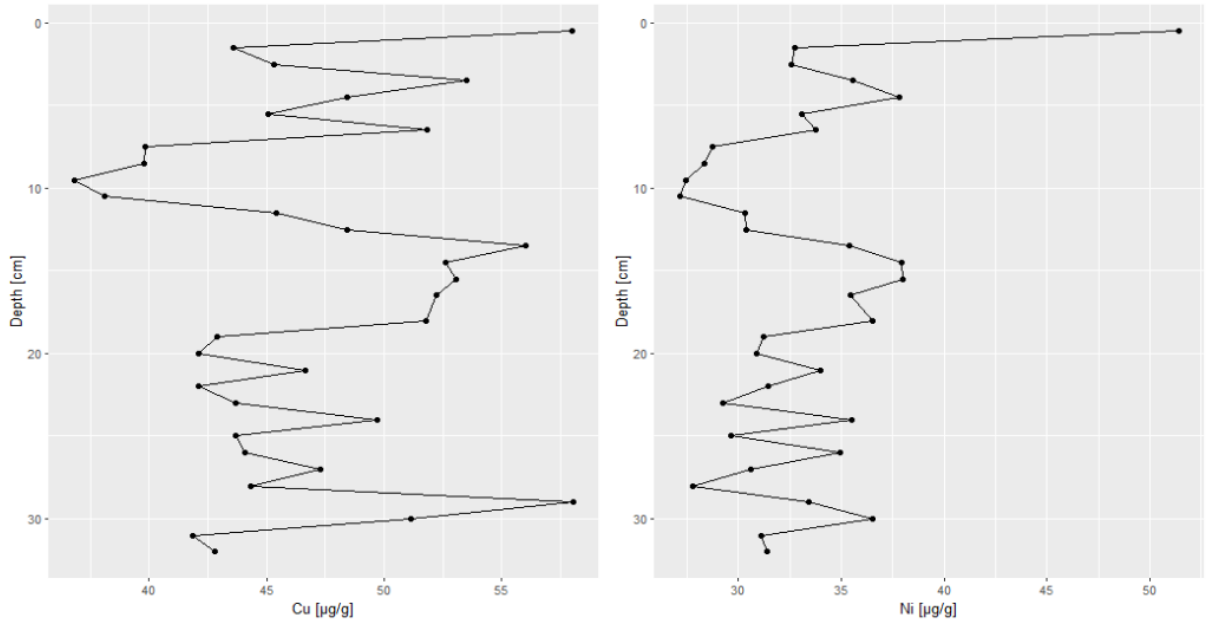

Figure 9 Copper and nickel in µg/g from 0-32 cm depth.

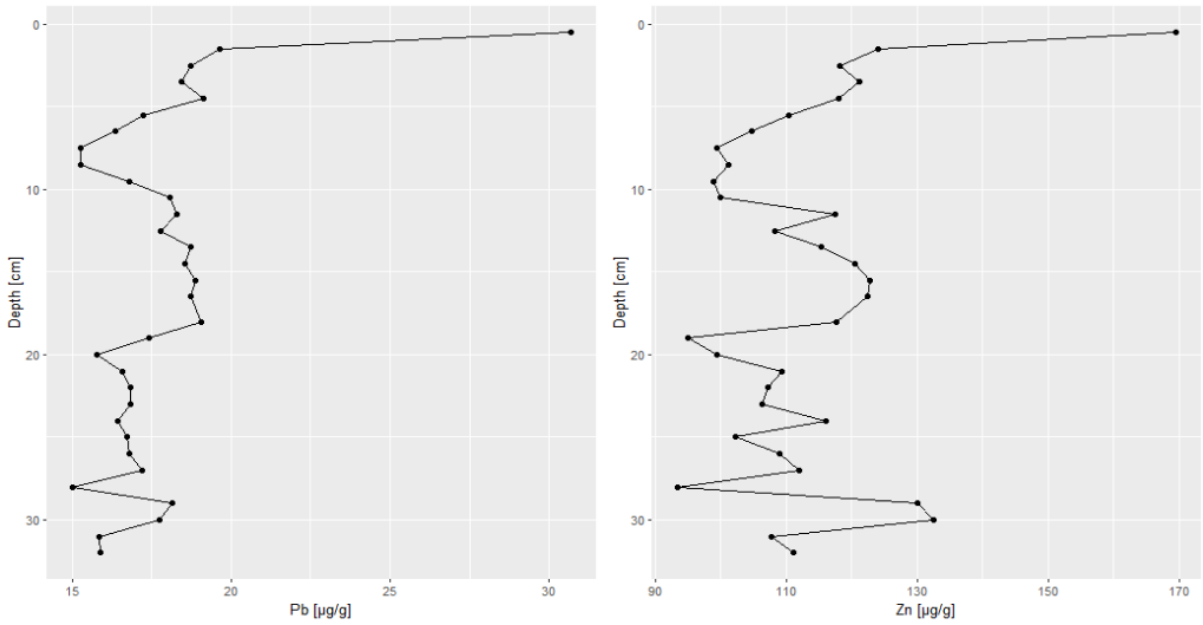

Figure 10 Lead and zinc in µg/g from 0-32 cm depth.

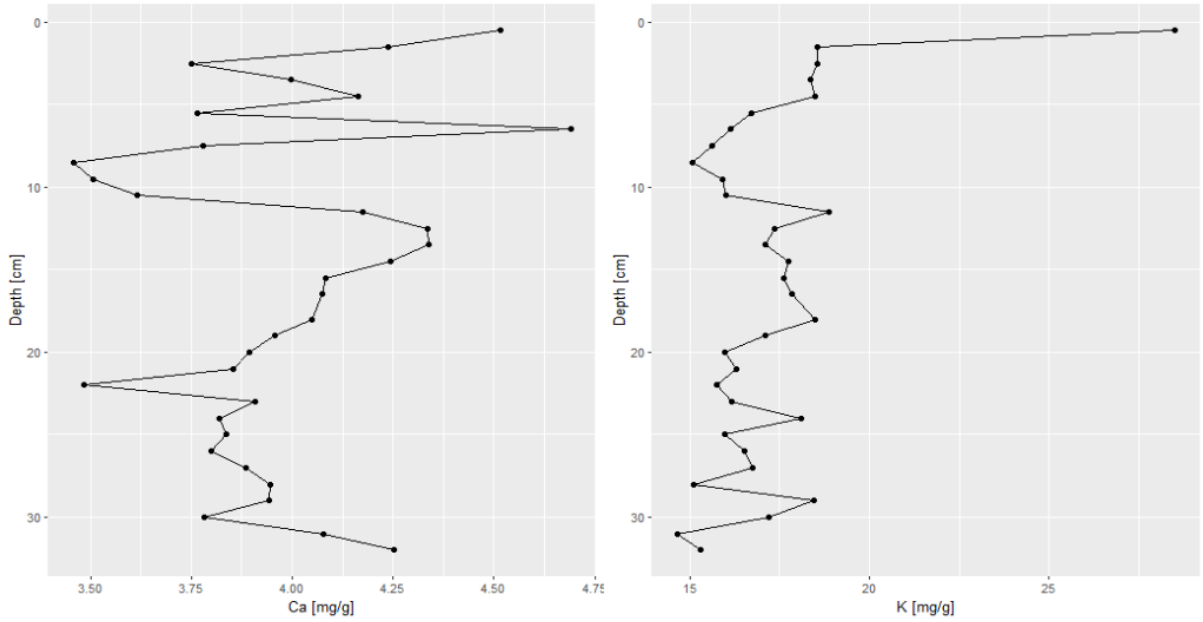

Figure 11 Calcium and potassium in mg/g from 0-32 cm depth.

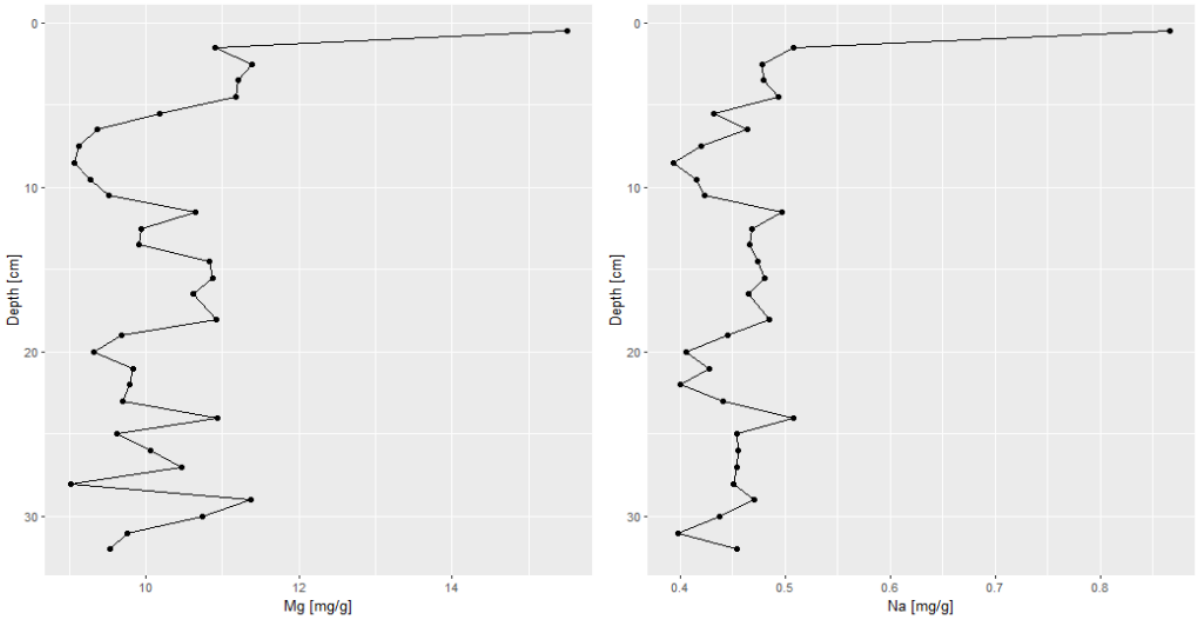

Figure 12 Magnesium and sodium in mg/g from 0-32 cm depth.

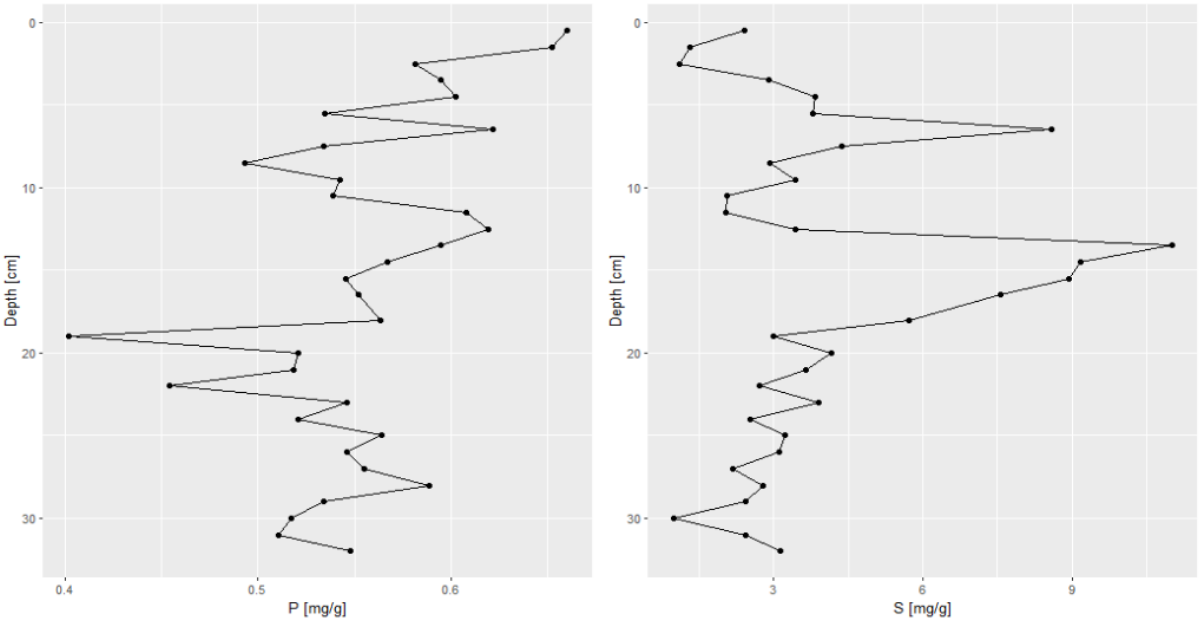

Figure 13 Phosphorus and sulphur in mg/g from 0-32 cm depth.

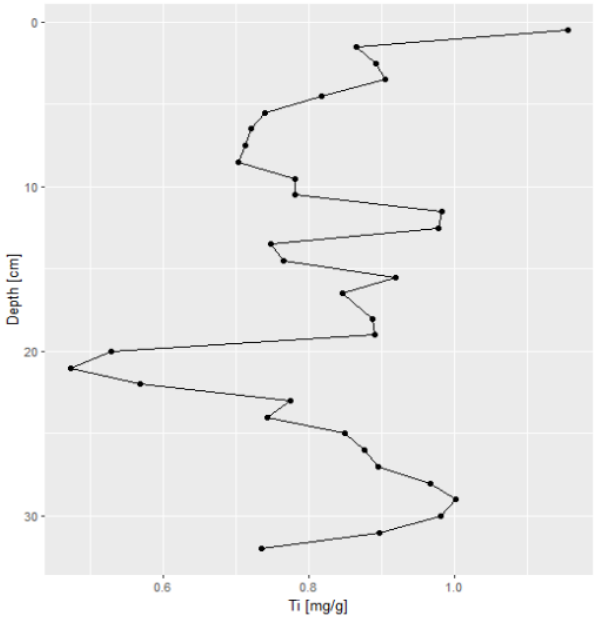

Figure 14 Titanium in mg/g from 0-32 cm depth.

All elements have, in varying degrees, an enrichment of the first sample of 0.5 cm depth (20th century) compared to the next sample at 1.5 cm depth (late 1800; Figures 6-14). Furthermore, all elements but Mn follow a similar enrichment trend in the depths around 11.5/13.5 to 18/19 cm, i.e., from the late 13th century to the early 16th century. Greater troughs down the core are found at 7.5-10.5 cm depths (early 16th century to 17th century), but especially from 19 cm depth to 32 cm depth (early 14th century to early 10th century). Although enriched, only Al, Fe, Mn, Cr, Ni, Pb, Zn, K, Mg, and Na have a distinct enrichment compared to the reference variations at lower depths. However, only Mn, Pb, K, and P have a significant Mann-Kendall trend of enrichment in the upper layer ($p = 0.0011$, 0.01195, 0.0068, and 0.041, respectively; $n = 32$) (Appendix 6). Sen's slope of the latter parameters showed a consistent negative trend downward the sediments ($Q = -0.0036$, -0.0822, -0.0691, -0.0026, and -0.0828, respectively), i.e., a trend of accumulation in the first layer, which is comparable with the Mann-Kendall Trend Test.

Two aliquots of each CRM were decomposed and analysed to determine the reproducibility. The method's precision is determined by the relative standard deviation (RSD). The following were obtained:

RSD <10%: Al, Fe, Mn, As, Cd, Cr, Cu, Ni, Zn, Ca, K, Mg, Na, P, S, Pb, and Ti (Both MESS-4 Marine Sediments and MODAS M-2 BotSed)

RSD 20%: Pb (MESS-4 Marine Sediments)

The method's accuracy was determined by comparing the measured values of CRM with the certified interval. There were no certified values of Na, Mg, S, Fe, Cr, and K in MODAS M-2

BotSed, whereas P, Ca, Mn, Co, Ni, Cu, Zn, As, Cd and Pb were within 10% of the certified interval. Al was within 25-35%, while Ti was within 93% of the certified interval. As for MESS-4 Marine Sediments, only S was within the certified interval, whereas Mg, P, Ca, Fe, Co, Ni, Zn, As, and Cd were within 10% of the certified interval. Mn, Cu, and Pb were within 11-15%, whereas Na, Al, and K were within the 15-40% interval with high variations between the aliquots. Ti was 96% from the certified values, like the obtained values from the MODAS M-2 BotSed.

Precalculated detection limits (DL) of the ICP-MS analysis are given in Appendix 2.

3.4 Principal Component Analysis and Correlation

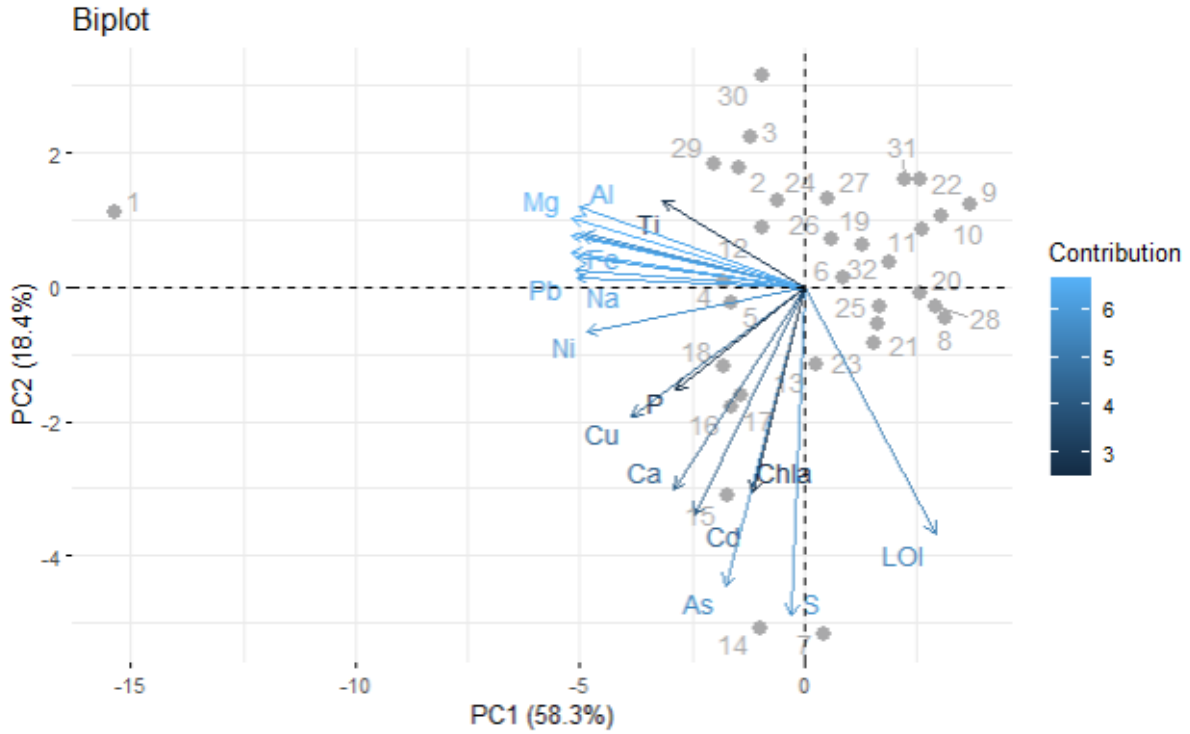

Figure 15 Biplot of first and second principal component from layers S1.S14-S42, S45-S46, i.e., the layers S2-S13 and S43-S44 are excluded. However, the numeric values continue, meaning that S14 corresponds to sample 2, and the last sample 32, corresponds to layer S46. "Chla" stands for chlorophyll a.

The first principal component describes 58.3% of the total variation in the dataset, while the second principal component stands for 18.4% of all variations. Together they describe 76.7% of the total variation. Since the third principal component describes 6%, and thus is close to the 5% background noise, PC3 was not further investigated. Nineteen principal components are required to describe 100% of the total variation in the dataset, whereas five principal components are required to describe 92 % of the total variation.

From the biplot of the first and second principal components, shown in Figure 15, there are two groups of importance. K, Mg, Cr, Pb, Fe, and Na, respectively, are correlated and have strong loadings on the first principal component. Additionally, these are strongly associated with S1

at 0.5 cm depth compared to samples closer to the origin. Hence, score 1 has a higher concentration of K, Mg, Cr, Pb, Fe, and Na, than other scores (layers). The second group consists of the parameters S, As, LOI, Cd, Chlorophyll *a*, and Ca, respectively, which have strong loadings on the second principal component and are associated with scores 7 and 14, i.e., S19 at 6.5 cm depth and S26 at 14.5 cm depth. In other words, the scores 7 and 14 have higher concentrations of especially As, S, and Cd compared to other points. The cluster of scores in the upper right side of the origin have relatively low or monotonic values of the tested parameters. Hence, they are associated with neither of the loadings. The blue shaded colours visualise what loadings contribute the most, as presented above.

Correlations between the variables are better presented in Figure 16. As visual in the biplot, variables with high loadings on the first principal component have high correlations. For instance, aluminium is highly correlated with chrome, potassium, and magnesium (R^2 = 0.93, 0.96, 0.92, respectively). While for instance, Loss on Ignition is low to moderate negative correlated with iron, magnesium, zinc, and nickel (R^2 = -0.48, -0.37, -0.44, and -0.36, respectively). Loadings having approximately 90 degrees toward each other are not correlated/ trivial correlated, for instance, between LOI and copper or manganese and arsenic (R^2 = 0.09 and 0.02, respectively). Nevertheless, the position of LOI and thus the correlation might have been different if the LOI result of S1 was available.

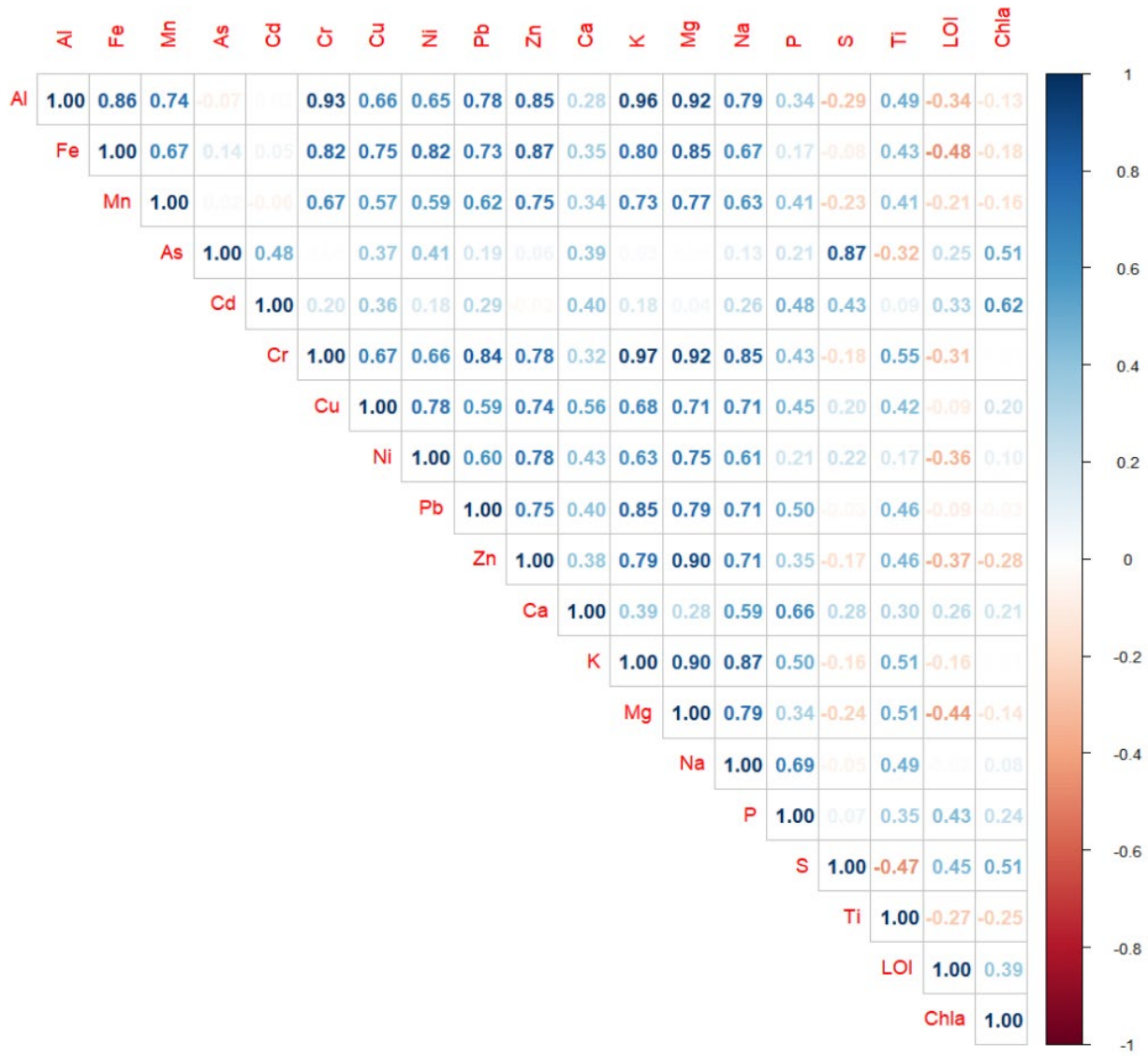

Figure 16 Correlation plot between the chosen variables. Shades of blue indicate positive correlation, whereas shades of red indicate negative correlation. Weak colours indicate more or less no correlation between the two variables. Chlorophyll a is abbreviated to "Chla".

4 Discussion

4.1 Quality Assurance and Quality Control

Per ISO 16729:2013 (Standardization, 2013), utilising HNO_3 as a dissolving acid in the decomposition of sediment samples gives only the labile fraction of the elements in the sample. Thus, several elements fell within 10-20% under the 95% confidence interval of the certified reference material (CRM). The accuracy of the method is therefore difficult to assess.

Only one sediment core was retrieved from Sarsvatnet with no replica but the obtained results. Hence, there is no estimation of the spatial variation. However, the results are comparable with results obtained by Birks et al. (2004b). Three scans of each sample were conducted, and thus the precision is presented as relative standard deviations (RSD; Appendix 1).

The accuracy and precision of analytical measurements depend on the sampling procedure and the management of samples prior to analysis. Potential human errors in data collection include contamination from fingerprints on the sediment corer and its instrumental parts. Better field procedures, e.g., using disposable gloves, could minimise the contamination. Elements that may contaminate are mainly salts associated with human sweat, i.e., sodium, potassium, and calcium (Patterson et al., 2000). Other elements from skin contaminants have previously been reported with trace minerals (e.g., iron, zinc, magnesium, calcium, and copper; Baker (2017)). From the biplot, contamination is assessed as low.

Indirect dating is one of the most significant errors as the dating is based on interpolation from previous estimations (Appleby, 2004), in addition to interpolating of extrapolated sedimentation rate. However, in further discussions, the estimated decades and centuries are instead used than the actual estimated year when compared to findings from previous research. Furthermore, similarities with other research are used to control the reliability of indirect dating.

4.2 Episodic accumulation event

A greyish segment in the upper core (S2-S13) at 1-7.5 cm has been identified. (Boyle et al., 2004) and (Bjerkås, 2019) explored explanatory causes of this episodic accumulation event with higher clay content and lower LOI and chlorophyll *a* concentrations, the latter being a response to dilution (Krajewska et al., 2020). Boyle et al. (2004) argued that neither rapid catchment erosion nor the redistribution of older marginal lake sediments can determine the cause of the rapid accumulation event, as both reasons would give similar sediment characteristics. Bjerkås (2019) suggested that an accumulation could respond to a surge from the Kongsbreen glacier but most likely from increased winter precipitation during the Little Ice Age (LIA). Either way, the layers of S2-S13 and S43-S44 are excluded from the trend Figures 5-14 to assess the continuity of the variables in the core.

4.3 Indication of the historical climate

Chlorophyll and organic matter (OM) are among several proxies used to reconstruct the historical environment and climate (Boldt et al., 2015; Czeczuga, 1965; Overpeck et al., 1997). The following section will not include a complete reconstruction of the historical climate but rather discuss important peaks and troughs of Loss on Ignition (LOI) and Chlorophyll *a* trends of the sediment core (Figure 5) from the last 1100 years. For reconstruction work of Kongsfjorden, see Bjerkås (2019) or Grant (2016).

From the period 900-1400 (i.e., 15.5 cm to 32 cm depths), there are rapid rises and falls of chlorophyll *a* and LOI, yet less prominent as the upper peaks and troughs of the core. Furthermore, the samples from this period contained much brown and green, sticky organic matter-rich sediments. The same period is recognised as the Medieval Climate Anomaly (MCA), i.e., distinct warming of the Northern Hemisphere in north-western Europe (Zamelczyk et al., 2020). This could describe the LOI and chlorophyll *a* trends. As a response to an increased presence of warm Atlantic Water through the Fram Strait into the Arctic Ocean (Zamelczyk et al., 2020), there are reports of increased temperatures (Divine et al., 2011; Spielhagen et al., 2011), high runoff due to melting of glaciers (Grinsted et al., 2006), reimmigration of thermophilous marine molluscs (Mangerud & Svendsen, 2018), and increased primary production (van der Bilt et al., 2015) in Svalbard. Studies, e.g., Grinsted et al. (2006), suggest that the temperatures during the MCA were similar to or warmer than present-day temperatures in the Northern Hemisphere. Despite this, D'Andrea et al. (2012) describe a cooling period between 910 to 990, 1100-1160, and 1250-1300 in Isfjorden, Svalbard. This could explain the few drops in primary production throughout the late 10th century to 15th century.

A rapid decline at 31 cm depth (mid-10th century) of both variables can be attributed to either 1) a response to a colder climate before the MCA (D'Andrea et al., 2012; Werner et al., 2011), or 2) a supply of glacier sediments. Bjerkås (2019) observed periodically increased glacier supply in the 900-1600. The layers S43 and S44 were excluded from the trend plots based on low chlorophyll *a* content, low LOI (below 5%), and a distinct greyish colour. However, mixing of layers could have occurred and thus a decline in concentrations of both variables. Low sedimentation rate and mixing of layers are problems in deep lakes (Smol, 2016). Nevertheless, from Figure 4, the sediments are somewhat laminated. The LOI is, however, not as low as the excluded values.

Studies suggest a relatively cold period between the 16th and 19th centuries, but mainly a cold period during the 19th century (Isaksson et al., 2003; Overpeck et al., 1997). The Little Ice Age (LIA) occurred asymmetrically around the North Atlantic (Grove, 2001). Initiative attributes to

the Little Ice Age are proposed to lower temperatures (Humlum et al., 2005; Isaksson et al., 2003; Svendsen & Mangerud, 1997) as a response to summer insolation (Overpeck et al., 1997), changing solar irradiance (Crowley, 2000), reduced meridional overturning circulation in the North Atlantic (Bianchi & McCave, 1999), and increased volcanic activity (Porter, 1981) However, D'Andrea et al. (2012) argued that the recent glacier advances had similar positions as the occurring glaciers in 1300, although the summer temperatures are estimated to be 1-2.5ºC higher than the recent advances. Therefore, increased winter precipitation and snowfall with mild and humid winters as a response to a prevailing positive North Atlantic Oscillation are a suggestion that led to glacier advances rather than colder summer temperatures (D'Andrea et al., 2012; Nesje et al., 2008; Røthe et al., 2015). Nevertheless, as Farnsworth et al. (2020) pointed out, historical precipitation records are sparse, and several workers suggest that cool air and ocean temperatures favour glaciers during the late Neoglacial (i.e., the widespread Late Holocene glacier expansion) and the Little Ice Age. However, an observation of a sharp peak of both LOI and chlorophyll *a* at 13.5 cm depth (the mid-1650s) indicates warm summer temperatures could occur, despite glacier advances during the winter.

Alternatively, a peak of chlorophyll *a* could be due to a good preservation effect to degradation of pigments (Jiang et al., 2011). The Native Chlorophyll (NC) had a significant medium correlation (R^2 = 0.575) with Chlorophyll Derivatives (CD), indicating that the preservation conditions were good. However, degradation of pigments should be higher in oligotrophic lakes (Swain, 1985). Similar patterns can be attributed to the peak at 13.5-14.5 cm depth of chlorophyll *a* but particularly of LOI, dated to the 15th century. This observation relates to findings by Brooks and Birks (2004), who reported a sudden rise in *Orthocladius consobrinus*-type at about 1470, concluded to as a response to climate variables.

An extensive increase of chlorophyll *a* is observed in the first layer, dated to the 20th and 21st centuries. This can be credited to warmer background temperatures (Isaksen et al., 2016) which corresponds to findings by Krajewska et al. (2020) of chlorophyll *a* in a marine sediment core in Kongsfjorden. Although missing Loss on Ignition (LOI) data of the first layer, Brooks and Birks (2004) argued for a similar LOI trend as chlorophyll *a*. Despite increasing primary production trends, Brooks and Birks (2004) suggested that Sarsvatnet is now in its most oligotrophic state and did not become as productive as several of the assessed lakes in Svalbard. Regional differences could explain this. Compared to several of the lakes evaluated by Brooks and Birks (2004), Ossian Sars is located further inland, where Kongsbreen was present until the 1950s after the recent glacier advance (Bennet et al., 1998). Subsequently, meltwater could cool the lake water and thus reduce the primary production potential in Sarsvatnet. However, their

assessment includes samples from the 19th and 20th centuries (1810-1995). This corresponds to the trough in 1.5-2.5 cm depth, dated to the 19th century. Consequently, biological changes synchronise with the termination of the Little Ice Age. Depending on the proxy used and its sensitivity (Luoto et al., 2016), the termination of the LIA differs from 1840 to 1900 in the Arctic (Fujii et al., 1990; Grinsted et al., 2006; Isaksson et al., 2005; Overpeck et al., 1997). Nevertheless, several workers agree that the 19th century was the coldest period in the Arctic. Hence the primary production in the upper sediment is a response to global warming during the last 100 years (Krajewska et al., 2020; Overpeck et al., 1997).

The Arctic environment is not in a steady state; climate variabilities in the Arctic cryosphere and biosphere have changed throughout the centuries and will continue to shift. The Arctic has, however, been subjected to an immense change during the past century, caused by natural and anthropogenic forces (Macdonald et al., 2005; Overpeck et al., 1997). A negative Mann-Kendall Trend Test of Loss on Ignition reveals a trend of reduced primary production with depth, i.e., increased primary production with time. The organic matter originates primarily from allochthonous soil organic matter (Boyle et al., 2004). With expected and recorded higher atmospheric temperatures (Macdonald et al., 2005) and increased precipitation (Førland et al., 2011), it is estimated an elevated inwash of terrestrial primary production and soil organic matter (Bintanja & Andry, 2017), and lake primary production (Jiang et al., 2011).

4.4 Element changes with time

The biplot (Figure 15) reveals that the upper layer, controlling PC1, is enriched in major and trace element concentrations compared to pre-industrial values (Figure 6-14; Evenset et al. (2007)). PC2, on the other hand, is controlled by layers 7 and 14. These layers are high in especially sulphur, arsenic, and cadmium. The similarity between the three points in the first and second principal components is more outstanding primary production as a response to climate, although the variable concentrations differ.

Of elements that may be transported through atmospheric processes, lead, cadmium, and mercury are carefully monitored in the Arctic due to their bioaccumulation and biomagnifying properties (Macdonald et al., 2003). However, Pb and Cd have a weak correlation, indicating two different control mechanisms. On the contrary, lead strongly correlates with geochemical elements, such as potassium, which is found in enriched concentrations in micas and K-feldspars as documented on Ossian Sars (Boyle et al., 2004; Kern et al., 2019). Similar observations between Zn and Cu, and geochemical elements, e.g., Ti, Mn, Fe, and Ca (Røthe et al., 2015), are described mainly by geological processes, originated in basic rock types, and biotite (Boyle et al., 2004). The first principal component is predominantly influenced by

geological processes, despite that several of the elements in PCA is associated with long-range pollution. This is consistent with results by Aslam et al. (2019).

Although weak correlations between chlorophyll *a* with heavy metals and major elements, enrichment in the upper layer suggests a similar process of lake input. A weak correlation could indicate post-burial remobilisation of elements but is rejected by Boyle et al. (2004) since there is little fractionation between the elements Pb, Zn, Cu, Fe, and Mn. Rather, two natural allochthonous pathways would supply Sarsvatnet with elements. Firstly, colloids and particles rich in Fe, Mn, heavy metals, and organic matter. Weak correlation between LOI and chlorophyll *a* suggest that soil organic matter (SOM) is not the material sources. Secondly, inwash of clastic materials, such as micas and amphiboles. Variation of element concentration depends on the sediment supply rate, which imply that the erosion intensity influences separation. Supplementary fractionation of elements depending on depth, and biogeochemical cycling of elements, would give further variations in the element concentrations (Boyle et al., 2004).

On the other hand, Boyle et al. (2004) also argued that although the organic matter had a weak to moderate correlation with Fe and Mn, indicating different geochemical control mechanisms, both Mn and Fe could be derived from soil organic matter (SOM). The origin of Fe and Mn are presumably from the weathering of post-glacial rock fragments, which corresponds to the geology of Ossian Sars (Ottesen et al., 2010). An enrichment of Fe and Mn in the top sediments is natural due to post-burial remobilisation and upward diffusion (Davison, 1993; Tessier et al., 1996) and follows similar properties (Kostka & Leśniak, 2021; Wetzel, 2001). However, dissolved iron is unlikely to be significant in clear water with a high pH such as Sarsvatnet (Boyle et al., 2004; Gorseth, 2022), hence the conclusion of derivation from SOM from the catchment. Nevertheless, an enrichment of elements also supports an allochthonous supply of organic matter from SOM, as an autochthonous supply would result in dilution and reduced element concentrations (Boyle et al., 2004).

Cadmium, sulphur, and arsenic influence the second principal component. The weak correlation of As with several geochemical elements is not fully aligned with findings by Aslam et al. (2019). There, it was suggested that arsenic had a common source of origin as Al, Cr, Cu, Fe, and Ni, potentially from the geology. Hence, although the geology can originate elemental concentrations, an enrichment of As, S, and Cd in the layers 7 and 14 could be controlled by other factors. S and As have a strong correlation, corresponding to their affinity to each other (O'Day, 2006). This may indicate reducing conditions in the sediments and thereby the enrichment of Cd as being redox-sensitive (Grotti et al., 2017; O'Day, 2006). Furthermore, Cd

generally increases with rocks' rising P, S, and C concentrations (Alloway, 2012). The denominator for the three elements is the correlation with chlorophyll *a* and LOI, respectively. This indicates an allochthonous supply of Cd, As, and S from other sources than elements associated with PC1.

There are different sources of Cd, As, and S, and perhaps not only one primary source contributing to the elements. An enrichment in layers 7 and 14 may correspond to volcanic activity or major forest fire in previous centuries, as sulphur may be used as a signal of volcanic activity (Overpeck et al., 1997). This could explain the declining chlorophyll *a* and LOI levels after the temperature rises during AD 1400 and AD 1600, and thus the initiation of the Little Ice Age as a response to cloud cover and thus reduced solar radiation. Low volcanic activity in the 20th century is partially accounted for the reduction of both As and S in the last 100-200 years, and hence the warming of the Northern Hemisphere (Overpeck et al., 1997). In contrast, such an accumulation in layers 7 and 14 cannot be explained by volcanic activities or forest fires alone due to the low sedimentation rate and thus the potential of dilution of elements compared to the high contribution in these two layers.

Instead, the elements may originate from marine sources, transported via bird guano, and thereby contributing considerably. S and As are abundant in the marine environment, whereas Cd can display calcium ions in the calcium metabolism and thus accumulate Cd in shellfish, digested by birds (Faubel et al., 2008). Although the bird cliff is further south at Ossian Sars, the observation of much bird guano indicates that Sarsvatnet is heavily influenced by bird activity. As there is a continuous seeping of water from the southern part of the catchment down to the lake, bird guanos and thus contaminants may regularly supply the sediments. This could also justify the correlation with LOI. A medium correlation with phosphorus, which Lakså (2021) concluded was significant in bird-influenced soil samples from Ossian Sars, indicates that bird life near Sarsvatnet is essential for the element composition in the sediments. Increasing P supply from bird activity could also enhance primary production in the area (Yang et al., 2021), hence the correlation between P and LOI, and increased OM in the sediments. Similar patterns may have occurred during the 1400 and 1600, seemingly warm periods (Chapter 4.3). Direct marine influence from e.g., sea spray may also contribute with As and S, however with limited supply due to the location of Sarsvatnet (100 m.a.s.l.) in the innermost of Kongsfjorden, in addition to the dilution of sea spray.

Although reducing As and S concentrations in the sediment surface, this is opposite for Cd. Guanos from migrating birds are likely to impact Sarsvatnet and thus contribute with toxic elements, such as Cd, as described above. Lakså (2021) and Syvertsen (2022) implied that the

phenomenon of ornithogenic drainage (Smol, 2016) at Ossian Sars is of significance. Black-legged kittiwakes in the Barents Sea, which dominates at Ossian Sars, are found to have elevated levels of Cd compared to other birds found on Ossian Sars, such as common eiders and barnacle goose (Savinov et al., 2003; Syvertsen, 2022). Nevertheless, all mentioned birds, in addition to fulmars, have concerningly high levels of Cd due to their high trophic level, age and contaminated food exposure (Savinov et al., 2003). In addition, Lakså (2021) reported a high mercury concentration at Ossian Sars, which attributes to the local geology rather than anthropogenic activity as in Ny-Ålesund (Yang et al., 2020). In this thesis and methodology, mercury could not be quantified because of the volatile properties of the element.

Atmospheric deposition is another pathway of contaminants. Aslam et al. (2019) observed no spatial distribution of Cd between Kongsfjorden and Adventdalen, suggesting an enrichment is due to anthropogenic activities at lower latitudes. Local anthropogenic pollution in Ny-Ålesund is reported by Aslam et al. (2019). Bazzano et al. (2016) reported anthropogenic origin of Cd, Cr, Cu, Mo, Ni, Pb, and Zn in atmospheric aerosols in Ny-Ålesund, with seasonal differences for Cd, Pb and Cu, and others. The seasonal changes are due to the characteristics of weather systems during winter and summer. A negative correlation between LOI and Fe, and a positive correlation between LOI and Cd, S, As, and P suggest two different driving mechanisms. Increased Cd concentrations in the upper layer, although not high loading on the PC1, are therefore likely to be originated from sources other than the geology and have little association with PC1.

Several anthropogenic pollutants have been banned or reduced through international legislation, for instance a reduction of lead in soils from Ny-Ålesund after 1970

such as the Convention on Long-Range Transboundary Air Pollution and Stockholm Convention. Liu et al. (2012), observed a reduction in lead in soil from Ny-Ålesund after 1970 as a response to the worldwide reduction of Pb in gasoline. This is consistent with findings from Europe (Renberg et al., 2000) and Canada (Weiss et al., 2002).

A reduction of lead in soils from Ny-Ålesund has been observed after 1970 as a response to the worldwide reduction of Pb in gasoline. On the contrary, although the lead contribution in this sediment core is predominantly from geological processes, Rose et al. (2004) concluded that the Pb concentration profile exceeded natural variations in post- 1970 sediments from Sarsvatnet. However, the conclusion of the anthropogenic contamination signal is open to doubt based on where the baseline of natural geochemical processes is set. Since PC1 explains 58 % accounting for geological processes, an influence from atmospheric deposited lead cannot be

rejected. However, it could be hidden by natural variability (Birks et al., 2004b). A more careful approach to dating the sediment core could potentially reveal any reduction in Pb patterns to indicate anthropogenic long-range exposure of Sarsvatnet. However, such fine adjusted approach is better suitable for shallower lakes since the sedimentation rate is greater in ponds, and thus the potential problems with the mixing of layers are minimal compared to deep lakes as Sarsvatnet (Smol, 2016). In contrast, the core in Figure 4 reveal layered sedimentation in Sarsvatnet. Nevertheless, the sedimentation rate is low (Appleby, 2004). Consequently, to better assess the influence of long-range pollution to the Arctic the last centuries, it is advised to investigate in ponds rather than deep lakes.

4.5 Linking climate change and element distribution

Several workers have observed similar trends of increasing element concentrations in the upper horizon in soil samples (Yang et al., 2020), sediment samples (Boyle et al., 2004; Outridge et al., 2017), and surface waters (Kozak et al., 2016). Anthropogenic activity can explain some of the enrichment, but not all. Environmental changes contribute mainly to the elements associated with the local geology in the upper sediments. Consequently, the background concentration of elements changes simultaneously. Temperature is the primary external catalysator in the catchment, which influences the soil stability, the length of the growing season, and thus the physical and chemical weathering, soil development, vegetation type, cover, and primary production (Birks et al., 2004b). Precipitation influences the scavenging of aerosols and gasses from the atmosphere depositing on Sarsvatnet and the catchment (Macdonald et al., 2005), the inwash of remobilised organic matter and minerogenic, and weathering of nutrients (Birks et al., 2004b; Outridge et al., 2017). Historical climate variabilities can, therefore, partly explain the variation of elements in the sediment core. An Arctic temperature rise twice the global warming (Isaksen et al., 2016) accelerates the primary production in Sarsvatnet and in the catchment. A significant increasing trend of Mn, Pb, K, and P in the upper layer indicates that the biogeochemical processes in the catchment, apparently from changing climate rather than anthropogenic contaminants directly, is the major source of trace elements in Sarsvatnet. However, although most of the elements are induced by natural processes, climate change is partially accelerated by human activities (Stern & Kaufmann, 2014).

Notwithstanding, climate change associated impacts have negative consequences on several Arctic birds and mammals. For instance, increased sea ice and air temperatures, and “rain-on-snow” days, reducing spring sea ice concentration and spring sea ice cover, will negatively impact Brünnich’s guillemot, little auk, black-legged kittiwake, and pink-rooted goose with lower survival rates, lower fledging success, decreasing population size and higher prevalence

of ticks. Although some Arctic species benefit from increasing Arctic temperatures, most Arctic endemic species on Svalbard suffer in a warming Arctic environment (Descamps et al., 2017). A reduction in population size could influence the nearby bird cliff soils and thus Sarsvatnet. However, more research is needed to monitor Arctic wildlife and migrating flora and fauna that will alter the environment, thus increasing, reducing, or continuing to supply phosphorus and long-range pollution to Sarsvatnet.

5 Conclusions

The objective of this master's thesis was to assess the extent of influence from long-range pollution in Lake Sarsvatnet, Svalbard, and to discuss the forcing mechanisms of trends in elements and climate proxies over the last 1100 years from a sediment core.

The extent of influence from long-range pollution in Sarsvatnet, Svalbard, is prominent. The results indicate that cadmium (Cd) is derived from bird guano and atmospheric deposition from lower latitudes. The element concentrations have varied over the last 1100 years. An enrichment of most elements the last century is rather from increased weathering of the local geology than from atmospheric deposition and local and long-range pollution. However, more thoroughly research is needed to assess the fraction of lead (Pb) originated from atmospheric deposited lead, as the geological input dominates the source of lead.

Climate proxies, i.e., Loss on Ignition and chlorophyll *a*, reflect the climate variations over the last 1100 years. Historical periods, e.g., the Little Ice Age and Medieval Climate Anomaly, were recognised, yet anomalies were observed. These indicate periods with warmer temperatures, thus increasing primary production despite expected colder temperatures. One of the most important findings is the increased primary production in the 20th century credited to global warming. Rising temperatures in the Arctic, and thus a changing environment, it is expected increased primary production, precipitation, and weathering of bedrock. It is therefore fair to expect higher background concentrations of elements, primary production derivatives, and soil organic matter in the sediments of Sarsvatnet. Nevertheless, climate change will also alter the transportation of pollutants from lower latitudes, expecting to change loads.

Further monitoring of Sarsvatnet in the following years will be necessary to assess the development of toxic elements and the mechanisms contributing to these. This thesis provides an updated evaluation of the status quo in Sarsvatnet and could be of relevance to further research. Additionally, the attached results not processed here could initiate further necessary research in the future.

References

Allen, J., Rae, J., Longworth, G., Hasler, S. & Ivanovich, M. (1993). A comparison of the210Pb dating technique with three other independent dating methods in an oxic estuarine salt-marsh sequence. *Estuaries*, 16 (3): 670-677.

Alloway, B. J. (2012). *Heavy metals in soils: trace metals and metalloids in soils and their bioavailability*, vol. 22: Springer Science & Business Media.

AMAP. (2016). *Influence of Climate Change on Transport, Levels, and Effects of Contaminants in Northern Areas- Part 2*. In Carlsson, P., Christensen, J. H., Borgå, K., R., K., Aspmo Pfaffhuber, K., Odland, J. Ø., Reiersen, L.-O. & Pawlak, J. F. (eds). AMAP Technical Report No 10. Oslo: Arctic Monitoring and Assessment Programme (AMAP).

Appleby, P. (1998). *Dating recent sediments by 210 Pb: Problems and solutions*.

Appleby, P. (2004). Environmental change and atmospheric contamination on Svalbard: sediment chronology. *Journal of Paleolimnology*, 31 (4): 433-443.

Arunachalam, J., Mohl, C., Ostapczuk, P. & Emons, H. (1995). Multielement characterization of soil samples with ICP-MS for environmental studies. *Fresenius' journal of analytical chemistry*, 352 (6): 577-581.

Aslam, S. N., Huber, C., Asimakopoulos, A. G., Steinnes, E. & Mikkelsen, Ø. (2019). Trace elements and polychlorinated biphenyls (PCBs) in terrestrial compartments of Svalbard, Norwegian Arctic. *Science of the Total Environment*, 685: 1127-1138. doi: https://doi.org/10.1016/j.scitotenv.2019.06.060.

Baker, L. B. (2017). Sweating rate and sweat sodium concentration in athletes: a review of methodology and intra/interindividual variability. *Sports Medicine*, 47 (1): 111-128.

Barnes, R. M., Júnior, D. S. & Krug, F. J. (2014). Introduction to sample preparation for trace element determination. In *Microwave-assisted sample preparation for trace element analysis*, pp. 1-58: Elsevier.

Batley, G. (1999). Quality assurance in environmental monitoring. *Marine Pollution Bulletin*, 39 (1-12): 23-31.

Bazzano, A., Ardini, F., Grotti, M., Malandrino, M., Giacomino, A., Abollino, O., Cappelletti, D., Becagli, S., Traversi, R. & Udisti, R. (2016). Elemental and lead isotopic composition of atmospheric particulate measured in the Arctic region (Ny-Ålesund, Svalbard Islands). *Rendiconti Lincei*, 27: 73-84.

Bennet, M. R., Hambrey, M. J., Huddart, D., Glasser, N. F. & Crawford, K. (1998). The ice-dammed lakes of Ossian Sarsfjellet (Svalbard): their geomorphology and significance. *Boreas*, 27 (1): 25-43.

Bianchi, G. G. & McCave, I. N. (1999). Holocene periodicity in North Atlantic climate and deep-ocean flow south of Iceland. *Nature*, 397 (6719): 515-517.

Bintanja, R. & Andry, O. (2017). Towards a rain-dominated Arctic. *Nature Climate Change*, 7 (4): 263-267.

Birks, H. J. B., Jones, V. J. & Rose, N. L. (2004a). Recent environmental change and atmospheric contamination on Svalbard as recorded in lake sediments–an introduction. *Journal of Paleolimnology*, 31 (4): 403-410.

Birks, H. J. B., Jones, V. J. & Rose, N. L. (2004b). Recent environmental change and atmospheric contamination on Svalbard as recorded in lake sediments–synthesis and general conclusions. *Journal of Paleolimnology*, 31 (4): 531-546.

Birks, H. J. B., Monteith, D. T., Rose, N. L., Jones, V. J. & Peglar, S. M. (2004c). Recent environmental change and atmospheric contamination on Svalbard as recorded in lake sediments–modern limnology, vegetation, and pollen deposition. *Journal of Paleolimnology*, 31 (4): 411-431.

Bjerkås, A. M. B. (2019). *Holocen rekonstruksjon av Kongsbreen, Svalbard*: The University of Bergen.

Bojko, O. & Kabała, C. (2014). Loss-on-ignition as an estimate of total organic carbon in the mountain soils. *Polish Journal of Soil Science*, 47 (2).

Boldt, B. R., Kaufman, D. S., McKay, N. P. & Briner, J. P. (2015). Holocene summer temperature reconstruction from sedimentary chlorophyll content, with treatment of age uncertainties, Kurupa Lake, Arctic Alaska. *The Holocene*, 25 (4): 641-650.

Bottenheim, J. W., Dastoor, A., Gong, S.-L., Higuchi, K. & Li, Y.-F. (2004). Long range transport of air pollution to the Arctic. In *Air Pollution*, pp. 13-39: Springer.

Boyle, J. F., Rose, N. L., Appleby, P. & Birks, H. J. B. (2004). Recent environmental change and human impact on Svalbard: the lake-sediment geochemical record. *Journal of Paleolimnology*, 31 (4): 515-530.

Brooks, S. J. & Birks, H. J. B. (2004). The dynamics of Chironomidae (Insecta: Diptera) assemblages in response to environmental change during the past 700 years on Svalbard. *Journal of Paleolimnology*, 31 (4): 483-498.

Chakole, R. D., Deshmukhe, P. M. & Charde, M. S. (2021). A Review on HPLC Method Development and Validation. *International Journal of Pharmacy and Pharmaceutical Research*, 21 (4): 66-82.

Corver, J. (2009). The Evolution of Freeze-Drying. *Innovations in Pharmaceutical Technology*, 29: 66-70.

Crawley, M. J. (2012). *The R book*: John Wiley & Sons.

Crowley, T. J. (2000). Causes of climate change over the past 1000 years. *Science*, 289 (5477): 270-277.

Czeczuga, B. (1965). Quantitative changes in sedimentary chlorophyll in the bed sediment of the Mikolajki Lake during the post-glacial period. *Schweizerische Zeitschrift für Hydrologie*, 27 (1): 88-98.

D'Andrea, W. J., Vaillencourt, D. A., Balascio, N. L., Werner, A., Roof, S. R., Retelle, M. & Bradley, R. S. (2012). Mild Little Ice Age and unprecedented recent warmth in an 1800 year lake sediment record from Svalbard. *Geology*, 40 (11): 1007-1010.

Dallmann, Q. K. (2015). *Geoscience Atlas of Svalbard*. In Dallmann, Q. K. (ed.). Oslo: Norwegian Polar Institute

Davison, W. (1993). Iron and manganese in lakes. *Earth-Science Reviews*, 34 (2): 119-163.

Decorte, L. (2020). Inferring past environmental changes in High Arctic lake ecosystems using ancient DNA.

Descamps, S., Aars, J., Fuglei, E., Kovacs, K. M., Lydersen, C., Pavlova, O., Pedersen, Å. Ø., Ravolainen, V. & Strøm, H. (2017). Climate change impacts on wildlife in a High Arctic archipelago–Svalbard, Norway. *Global Change Biology*, 23 (2): 490-502.

Ding, M., Wang, S. & Sun, W. (2018). Decadal climate change in Ny-Ålesund, Svalbard, a representative area of the Arctic. *Condensed Matter*, 3 (2): 12.

Divine, D., Isaksson, E., Martma, T., Meijer, H. A., Moore, J., Pohjola, V., van de Wal, R. S. & Godtliebsen, F. (2011). Thousand years of winter surface air temperature variations

in Svalbard and northern Norway reconstructed from ice-core data. *Polar Research*, 30 (1): 7379.

Dong, M. (2013). The essence of modern HPLC: advantages, limitations, fundamentals, and opportunities.

Eckhardt, S., Stohl, A., Beirle, S., Spichtinger, N., James, P., Forster, C., Junker, C., Wagner, T., Platt, U. & Jennings, S. (2003). The North Atlantic Oscillation controls air pollution transport to the Arctic. *Atmospheric Chemistry and Physics*, 3 (5): 1769-1778.

Elvebakk, A. (1997). Tundra diversity and ecological characteristics of Svalbard. *Ecosystems of the world*: 347-360.

Evenset, A., Christensen, G., Carroll, J., Zaborska, A., Berger, U., Herzke, D. & Gregor, D. (2007). Historical trends in persistent organic pollutants and metals recorded in sediment from Lake Ellasjøen, Bjørnøya, Norwegian Arctic. *Environmental Pollution*, 146 (1): 196-205.

Farnsworth, W. R., Allaart, L., Ingólfsson, Ó., Alexanderson, H., Forwick, M., Noormets, R., Retelle, M. & Schomacker, A. (2020). Holocene glacial history of Svalbard: Status, perspectives and challenges. *Earth-Science Reviews*, 208: 103249.

Faubel, D., Lopes-Lima, M., Freitas, S., Pereira, L., Andrade, J., Checa, A., Frank, H., Matsuda, T. & Machado, J. (2008). Effects of Cd2+ on the calcium metabolism and shell mineralization of bivalve Anodonta cygnea. *Marine and Freshwater Behaviour and Physiology*, 41 (2): 131-146.

Forskrift om Ossian Sars naturreservat. (2003). *Forskrift om fredning av Ossian Sars naturreservat*. Available at: https://lovdata.no/dokument/SF/forskrift/2003-09-26-1188 (accessed: 01.10.2021).

Fujii, Y., Kamiyama, K., Kawamura, T., Kameda, T., Izumi, K., Satow, K., Enomoto, H., Nakamura, T., Hagen, J. & Gjessing, Y. (1990). 6000-year climate records in an ice core from the Høghetta ice dome in northern Spitsbergen. *Annals of Glaciology*, 14: 85-89.

Førland, E. J., Benestad, R., Hanssen-Bauer, I., Haugen, J. E. & Skaugen, T. E. (2011). Temperature and precipitation development at Svalbard 1900–2100. *Advances in Meteorology*, 2011.

Førland, E. J., Isaksen, K., Lutz, J., Hanssen-Bauer, I., Schuler, T. V., Dobler, A., Gjelten, H. M. & Vikhamar-Schuler, D. (2020). Measured and modeled historical precipitation trends for Svalbard. *Journal of Hydrometeorology*, 21 (6): 1279-1296.

Gauthier, T. D. (2001). Detecting trends using Spearman's rank correlation coefficient. *Environmental forensics*, 2 (4): 359-362.

Gorseth, L. K. (2022). *Factors Affecting the Water Chemistry of Non-Glaciated High Arctic Catchments: A Snapshot study of Lake Sarsvatnet, Svalbard*. Master's thesis. Ås: Norwegian University of Life Sciences.

Grant, O. R. (2016). *The deglaciation of Kongsfjorden, Svalbard—based on surface exposure dating of glacial erratics and Quaternary geological mapping of Blomstrandhalvøya*: The University of Bergen.

Grinsted, A., Moore, J. C., Pohjola, V., Martma, T. & Isaksson, E. (2006). Svalbard summer melting, continentality, and sea ice extent from the Lomonosovfonna ice core. *Journal of Geophysical Research: Atmospheres*, 111 (D7).

Grotti, M., Soggia, F., Ardini, F., Bazzano, A., Moroni, B., Vivani, R., Cappelletti, D. & Misic, C. (2017). Trace elements in surface sediments from Kongsfjorden, Svalbard: occurrence, sources and bioavailability. *International Journal of Environmental Analytical Chemistry*, 97 (5): 401-418. doi: https://doi.org/10.1080/03067319.2017.1317762.

Grove, J. M. (2001). The initiation of the" Little Ice Age" in regions round the North Atlantic. *Climatic change*, 48 (1): 53-82.

Hagman, C. H. C., Rohrlack, T., Uhlig, S. & Hostyeva, V. (2019). Heteroxanthin as a pigment biomarker for Gonyostomum semen (Raphidophyceae). *PloS one*, 14 (12): e0226650. doi: https://doi.org/10.1371/journal.pone.0226650.

Hanoa, R. (2016). *Kings Bay på Svalbard 1916-2016; Fra gruvedrift til forskingsservice og klimaobservatorium* Fagbokforlaget.

Hipel, K. W. & McLeod, A. I. (1994). *Time series modelling of water resources and environmental systems*: Elsevier.

Hjelle, A. (1993). *Geology of Svalbard*. Oslo: Norsk Polarinstitutt.

Humlum, O., Elberling, B., Hormes, A., Fjordheim, K., Hansen, O. H. & Heinemeier, J. (2005). Late-Holocene glacier growth in Svalbard, documented by subglacial relict vegetation and living soil microbes. *The Holocene*, 15 (3): 396-407.

International Standard. (2013a). *ISO 16729 Soil quality- Digestion of nitric acid soluble fractions of elements*. Available at: https://standard.no/no/Nettbutikk/produktkatalogen/Produktpresentasjon/?ProductID=668218 (accessed: 13.06.2022).

International Standard. (2013b). *ISO/TS 16965:2013 Soil quality- Deteermination of trace elements using inductively coupled plasma mass spectrometry (ICP-MS)*. Available at: https://www.iso.org/standard/58056.html (accessed: 13.07.2022).

Isaksen, K., Nordli, Ø., Førland, E. J., Łupikasza, E., Eastwood, S. & Niedźwiedź, T. (2016). Recent warming on Spitsbergen—Influence of atmospheric circulation and sea ice cover. *Journal of Geophysical Research: Atmospheres*, 121 (20): 11,913-11,931.

Isaksson, E., Hermanson, M., Hicks, S., Igarashi, M., Kamiyama, K., Moore, J., Motoyama, H., Muir, D., Pohjola, V. & Vaikmäe, R. (2003). Ice cores from Svalbard—useful archives of past climate and pollution history. *Physics and Chemistry of the Earth, Parts A/b/c*, 28 (28-32): 1217-1228.

Isaksson, E., Kohler, J., Pohjola, V., Moore, J., Igarashi, M., Karlöf, L., Martma, T., Meijer, H., Motoyama, H. & Vaikmäe, R. (2005). Two ice-core δ18O records from Svalbard illustrating climate and sea-ice variability over the last 400 years. *The Holocene*, 15 (4): 501-509.

Jiang, S., Liu, X., Sun, J., Yuan, L., Sun, L. & Wang, Y. (2011). A multi-proxy sediment record of late Holocene and recent climate change from a lake near Ny-Ålesund, Svalbard. *Boreas*, 40 (3): 468-480.

Kassambara, A. & Mundt, F. (2020). *Factoextra: Extract and Visualize the Results of Multivariate Data Analyses* (Version 1.0.7). Available at: http://www.sthda.com/english/rpkgs/factoextra

Keith, L. H. (1999). *Environmental Sampling and Analysis: A Practical Guide*. Boca Raton, Florida: Lewis Publishers.

Kern, R., Hotter, V., Frossard, A., Albrecht, M., Baum, C., Tytgat, B., De Maeyer, L., Velazquez, D., Seppey, C., Frey, B., et al. (2019). Comperative vegetation survey with focus on cryptogamic covers in the high Arctic along two differing catenas. *Polar Biology*, 42. doi: https://doi.org/10.1007/s00300-019-02588-z.

Kostka, A. & Leśniak, A. (2021). Natural and anthropogenic origin of metals in lacustrine sediments; assessment and consequences—A case study of Wigry lake (Poland). *Minerals*, 11 (2): 158.

Kozak, K., Polkowska, Ż., Stachnik, Ł., Luks, B., Chmiel, S., Ruman, M., Lech, D., Kozioł, K., Tsakovski, S. & Simeonov, V. (2016). Arctic catchment as a sensitive indicator of the environmental changes: distribution and migration of metals (Svalbard). *International Journal of Environmental Science and Technology*, 13 (12): 2779-2796.

Krajewska, M., Szymczak-Żyła, M., Tylmann, W. & Kowalewska, G. (2020). Climate change impact on primary production and phytoplankton taxonomy in Western Spitsbergen fjords based on pigments in sediments. *Global and Planetary Change*, 189: 103158.

Krogstad, T. & Børresen, T. (2015). *JORD200: Field and laboratory methods*. Ås, Norway: Norwegian University of Life Sciences.

Lakså, S. B. (2021). *The role of migratory birds in the transport of pollutants to the Arctic*. M.Sc. Trondheim: Norwegian University of Science and Technology.

Law, K. S. & Stohl, A. (2007). Arctic air pollution: Origins and impacts. *science*, 315 (5818): 1537-1540.

Lee, Y. K. (2020). *Arctic Plants in Svalbard*: Springer.

Lindbäck, K., Kohler, J., Pettersson, R., Nuth, C., Langley, K., Messerli, A., Vallot, D., Matsuoka, K. & Brandt, O. (2018). Subglacial topography, ice thickness, and bathymetry of Kongsfjorden, northwestern Svalbard. *Earth System Science Data*, 10 (4): 1769-1781.

Lindström, E. & Leskinen, E. (2002). Do neighboring lakes share common taxa of bacterioplankton? Comparison of 16S rDNA fingerprints and sequences from three geographic regions. *Microbial Ecology*, 44 (1): 1-9.

Liu, X., Jiang, S., Zhang, P. & Xu, L. (2012). Effect of recent climate change on Arctic Pb pollution: A comparative study of historical records in lake and peat sediments. *Environmental Pollution*, 160: 161-168.

Luoto, T., Oksman, M. & Ojala, A. E. (2016). Invertebrate communities of the High Arctic ponds in Hornsund. *Polish Polar Research*, 37.

Macdonald, R., Harner, T. & Fyfe, J. (2005). Recent climate change in the Arctic and its impact on contaminant pathways and interpretation of temporal trend data. *Science of the total environment*, 342 (1-3): 5-86. doi: https://doi.org/10.1016/j.scitotenv.2004.12.059.

Macdonald, R. W., Hamer, T., Fyfe, J., Loeng, H. & Weingartner, T. (2003). *AMAP Assessment 2002: The Influence of Global Change on Contaminant Pathways to, within, and from the Arctic*: Arctic Monitoring and Assessment Programme (AMAP).

Mangerud, J. & Svendsen, J. I. (2018). The Holocene thermal maximum around Svalbard, Arctic North Atlantic; molluscs show early and exceptional warmth. *The Holocene*, 28 (1): 65-83.

Marx, S. K., Rashid, S. & Stromsoe, N. (2016). Global-scale patterns in anthropogenic Pb contamination reconstructed from natural archives. *Environmental Pollution*, 213: 283-298.

Moroni, B., Cappelletti, D., Ferrero, L., Crocchianti, S., Busetto, M., Mazzola, M., Becagli, S., Traversi, R. & Udisti, R. (2016). Local vs. long-range sources of aerosol particles upon Ny-Ålesund (Svalbard Islands): Mineral chemistry and geochemical records. *Rendiconti Lincei*, 27 (1): 115-127.

Muraoka, H., Uchida, M., Mishio, M., Nakatsubo, T., Kanda, H. & Koizumi, H. (2002). Leaf photosynthetic characteristics and net primary production of the polar willow (Salix polaris) in a High Arctic polar semi-desert, Ny-Ålesund, Svalbard. *Canadian Journal of Botany*, 80 (11): 1193-1202.

Nesje, A., Dahl, S. O., Thun, T. & Nordli, Ø. (2008). The 'Little Ice Age'glacial expansion in western Scandinavia: summer temperature or winter precipitation? *Climate dynamics*, 30 (7): 789-801.

Norwegian Polar Institute. (2016). *Geological map of Svalbard (1:250000)* Data set: Norwegian Polar Institute.

Noyes, P. D., McElwee, M. K., Miller, H. D., Clark, B. W., Van Tiem, L. A., Walcott, K. C., Erwin, K. N. & Levin, E. D. (2009). The toxicology of climate change: environmental contaminants in a warming world. *Environment international*, 35 (6): 971-986.

O'Day, P. A. (2006). Chemistry and mineralogy of arsenic. *Elements*, 2 (2): 77-83.

Ottesen, R. T., Bogen, J., Finne, T. E., Andersson, M., Dallmann, W. K., Eggen, O. A., Jartun, M., Lundkvist, Q., Pedersen, H. R. & Volden, T. (2010). *Geochemical atlas of Norway Part 2: Geochemical atlas of Spitsbergen*. Geochemical atlas of Norway Trondheim, Norway: Geological Survey of Norway & Norges Vassdrag- og Energidirektorat.

Outridge, P., Sanei, H., Mustaphi, C. C. & Gajewski, K. (2017). Holocene climate change influences on trace metal and organic matter geochemistry in the sediments of an Arctic lake over 7,000 years. *Applied Geochemistry*, 78: 35-48.

Overpeck, J., Hughen, K., Hardy, D., Bradley, R., Case, R., Douglas, M., Finney, B., Gajewski, K., Jacoby, G. & Jennings, A. (1997). Arctic environmental change of the last four centuries. *Science*, 278 (5341): 1251-1256. doi: 10.1126/science.278.5341.1251.

Pacyna, J. M. & Pacyna, E. G. (2001). An assessment of global and regional emissions of trace metals to the atmosphere from anthropogenic sources worldwide. *Environmental reviews*, 9 (4): 269-298.

Patterson, M. J., Galloway, S. D. & Nimmo, M. A. (2000). Variations in regional sweat composition in normal human males. *Experimental physiology*, 85 (6): 869-875.

Pearce, D. A., Cockell, C. S., Lindström, E. S. & Tranvik, L. J. (2007). First evidence for a bipolar distribution of dominant freshwater lake bacterioplankton. *Antarctic Science*, 19 (2): 245-252.

Pohlert, T. (2020). *Trend: Non-Parametric Trend Test and Change-Point Detection* (Version 1.1.4). Available at: https://cran.r-project.org/web/packages/trend/index.html.

Pommeresche, R., Frøseth, R. B. & Riley, H. (2019). Hvordan måles innholdet av organisk materiale og karbon i norsk jord?

Porter, S. C. (1981). Recent glacier variations and volcanic eruptions. *Nature*, 291 (5811): 139-142.

R Core Team. (2013). *The R Stats Package* (Version Version 4.3.0): R Foundation for Statistical Computing. Available at: https://stat.ethz.ch/R-manual/R-devel/library/stats/html/stats-package.html.

Renberg, I., Brännvall, M.-L., Bindler, R. & Emteryd, O. (2000). Atmospheric lead pollution history during four millennia (2000 BC to 2000 AD) in Sweden. *AMBIO: A Journal of the Human Environment*, 29 (3): 150-156.

Reymert, P. K. (2016). *Ny-Ålesund; Verdens nordligste gruveby*. Longyearbyen, Norge: Sysselmannen på Svalbard, Miljøvernavdelingen.

Rose, N. L., Rose, C. L., Boyle, J. F. & Appleby, P. G. (2004). Lake-sediment evidence for local and remote sources of atmospherically deposited pollutants on Svalbard. *Journal of Paleolimnology*, 31: 499-513.

Røthe, T. O., Bakke, J., Vasskog, K., Gjerde, M., D'Andrea, W. J. & Bradley, R. S. (2015). Arctic Holocene glacier fluctuations reconstructed from lake sediments at Mitrahalvøya, Spitsbergen. *Quaternary Science Reviews*, 109: 111-125.

Sagar, V., Kannan, V. M., Gopikrishna, V. G., Krishnan, K. P. & Mohan, M. (2021). Geochemistry and distribution of Metals in the Sediments of Kongsfjorden, Svalbard, Arctic. *Regional Studies in Marine Science*, 44: 101729.

Salmi, T. (2002). *Detecting trends of annual values of atmospheric pollutants by the Mann-Kendall test and Sen's slope estimates-the Excel template application MAKESENS*: Ilmatieteen laitos.

Savinov, V. M., Gabrielsen, G. W. & Savinova, T. N. (2003). Cadmium, zinc, copper, arsenic, selenium and mercury in seabirds from the Barents Sea: levels, inter-specific and geographical differences. *Science of the Total Environment*, 306 (1-3): 133-158.

Schmale, J., Arnold, S., Law, K. S., Thorp, T., Anenberg, S., Simpson, W., Mao, J. & Pratt, K. (2018). Local Arctic air pollution: A neglected but serious problem. *Earth's Future*, 6 (10): 1385-1412.

Shears, J., Theisen, F., Bjørdal, A. & Norris, S. (1998). *Environmental impact assessment: Ny-Ålesund international scientific research and monitoring station, Svalbard*. Norsk Polarinstitutt Meddelelser. Tromsø: Norwegian Polar Institute.

Shukla, S. (2011). Freeze drying process: A review. *International journal of pharmaceutical sciences and research*, 2 (12): 3061.

Skoglund, A. (not released). *NP_Basiskart_Svalbard_WMS [Data set]*: Norwegian Polar Institute.

Skoog, D. A., West, D. M., Holler, F. J. & Crouch, S. R. (2014). *Fundamentals of Analytical Chemistry*. 9. ed. Belmount, USA: Brooks/Cole.

Smol, J. P. (2016). Arctic and Sub-Arctic shallow lakes in a multiple-stressor world: a paleoecological perspective. *Hydrobiologia*, 778 (1): 253-272.

Spielhagen, R. F., Werner, K., Sørensen, S. A., Zamelczyk, K., Kandiano, E., Budeus, G., Husum, K., Marchitto, T. M. & Hald, M. (2011). Enhanced modern heat transfer to the Arctic by warm Atlantic water. *Science*, 331 (6016): 450-453.

Standard Norge. (2007). *NS-EN ISO 16720: 2007 Jordkvalitet; Forbehandling ved hjelp av frysetørking av prøver for senere analyse*. Available at: https://infostore.saiglobal.com/en-gb/standards/product-details-38754_SAIG_AFNOR_AFNOR_86188/?ProductID=38754_SAIG_AFNOR_AFNOR_86188 (accessed: 07.07.2022).

Standard Norge. (2017). *NS-ISO 5667-12:2017 Vannundersøkelse- Prøvetaking- Del 12: Veiledning i prøvetaking av bunnsedimenter fra elver, innsjøer og estuarine områder*. Available at:

https://www.standard.no/no/Nettbutikk/produktkatalogen/Produktpresentasjon/?ProductID=941609 (accessed: 07.07.2022).

Standard Norge. (2021). *NS-EN 15935:2021 Jord, avfall, behandlet organisk avfall og slam; Bestemmelse av glødetap*. Available at: https://www.standard.no/no/Nettbutikk/produktkatalogen/Produktpresentasjon/?ProductID=1370713.

Standardization, I. O. f. (2013). *ISO 16729:2013 Soil quality- Digestion of nitric acid soluble fractions of elements*. Available at: https://www.iso.org/standard/57562.html (accessed: 13.06.2022).

Stern, D. I. & Kaufmann, R. K. (2014). Anthropogenic and natural causes of climate change. *Climatic change*, 122 (1): 257-269.

Stohl, A. (2006). Characteristics of atmospheric transport into the Arctic troposphere. *Journal of Geophysical Research: Atmospheres*, 111 (D11).

Sun, Q., Chu, G., Liu, J. & Gao, D. (2006). A 150-year record of heavy metals in the varved sediments of Lake Bolterskardet, Svalbard. *Arctic, Antarctic, and Alpine Research*, 38 (3): 436-445.

Svendsen, J. I. & Mangerud, J. (1997). Holocene glacial and climatic variations on Spitsbergen, Svalbard. *The Holocene*, 7 (1): 45-57.

Swain, E. B. (1985). Measurement and interpretation of sedimentary pigments. *Freshwater Biology*, 15 (1): 53-75.

Syvertsen, M. (2022). *Long-range transport of pollutants to Arctic areas by seabirds*. M.Sc. Trondheim: Norwegian University of Science and Technology.

Tabari, H. & Talaee, P. H. (2011). Analysis of trends in temperature data in arid and semi-arid regions of Iran. *Global and Planetary Change*, 79 (1-2): 1-10.

Tessier, A., Fortin, D., Belzile, N., DeVitre, R. & Leppard, G. (1996). Metal sorption to diagenetic iron and manganese oxyhydroxides and associated organic matter: narrowing the gap between field and laboratory measurements. *Geochimica et Cosmochimica Acta*, 60 (3): 387-404.

Thusen, N. P. B., S. (2021). *Svalbard* Encyclopedia Store Norske Leksikon. Available at: https://snl.no/Svalbard (accessed: 27.04.2021).

van der Bilt, W. G., Bakke, J., Vasskog, K., D'Andrea, W. J., Bradley, R. S. & Ólafsdóttir, S. (2015). Reconstruction of glacier variability from lake sediments reveals dynamic Holocene climate in Svalbard. *Quaternary Science Reviews*, 126: 201-218.

Vidushi, Y. & Meenakshi, B. (2017). A review on HPLC method development and validation. *Res J Life Sci, Bioinform, Pharm Chem Sci*, 2 (6): 178.

Weckström, K., Saunders, K. M., Gell, P. A. & Skilbeck, C. G. (2017). *Applications of paleoenvironmental techniques in estuarine studies*, vol. 20: Springer.

Wei, T., Simko, V., Levy, M., Xie, Y., Jin, Y., Zemla, J., Freidank, M., Cai, J. & Protivinsky, T. (2021). *R package "corrplot": Visualization of a Correlation Matrix* (Version Version 0.92). Available at: https://github.com/taiyun/corrplot.

Weiss, D., Shotyk, W., Boyle, E. A., Kramers, J. D., Appleby, P. G. & Cheburkin, A. K. (2002). Comparative study of the temporal evolution of atmospheric lead deposition in Scotland and eastern Canada using blanket peat bogs. *Science of the total environment*, 292 (1-2): 7-18.

Werner, K., Spielhagen, R. F., Bauch, D., Hass, H. C., Kandiano, E. & Zamelczyk, K. (2011). Atlantic Water advection to the eastern Fram Strait—Multiproxy evidence for late Holocene variability. *Palaeogeography, Palaeoclimatology, Palaeoecology*, 308 (3-4): 264-276.

Wetzel, R. G. (2001). *Limnology: lake and river ecosystems*: gulf professional publishing.

Willis, M. D., Leaitch, W. R. & Abbatt, J. P. (2018). Processes controlling the composition and abundance of Arctic aerosol. *Reviews of Geophysics*, 56 (4): 621-671.

Wilschefski, S. C. & Baxter, M. R. (2019). Inductively coupled plasma mass spectrometry: introduction to analytical aspects. *The Clinical Biochemist Reviews*, 40 (3): 115.

Yang, Z., Yuan, L., Xie, Z., Wang, J., Li, Z., Tu, L. & Sun, L. (2020). Historical records and contamination assessment of potential toxic elements (PTEs) over the past 100 years in Ny-Ålesund, Svalbard. *Environmental Pollution*, 266: 115205. doi: https://doi.org/10.1016/j.envpol.2020.115205.

Yang, Z., Zhang, Y., Xie, Z., Wang, J., Li, Y., Du, J. & Sun, L. (2021). Potential influence of rapid climate change on elemental geochemistry distributions in lacustrine sediments-A case study at high Arctic site in Ny-Ålesund, Svalbard. *Science of The Total Environment*, 801 (149784). doi: https://doi.org/10.1016/j.scitotenv.2021.149784.

Zamelczyk, K., Rasmussen, T. L., Raitzsch, M. & Chierici, M. (2020). The last two millennia: climate, ocean circulation and paleoproductivity inferred from planktic foraminifera, south-western Svalbard margin.

Appendix 1: Collected data

Appx 1 Concentrations [µg/g or mg/g] and Relative Standard Deviation (RSD) [%] of all elements, chlorophyll a, Loss on Ignition (LOI), and indirect dating. Here, conditional presentation of elements, LOI and chlorophyll a is given to visualise the trends through time. The redder background colours, the higher the number. The numbers are, however, not compared to given limit values The excluded samples, i.e., S2-S13 and S43 and S44 (chapter 2.2.8), are presented within the firm line.

Layer	Depth (incl. external input)	Depth (excl. external input)	Dating	Chloro-phyll *a*	Loss on Ignition	Na		Mg		Al		P		S		K	
	[cm]	[cm]	[AD]	[µg/g]	[%]	[mg/g]	RSD [%]	[mg/g]	RSD [%]	[mg/g]	RSD [%]	[mg/g]	RSD [%]	[mg/g]	RSD [%]	[mg/g]	RSD [%]
	0	0	2021														
S1	0.5	0.5	1909	169	0	0.87	0.5	15.51	0.4	75.20	2.6	0.66	0.1	2.40	0.5	28.53	0.8
S2	1			16.4	6.77	1.00	2.3	18.23	1.2	87.94	1.2	0.42	0.7	1.23	1.5	33.26	0.8
S3	1.5			5.70	4.78	1.00	2.1	18.54	1.8	85.37	0.5	0.34	0.6	0.72	2.1	33.40	1.4
S4	2			1.39	4.35	1.01	1.6	18.98	1.2	83.88	1.8	0.35	0.1	0.47	0.7	33.70	0.5
S5	2.5			0.942	4.39	0.90	0.9	17.39	3.1	81.71	1.5	0.34	3.3	0.22	1.5	29.57	1.2
S6	3			0.284	4.38	0.93	2.7	16.71	2.7	74.48	2.0	0.38	1.3	0.18	1.2	29.03	0.9
S7	3.5			0.139	4.41	0.91	2.1	16.05	2.0	74.80	2.4	0.38	1.1	0.14	2.6	28.12	1.9
S8	4			0.736	4.41	0.91	1.6	17.00	2.2	79.84	0.7	0.43	2.2	0.17	2.2	29.82	0.9
S9	4.5			1.83	5.42	0.84	2.1	15.91	0.7	76.57	2.2	0.47	0.6	0.25	2.3	27.82	0.5
S10	5			10.23	5.74	0.79	1.2	15.27	1.3	73.62	2.5	0.56	1.6	0.41	1.8	26.69	0.6
S11	5.5			8.60	5.78	0.71	2.2	14.44	0.5	67.96	2.4	0.62	2.0	0.35	0.9	24.54	0.4
S12	6.5			1.85	5.42	0.74	1.2	14.38	2.5	73.48	2.0	0.66	2.0	0.25	2.4	26.18	0.6
S13	7.5			9.66	6.46	0.82	1.8	15.07	2.3	78.13	2.9	0.60	1.5	0.56	2.6	28.17	0.6
S14	8.5	1.5	1889	41.7	11.26	0.51	2.4	10.91	3.4	56.97	1.6	0.65	2.0	1.32	3.3	18.56	2.1
S15	9.5	2.5	1843	38.2	8.81	0.48	1.0	11.38	1.4	56.60	1.9	0.58	1.6	1.10	1.3	18.55	2.5
S16	10.5	3.5	1796	91.04	10.2	0.48	0.8	11.21	0.8	54.22	2.4	0.59	0.6	2.91	0.3	18.35	0.7
S17	11.5	4.5	1741	120	10.88	0.49	2.5	11.17	3.1	53.65	0.9	0.60	2.2	3.83	1.7	18.50	1.5
S18	12.5	5.5	1694	117	10.85	0.43	2.5	10.18	4.1	50.62	3.3	0.53	1.9	3.79	3.0	16.72	2.5
S19	13.5	6.5	1656	221	18.21	0.46	2.4	9.37	2.6	48.10	1.3	0.62	1.2	8.59	4.1	16.12	1.8
S20	14.5	7.5	1620	139	12.59	0.42	2.2	9.12	2.5	45.66	3.0	0.53	3.7	4.36	2.9	15.61	2.6
S21	15.5	8.5	1586	57.2	10.85	0.39	2.2	9.07	2.0	46.38	2.4	0.49	4.0	2.93	2.6	15.05	2.8

Layer	Depth (incl. external input)	Depth (excl. external input)	Dating	Chloro-phyll *a*	Loss on Ignition	Na		Mg		Al		P		S		K	
	[cm]	[cm]	[AD]	[µg/g]	[%]	[mg/g]	RSD [%]	[mg/g]	RSD [%]	[mg/g]	RSD [%]	[mg/g]	RSD [%]	[mg/g]	RSD [%]	[mg/g]	RSD [%]
S22	16.5	9.5	1559	55.1	10.88	0.42	1.9	9.28	3.2	45.97	1.4	0.54	1.5	3.43	2.7	15.91	2.3
S23	17.5	10.5	1541	81.2	11.95	0.42	3.2	9.51	4.1	47.56	1.3	0.54	2.2	2.07	3.8	16.00	3.7
S24	18.5	11.5	1522	57.2	11.95	0.50	3.2	10.65	4.2	55.82	3.5	0.61	3.6	2.03	4.3	18.88	4.0
S25	19.5	12.5	1503	92.9	15.81	0.47	0.4	9.95	1.1	50.85	3.0	0.62	1.4	3.43	0.3	17.37	1.7
S26	20.5	13.5	1480	95.1	15.7	0.47	2.6	9.91	3.0	49.00	2.5	0.59	1.5	11.02	2.0	17.09	1.8
S27	21.5	14.5	1445	89.8	11.53	0.47	3.4	10.82	2.6	51.41	1.7	0.57	3.2	9.17	3.7	17.73	3.1
S28	22.5	15.5	1410	60.49	10.51	0.48	6.0	10.87	3.4	51.78	1.4	0.55	2.5	8.92	2.2	17.61	3.1
S29	24	16.5	1380	71.2	10.51	0.47	1.6	10.62	2.7	53.66	1.7	0.55	0.5	7.56	2.4	17.85	1.6
S30	25	18.0	1360	125	10.17	0.48	1.9	10.92	3.6	53.38	2.2	0.56	2.6	5.71	2.8	18.50	1.3
S31	26	19.0	1324	121	9.86	0.45	2.1	9.68	3.5	50.80	1.2	0.40	1.5	2.99	1.9	17.10	2.6
S32	27	20.0	1286	81.9	10.2	0.41	3.7	9.31	3.2	48.20	1.5	0.52	3.2	4.17	3.3	15.99	3.5
S33	28	21.0	1256	140.9	11.19	0.43	2.4	9.84	2.4	48.83	1.1	0.52	2.3	3.64	2.5	16.31	2.8
S34	29	22.0	1226	73.7	7.74	0.40	4.0	9.79	3.6	48.53	1.6	0.45	3.9	2.71	4.5	15.75	4.3
S35	30	23.0	1195	155	11.22	0.44	2.7	9.70	2.3	48.43	2.4	0.55	2.7	3.89	1.2	16.17	2.4
S36	31	24.0	1165	81.8	8.78	0.51	2.4	10.94	3.2	55.31	3.1	0.52	2.5	2.51	2.8	18.11	2.1
S37	32	25.0	1135	123	10.88	0.45	2.7	9.62	4.3	47.04	1.8	0.56	3.4	3.23	3.3	15.97	2.9
S38	33	26.0	1104	80.6	9.06	0.45	3.4	10.06	4.9	50.55	1.6	0.55	2.7	3.11	4.1	16.51	3.4
S39	34	27.0	1074	73.2	9.15	0.45	2.6	10.47	2.4	49.99	0.7	0.55	2.0	2.19	3.0	16.74	3.1
S40	35	28.0	1044	101	12.88	0.45	3.0	9.01	2.8	44.07	1.3	0.59	1.8	2.78	2.2	15.09	1.9
S41	36	29.0	1014	51.8	7.8	0.47	2.6	11.38	2.3	56.60	1.3	0.53	1.5	2.43	2.9	18.44	2.1
S42	37	30.0	983	18.6	5.39	0.44	2.7	10.73	4.1	54.60	3.0	0.52	3.8	0.98	3.2	17.18	2.0
S43	38			2.043	5.07	0.46	1.8	11.90	0.9	57.96	3.6	0.51	2.0	0.80	1.7	19.36	2.0
S44	39			2.59	5.41	0.39	4.0	10.27	4.1	46.37	1.6	0.48	3.4	1.35	5.0	14.79	2.4
S45	40	31.0	953	17.1	7.43	0.40	2.6	9.75	3.3	44.35	3.5	0.51	2.8	2.43	2.4	14.64	2.4
S46	41	32.0	923	38.5	10.2	0.45	0.7	9.53	3.0	46.88	2.8	0.55	1.0	3.13	2.0	15.28	0.5

Layer	Depth (incl. external input)	Depth (excl. external input)	Ti		V		Cr		Mn		Fe		Co		Ni		Cu		Zn	
	[cm]	[cm]	[mg/g]	RSD [%]	[µg/g]	RSD [%]	[µg/g]	RSD [%]	[mg/g]	RSD [%]	[mg/g]	RSD [%]	[µg/g]	RSD [%]	[µg/g]	RSD [%]	[µg/g]	RSD [%]	[µg/g]	RSD [%]
	0	0																		
S1	0.5	0.5	1.16	1.1	94.04	1.2	83.10	1.4	1.21	2.1	59.92	0.7	30.69	1.1	51.43	1.4	58.02	0.7	169.60	0.7
S2	1		1.19	0.6	99.14	0.6	95.94	0.6	0.87	1.7	67.36	1.5	31.25	1.0	56.34	1.2	58.29	0.4	201.04	0.8
S3	1.5		1.26	0.7	100.38	1.1	96.09	1.3	0.84	1.3	67.68	0.7	29.09	0.8	54.81	1.5	56.17	0.7	196.20	0.7
S4	2		1.26	0.1	101.35	0.2	96.69	0.4	0.86	1.6	68.54	0.6	29.61	0.3	55.02	0.9	55.87	0.3	187.71	0.0
S5	2.5		1.16	2.3	89.30	2.1	87.49	2.6	0.82	2.2	68.99	2.0	27.77	1.2	49.60	3.4	48.31	2.0	183.81	1.6
S6	3		1.19	1.7	90.19	1.3	84.89	1.6	0.80	0.7	66.55	2.4	28.54	1.4	48.62	0.5	44.47	1.9	168.65	2.2
S7	3.5		1.14	0.7	89.78	2.1	82.02	1.0	0.77	1.5	68.58	2.0	27.56	1.0	45.95	1.5	41.38	0.2	165.30	1.8
S8	4		1.33	2.1	94.90	1.4	87.29	1.1	0.85	1.5	74.46	2.0	29.68	1.6	49.57	2.0	44.55	1.7	179.97	1.4
S9	4.5		1.23	0.5	88.61	0.9	81.52	0.8	0.79	0.9	70.83	3.5	27.22	1.1	47.00	1.8	42.35	0.1	171.91	3.7
S10	5		1.02	1.5	83.99	0.3	79.91	0.6	0.74	0.8	61.68	2.6	24.54	1.1	46.28	1.6	47.46	1.0	166.05	2.7
S11	5.5		1.09	0.8	79.66	0.8	74.51	1.4	0.71	0.3	59.59	2.7	25.26	0.8	44.86	1.9	45.76	1.1	158.22	4.4
S12	6.5		1.03	1.7	80.41	1.5	76.73	1.1	0.75	1.1	68.70	0.8	27.58	1.7	47.83	1.1	45.49	1.4	167.70	2.0
S13	7.5		0.87	0.7	82.97	0.9	80.37	1.0	0.70	0.3	60.90	1.5	24.43	1.2	46.65	2.0	45.42	1.3	173.04	1.4
S14	8.5	1.5	0.86	3.0	64.98	2.3	59.62	2.4	0.48	0.6	39.17	1.5	14.73	2.4	32.76	1.7	43.59	1.8	124.05	1.6
S15	9.5	2.5	0.89	1.1	66.03	0.7	60.37	1.6	0.50	1.6	38.47	2.6	14.64	0.3	32.57	2.5	45.33	1.0	118.18	2.8
S16	10.5	3.5	0.90	0.1	69.93	0.3	59.83	0.2	0.49	0.5	37.18	1.1	16.95	1.4	35.54	0.3	53.51	0.8	121.24	0.3
S17	11.5	4.5	0.82	1.1	69.39	1.2	60.09	1.4	0.48	1.1	36.47	0.8	19.40	1.6	37.82	0.9	48.44	1.8	118.11	0.3
S18	12.5	5.5	0.74	3.0	62.21	2.2	54.17	3.4	0.44	2.0	35.79	4.2	16.36	2.5	33.06	4.1	45.09	1.9	110.49	0.6
S19	13.5	6.5	0.72	1.8	64.47	2.3	51.34	2.7	0.42	1.2	34.80	1.6	18.08	2.7	33.76	3.1	51.81	1.9	104.76	1.8
S20	14.5	7.5	0.71	1.9	59.15	1.7	49.22	2.2	0.38	2.8	31.52	2.1	14.52	3.1	28.76	2.6	39.83	1.8	99.37	2.0
S21	15.5	8.5	0.70	2.3	56.82	2.8	48.90	2.8	0.37	2.3	31.82	1.2	13.96	1.8	28.36	3.3	39.80	2.1	101.28	0.9
S22	16.5	9.5	0.78	1.0	60.23	1.6	51.72	2.4	0.37	3.7	31.95	1.8	14.22	2.2	27.42	1.4	36.80	1.3	98.97	1.2
S23	17.5	10.5	0.78	2.4	60.71	2.6	52.04	2.5	0.36	1.9	31.16	3.2	13.02	4.0	27.14	2.3	38.12	1.7	99.95	3.8
S24	18.5	11.5	0.98	2.6	71.90	3.2	59.94	4.3	0.41	1.7	36.53	2.7	14.88	3.2	30.30	4.1	45.43	2.5	117.54	2.1

Layer	Depth (incl. external input)	Depth (excl. external input)	Ti		V		Cr		Mn		Fe		Co		Ni		Cu		Zn	
	[cm]	[cm]	[mg/g]	RSD [%]	[µg/g]	RSD [%]	[µg/g]	RSD [%]	[mg/g]	RSD [%]	[mg/g]	RSD [%]	[µg/g]	RSD [%]	[µg/g]	RSD [%]	[µg/g]	RSD [%]	[µg/g]	RSD [%]
S25	19.5	12.5	0.98	0.4	67.56	0.5	55.39	0.8	0.39	1.2	32.86	1.0	15.13	1.1	30.37	0.9	48.43	0.7	108.20	0.6
S26	20.5	13.5	0.75	1.2	68.42	2.4	54.85	2.1	0.39	2.6	37.85	1.3	23.77	3.1	35.39	2.2	56.04	2.1	115.31	3.5
S27	21.5	14.5	0.76	2.5	68.49	2.4	57.88	2.3	0.41	2.9	40.28	0.8	22.38	2.5	37.93	2.4	52.63	2.4	120.52	1.2
S28	22.5	15.5	0.92	0.9	69.46	2.4	57.70	2.2	0.40	3.0	40.35	0.9	22.96	1.9	38.01	0.6	53.08	0.8	122.74	2.7
S29	24	16.5	0.85	1.8	68.02	1.4	57.23	2.3	0.40	3.8	40.42	3.3	20.77	1.9	35.47	2.7	52.25	1.9	122.48	1.5
S30	25	18.0	0.89	1.4	70.12	2.4	60.49	2.3	0.40	3.9	39.41	1.8	19.77	3.6	36.51	3.8	51.79	3.2	117.72	1.8
S31	26	19.0	0.89	4.1	67.67	3.6	57.22	4.4	0.37	2.6	36.71	2.2	16.91	3.9	31.20	4.2	42.89	3.7	95.08	1.3
S32	27	20.0	0.53	2.5	59.46	2.7	52.43	3.3	0.34	4.9	34.76	1.4	16.51	4.3	30.86	2.9	42.11	2.5	99.45	1.5
S33	28	21.0	0.47	1.4	61.36	1.5	52.76	3.3	0.36	2.3	34.43	0.3	18.60	2.3	33.99	1.9	46.66	1.2	109.34	1.6
S34	29	22.0	0.57	4.5	57.70	3.4	51.73	3.2	0.35	4.6	35.07	1.2	16.16	3.2	31.42	4.2	42.10	2.8	107.21	2.9
S35	30	23.0	0.77	1.7	62.43	2.5	52.51	2.3	0.34	0.8	34.18	2.1	14.90	2.4	29.23	2.7	43.70	2.5	106.27	2.0
S36	31	24.0	0.74	2.2	68.62	2.3	58.99	2.9	0.40	0.8	38.68	1.8	17.82	0.9	35.50	2.9	49.70	1.6	116.01	2.2
S37	32	25.0	0.85	2.2	63.06	2.5	53.31	2.7	0.34	4.0	32.43	1.2	15.50	1.9	29.63	2.2	43.68	1.8	102.36	1.7
S38	33	26.0	0.88	2.9	63.89	2.9	55.45	3.8	0.36	6.3	35.94	1.5	17.69	2.3	34.97	3.9	44.08	3.5	109.01	2.7
S39	34	27.0	0.89	2.4	64.28	2.0	56.16	2.7	0.38	2.7	36.51	0.4	15.45	2.5	30.58	4.0	47.29	2.2	112.03	0.5
S40	35	28.0	0.97	1.7	62.62	1.1	50.27	2.1	0.31	2.3	28.82	2.2	14.27	2.1	27.79	2.8	44.31	1.7	93.36	2.3
S41	36	29.0	1.00	2.9	70.12	2.8	59.84	3.0	0.44	2.8	42.20	1.1	18.32	3.9	33.44	2.1	58.08	2.0	130.08	1.7
S42	37	30.0	0.98	3.3	61.89	1.9	56.62	3.7	0.43	2.8	40.89	2.7	18.27	3.4	36.49	3.9	51.15	2.2	132.49	3.5
S43	38	31.0	1.01	2.2	65.70	2.6	61.69	1.5	0.46	1.5	43.50	2.9	17.20	3.0	33.65	3.0	62.37	2.4	140.95	0.8
S44	39		0.87	3.4	56.35	2.8	50.14	4.1	0.41	2.9	36.96	2.7	16.93	3.7	33.89	6.2	43.64	4.0	114.19	2.1
S45	40		0.90	2.1	58.27	2.4	50.00	3.2	0.40	3.0	34.50	2.7	15.93	3.0	31.10	4.6	41.86	3.1	107.69	2.2
S46	41	32.0	0.73	1.1	60.13	1.4	50.92	1.0	0.37	3.0	33.53	3.3	16.12	1.3	31.39	0.8	42.81	0.7	111.06	2.9

Layer	Depth (incl. external input)	Depth (excl. external input)	As		Br		Cd		Pb		Li		Be		B [H2]		B [O2]		Si	
	[cm]	[cm]	[µg/g]	RSD [%]	[µg/g]	RSD [%]	[µg/g]	RSD [%]	[µg/g]	RSD [%]	[mg/g]	RSD [%]	[µg/g]	RSD [%]	[µg/g]	RSD [%]	[µg/g]	RSD [%]	[mg/g]	RSD [%]
	0	0																		
S1	0.5	0.5	13.75	0.3	83.63	2.5	0.42	11.8	30.70	0.3	54.77	1.0	3.46	15.1	70.52	1.9	68.53	1.4	2.08	1.9
S2	1		5.14	5.6	26.50	2.3	0.20	17.6	31.62	0.4	69.19	1.0	4.70	13.2	29.90	2.7	27.79	2.0	1.94	1.0
S3	1.5		2.10	4.8	15.45	4.9	0.27	10.1	29.13	0.6	70.10	2.5	4.29	12.9	24.62	9.4	24.23	1.9	1.95	0.2
S4	2		1.67	9.1	9.91	44.7	0.24	10.8	27.25	0.8	72.39	3.1	4.32	26.7	24.49	5.8	23.43	8.4	1.94	1.5
S5	2.5		1.41	6.5	<0.165	4.4	0.17	16.7	24.69	1.6	69.98	1.5	3.87	38.3	22.61	4.6	19.23	16.0	1.87	1.5
S6	3		2.05	5.1	<0.165	18.8	0.16	8.0	24.15	0.7	62.65	2.9	3.67	35.8	20.78	16.7	18.86	11.4	1.99	0.2
S7	3.5		2.82	10.5	<0.165	39.1	0.06	28.4	23.32	2.7	65.32	1.8	3.26	22.6	20.14	4.0	15.70	5.6	2.05	0.7
S8	4		4.16	2.9	11.15	67.0	0.06	49.8	26.77	1.2	69.61	2.0	4.32	52.8	22.02	7.5	18.54	5.5	1.93	0.2
S9	4.5		6.67	4.8	18.32	15.1	0.09	25.3	27.41	0.2	65.44	1.2	3.51	31.0	21.58	6.8	19.34	9.3	1.81	1.0
S10	5		8.32	5.9	29.76	13.8	0.14	39.0	27.74	0.7	60.47	2.3	3.09	38.1	22.88	14.3	22.45	17.8	1.92	1.9
S11	5.5		7.72	1.6	23.51	11.1	0.10	89.2	24.76	1.3	54.18	2.1	2.40	39.4	24.36	15.5	21.81	2.8	2.13	0.9
S12	6.5		13.09	4.4	15.49	10.7	0.12	10.2	24.22	2.7	56.26	1.5	3.40	31.8	24.46	6.5	21.51	6.7	2.05	0.5
S13	7.5		7.12	3.2	26.11	20.4	0.24	16.7	25.49	1.5	56.57	2.3	4.18	30.9	26.96	7.8	24.09	8.6	1.80	0.4
S14	8.5	1.5	4.53	4.4	40.55	11.6	0.07	10.0	19.64	2.3	42.52	2.4	3.72	32.7	25.32	18.2	21.46	4.7	1.68	0.7
S15	9.5	2.5	4.03	6.9	28.48	17.5	0.23	39.0	18.72	1.0	42.71	1.3	3.86	55.4	23.89	4.3	21.53	8.8	1.88	1.7
S16	10.5	3.5	7.97	7.9	41.29	17.9	0.27	30.0	18.45	0.5	37.95	0.5	3.17	12.8	25.49	6.4	21.26	3.5	1.46	1.6
S17	11.5	4.5	9.11	8.0	38.22	20.5	0.16	12.7	19.13	1.5	38.24	0.5	2.80	32.5	22.83	6.5	19.82	10.2	1.36	1.6
S18	12.5	5.5	9.35	5.4	31.49	17.1	0.16	22.3	17.23	3.2	34.62	1.2	2.84	18.6	24.18	18.3	17.39	13.8	1.07	1.0
S19	13.5	6.5	16.03	2.5	83.74	10.9	0.26	22.9	16.37	2.4	30.34	1.4	3.06	31.6	23.82	2.8	18.45	5.7	0.77	1.1
S20	14.5	7.5	8.39	6.7	50.96	13.4	0.17	31.4	15.26	2.1	34.79	2.7	3.26	7.4	20.51	6.6	18.54	14.5	0.63	1.5
S21	15.5	8.5	7.33	4.8	37.86	27.5	0.14	40.1	15.28	2.4	34.03	2.3	2.56	22.1	20.24	6.3	15.45	11.4	0.58	1.0
S22	16.5	9.5	8.88	2.7	30.88	5.8	0.14	21.7	16.79	1.6	33.63	0.8	2.65	8.4	17.94	1.3	17.12	8.9	0.50	1.0
S23	17.5	10.5	5.31	6.7	33.33	20.3	0.26	10.7	18.07	1.3	31.29	2.5	1.58	21.0	19.55	5.4	17.90	11.6	0.71	1.4
S24	18.5	11.5	5.15	9.0	36.10	8.0	0.23	7.3	18.28	2.0	40.19	1.4	3.33	21.7	24.50	7.8	20.97	21.9	0.88	1.6
S25	19.5	12.5	8.36	4.7	45.37	9.5	0.24	9.2	17.77	1.2	33.62	1.8	2.96	4.8	21.97	19.2	21.81	4.4	0.61	6.1

Layer	Depth (incl. external input)	Depth (excl. external input)	As		Br		Cd		Pb		Li		Be		B [H2]		B [O2]		Si	
	[cm]	[cm]	[µg/g]	RSD [%]	[µg/g]	RSD [%]	[µg/g]	RSD [%]	[µg/g]	RSD [%]	[mg/g]	RSD [%]	[µg/g]	RSD [%]	[µg/g]	RSD [%]	[µg/g]	RSD [%]	[mg/g]	RSD [%]
S26	20.5	13.5	19.35	4.4	51.22	16.4	0.46	13.6	18.74	1.1	33.16	1.5	2.69	38.6	23.37	3.2	20.61	10.4	1.09	1.3
S27	21.5	14.5	18.09	3.7	48.62	9.1	0.35	20.1	18.55	2.8	35.49	1.1	1.99	45.4	20.50	6.6	20.72	3.0	1.19	2.0
S28	22.5	15.5	17.72	5.1	35.36	10.9	0.20	31.5	18.88	3.8	36.49	1.8	2.90	32.7	23.34	13.1	20.77	8.0	1.47	1.6
S29	24	16.5	16.25	4.8	36.67	3.2	0.25	13.5	18.71	1.1	37.94	0.9	3.57	53.2	22.66	10.8	20.09	9.0	1.31	1.1
S30	25	18.0	12.12	2.4	45.10	18.2	0.28	20.0	19.07	1.8	39.56	0.6	3.17	46.5	21.80	18.5	20.58	6.3	1.26	1.3
S31	26	19.0	7.17	10.6	32.68	7.9	0.24	22.1	17.40	3.3	27.73	0.7	1.34	29.0	8.79	27.2	6.70	33.2	1.24	3.6
S32	27	20.0	9.05	3.4	12.98	7.1	0.18	12.9	15.78	2.0	34.46	0.9	2.94	47.7	20.30	7.7	20.16	6.9	0.38	4.1
S33	28	21.0	7.32	7.1	16.84	23.8	0.22	22.3	16.57	1.7	35.53	1.7	2.52	16.9	20.00	9.8	19.84	19.9	0.25	2.5
S34	29	22.0	7.91	6.7	<0.165	304.4	0.13	35.0	16.84	1.9	34.61	1.7	2.17	40.1	17.73	7.5	15.58	1.2	0.46	2.7
S35	30	23.0	9.25	2.3	42.38	14.7	0.27	10.2	16.82	2.2	35.22	1.9	1.69	14.9	22.47	10.2	18.88	4.0	0.83	1.2
S36	31	24.0	7.48	2.9	45.92	19.6	0.13	22.2	16.44	3.0	39.85	1.4	2.96	30.2	23.02	8.0	17.78	10.2	1.66	1.3
S37	32	25.0	7.62	5.9	52.91	7.1	0.28	21.1	16.73	1.8	35.72	2.6	2.12	57.8	19.86	8.5	18.86	7.6	1.59	1.6
S38	33	26.0	7.12	7.0	54.24	8.5	0.23	18.3	16.81	3.2	36.82	1.6	2.09	56.2	22.89	20.9	19.58	11.8	1.51	2.2
S39	34	27.0	5.43	1.7	42.48	21.5	0.16	7.4	17.19	2.1	35.95	1.0	2.05	26.8	22.54	11.3	20.30	6.9	1.45	0.3
S40	35	28.0	5.89	6.6	62.05	8.3	0.23	3.3	15.00	2.9	31.07	2.5	2.45	55.5	20.25	12.3	17.97	12.7	1.01	1.3
S41	36	29.0	6.08	6.7	37.01	8.6	0.12	38.8	18.16	2.6	40.63	1.5	3.49	24.2	23.01	5.6	21.64	11.2	1.89	2.3
S42	37	30.0	4.06	7.0	22.30	27.4	0.10	6.8	17.76	3.2	41.89	1.7	3.36	15.4	21.35	10.5	17.01	1.1	1.61	1.6
S43	38	31.0	6.19	3.9	9.90	40.1	0.12	30.8	20.88	1.5	46.81	2.9	3.76	12.0	23.49	16.2	21.58	20.8	1.84	0.9
S44	39		5.95	6.9	13.25	3.7	0.06	6.9	15.81	2.2	35.03	0.8	2.63	10.8	20.22	16.6	15.86	6.9	1.62	2.3
S45	40		6.12	1.8	19.59	7.8	0.14	23.1	15.87	2.7	35.42	1.6	2.01	22.7	18.03	9.4	14.46	17.5	1.91	6.7
S46	41	32.0	7.78	6.9	40.20	15.0	0.15	23.4	15.90	1.5	35.08	1.5	2.18	34.1	20.01	8.5	18.18	15.2	1.74	2.2

Layer	Depth (incl. external input)	Depth (excl. external input)	Cl		Sc		Ga		Se		Rb		Sr		Y		Zr		Nb	
	[cm]	[cm]	[mg/g]	RSD [%]	[µg/g]	RSD [%]	[µg/g]	RSD [%]	[µg/g]	RSD [%]	[mg/g]	RSD [%]	[µg/g]	RSD [%]	[µg/g]	RSD [%]	[µg/g]	RSD [%]	[µg/g]	RSD [%]
	0	0																		
S1	0.5	0.5	<54.19	N/A	18.93	0.8	25.64	1.8	1.99	15.5	0.20	2.8	22.01	0.1	19.74	0.4	8.58	0.2	0.01	5.8
S2	1		<54.19	N/A	22.55	0.9	29.89	0.5	1.08	5.4	0.23	2.0	21.86	0.6	20.44	0.5	6.62	2.5	-0.01	4.2
S3	1.5		<54.19	N/A	22.80	1.2	29.72	0.9	0.82	19.4	0.22	0.4	21.60	0.3	20.40	0.3	6.37	1.4	-0.02	16.4
S4	2		<54.19	N/A	23.34	1.3	29.24	1.0	0.65	21.4	0.23	2.1	21.93	1.1	21.62	0.6	6.47	0.9	-0.01	34.1
S5	2.5		<54.19	N/A	21.03	2.7	28.44	1.9	0.78	62.3	0.19	1.7	22.96	1.9	20.91	1.5	6.20	0.8	0.00	11.5
S6	3		<54.19	N/A	20.51	1.1	26.61	1.8	0.99	40.0	0.18	0.5	21.73	1.3	21.45	1.2	6.62	2.6	-0.02	10.9
S7	3.5		<54.19	N/A	19.88	0.5	26.21	2.7	0.63	42.2	0.18	0.5	22.56	2.0	20.60	2.2	6.38	1.2	-0.01	10.2
S8	4		<54.19	N/A	20.85	2.5	27.78	1.3	0.92	21.6	0.19	0.9	22.64	1.4	21.01	0.3	6.41	2.0	0.00	20.9
S9	4.5		<54.19	N/A	19.64	0.3	26.52	3.0	0.70	30.2	0.18	0.8	20.59	3.2	19.08	1.7	6.10	0.3	0.01	18.6
S10	5		<54.19	N/A	18.81	0.8	25.10	2.5	1.47	36.6	0.18	0.8	20.11	2.5	19.42	0.2	7.45	1.8	0.01	9.9
S11	5.5		<54.19	N/A	17.29	0.8	22.97	3.1	1.00	29.7	0.17	1.2	19.71	2.7	18.91	0.6	7.48	0.9	0.01	3.3
S12	6.5		<54.19	N/A	17.82	3.3	24.88	2.1	0.85	9.7	0.18	1.4	20.51	1.5	18.64	1.7	7.41	2.1	0.04	16.1
S13	7.5		<54.19	N/A	18.46	1.5	26.31	1.7	1.32	35.7	0.19	1.4	20.73	1.5	17.79	0.9	7.20	1.8	0.02	15.8
S14	8.5	1.5	<54.19	N/A	13.31	5.4	19.00	1.9	2.54	5.9	0.13	2.9	18.29	1.4	18.12	2.6	9.27	2.7	0.06	14.2
S15	9.5	2.5	<54.19	N/A	13.54	1.5	18.78	4.4	1.88	24.3	0.13	1.5	16.83	1.4	18.74	0.7	9.41	2.0	0.07	7.3
S16	10.5	3.5	<54.19	N/A	13.36	1.6	18.35	1.1	2.07	7.2	0.13	1.4	15.88	0.5	18.95	0.3	9.86	2.2	0.06	4.1
S17	11.5	4.5	<54.19	N/A	13.38	3.0	18.20	1.3	2.11	38.0	0.13	1.5	16.47	1.4	19.17	1.4	10.15	1.3	0.05	3.5
S18	12.5	5.5	<54.19	N/A	12.17	2.9	16.78	0.2	1.88	14.9	0.12	2.1	14.55	1.0	16.48	1.1	8.59	3.1	0.03	3.9
S19	13.5	6.5	<54.19	N/A	11.11	1.5	16.12	2.9	2.39	4.1	0.11	2.4	15.08	2.4	16.45	1.5	8.09	5.4	-0.01	9.3
S20	14.5	7.5	<54.19	N/A	10.86	1.2	15.38	1.9	1.61	29.1	0.11	2.5	14.05	1.1	15.53	1.7	8.01	2.4	0.00	12.0
S21	15.5	8.5	<54.19	N/A	10.87	3.3	15.44	3.1	2.19	11.0	0.11	2.2	13.91	2.7	15.23	1.6	7.78	1.7	0.01	14.4
S22	16.5	9.5	<54.19	N/A	11.36	1.2	15.75	0.7	1.78	7.3	0.11	2.3	14.22	0.3	16.38	1.9	8.75	2.8	0.02	5.9
S23	17.5	10.5	<54.19	N/A	11.44	3.1	15.77	2.0	2.33	27.7	0.11	3.3	15.23	1.5	16.13	1.4	8.44	1.7	0.03	8.0
S24	18.5	11.5	<54.19	N/A	13.19	2.9	18.94	3.5	2.16	25.1	0.13	3.1	17.75	1.8	18.36	2.7	9.70	0.9	0.03	9.7
S25	19.5	12.5	<54.19	N/A	12.18	1.7	16.89	3.7	2.68	27.4	0.12	1.1	16.55	1.5	18.12	1.3	9.76	2.6	0.02	18.2

Layer	Depth (incl. external input)	Depth (excl. external input)	Cl		Sc		Ga		Se		Rb		Sr		Y		Zr		Nb	
	[cm]	[cm]	[mg/g]	RSD [%]	[µg/g]	RSD [%]	[µg/g]	RSD [%]	[µg/g]	RSD [%]	[mg/g]	RSD [%]	[µg/g]	RSD [%]	[µg/g]	RSD [%]	[µg/g]	RSD [%]	[µg/g]	RSD [%]
S26	20.5	13.5	<54.19	N/A	12.23	2.9	16.62	0.7	2.92	14.7	0.12	1.6	15.87	1.0	18.29	0.8	9.85	2.6	0.01	9.3
S27	21.5	14.5	<54.19	N/A	12.96	3.0	17.70	2.0	2.53	15.8	0.13	3.3	15.67	1.3	18.35	2.3	9.87	4.7	0.05	13.6
S28	22.5	15.5	<54.19	N/A	12.90	1.3	17.51	1.1	2.52	35.9	0.13	2.7	15.93	0.2	18.45	2.7	10.13	3.1	0.05	9.5
S29	24	16.5	<54.19	N/A	12.84	1.3	17.95	1.4	2.12	25.6	0.12	1.8	15.73	0.3	18.46	1.8	10.07	2.3	0.05	6.5
S30	25	18.0	<54.19	N/A	13.76	2.4	18.26	3.2	1.98	18.3	0.13	3.2	16.77	2.0	19.24	1.4	10.05	2.0	0.04	18.2
S31	26	19.0	<54.19	N/A	12.65	3.3	17.44	0.9	2.24	23.9	0.12	2.1	17.12	1.8	22.52	7.6	12.61	7.0	0.14	16.0
S32	27	20.0	<54.19	N/A	11.83	0.8	16.40	3.1	1.99	25.3	0.11	3.3	14.50	2.3	17.32	1.7	7.69	2.0	0.02	25.2
S33	28	21.0	<54.19	N/A	11.75	3.1	16.61	1.0	1.49	13.2	0.11	2.8	13.87	1.8	17.55	2.0	7.79	2.3	0.01	61.2
S34	29	22.0	<54.19	N/A	11.48	4.1	16.84	1.3	1.31	12.4	0.11	3.0	13.51	0.7	16.55	1.4	7.11	3.1	0.02	29.5
S35	30	23.0	<54.19	N/A	11.96	2.9	16.58	1.3	2.24	28.7	0.11	1.5	16.04	1.6	17.76	1.8	9.84	4.4	0.09	21.0
S36	31	24.0	<54.19	N/A	13.07	3.4	18.70	1.6	1.94	32.1	0.13	1.1	15.89	2.7	19.86	3.5	9.91	3.5	0.06	22.9
S37	32	25.0	<54.19	N/A	11.69	3.2	16.24	2.0	2.44	17.8	0.11	2.7	16.22	1.7	19.03	1.6	10.37	1.5	0.09	14.9
S38	33	26.0	<54.19	N/A	12.17	3.3	17.23	2.5	1.92	10.1	0.12	4.3	16.12	2.0	18.88	3.2	10.16	2.4	0.11	5.9
S39	34	27.0	<54.19	N/A	12.46	2.4	17.35	3.2	2.13	21.2	0.12	2.6	15.85	0.4	18.68	2.6	9.85	2.6	0.13	3.5
S40	35	28.0	<54.19	N/A	10.87	2.4	15.06	2.6	2.78	6.4	0.10	2.4	16.99	1.2	18.32	2.1	10.64	1.0	0.08	5.8
S41	36	29.0	<54.19	N/A	13.05	3.0	19.29	2.2	2.14	4.3	0.13	2.1	14.27	1.4	18.13	2.6	9.21	3.3	0.14	13.7
S42	37	30.0	<54.19	N/A	12.44	4.2	19.20	2.9	1.54	18.4	0.12	2.0	15.77	3.4	18.65	2.7	8.90	4.1	0.10	14.3
S43	38	31.0	<54.19	N/A	13.73	2.1	20.14	3.0	1.62	38.2	0.14	2.2	16.01	3.2	19.17	2.1	8.65	4.0	0.08	4.4
S44	39		<54.19	N/A	11.21	4.3	16.70	3.6	1.88	18.9	0.11	4.1	13.92	1.3	18.32	2.3	8.81	2.0	0.07	15.4
S45	40		<54.19	N/A	10.95	3.0	15.91	2.4	2.10	20.4	0.11	2.2	15.16	2.7	19.57	1.9	9.98	4.7	0.11	9.0
S46	41	32.0	<54.19	N/A	11.32	1.3	16.34	1.6	2.15	18.6	0.11	0.4	16.92	2.9	19.83	1.2	10.95	2.8	0.08	9.8

Layer	Depth (incl. external input)	Depth (excl. external input)	Mo		Ru		Pd		In		Sn		Sb		Cs		Ba	
	[cm]	[cm]	[µg/g]	RSD [%]	[µg/g]	RSD [%]	[µg/g]	RSD [%]	[µg/g]	RSD [%]	[µg/g]	RSD [%]	[µg/g]	RSD [%]	[µg/g]	RSD [%]	[mg/g]	RSD [%]
	0	0																
S1	0.5	0.5	0.52	2.67	<0.000963	100.7	0.25	9.7	0.11	5.1	0.49	5.7	0.00	47.4	14.76	0.6	0.45	0.3
S2	1		0.16	10.73	<0.000963	432.1	0.27	3.0	0.13	7.5	0.26	4.6	0.00	98.9	16.94	0.9	0.53	0.5
S3	1.5		0.08	12.54	<0.000963	623.1	0.25	8.1	0.13	2.7	0.17	18.1	<0.000283	331.0	16.87	1.5	0.53	1.1
S4	2		0.10	2.14	<0.000963	N/A	0.26	4.4	0.13	3.3	0.10	4.3	<0.000283	227.8	16.45	1.0	0.52	0.8
S5	2.5		0.02	22.58	<0.000963	N/A	0.23	2.8	0.12	5.1	0.08	21.1	<0.000283	57.2	14.39	0.7	0.46	1.0
S6	3		0.02	5.13	<0.000963	N/A	0.24	5.1	0.11	8.9	0.08	38.5	0.01	76.1	13.96	0.6	0.46	0.5
S7	3.5		0.03	32.03	<0.000963	139.1	0.23	12.6	0.11	4.7	0.08	10.0	<0.000283	N/A	13.41	3.7	0.44	2.1
S8	4		0.04	47.88	<0.000963	250.9	0.24	14.2	0.11	8.2	0.12	1.3	<0.000283	256.7	14.44	0.6	0.46	0.6
S9	4.5		0.03	11.52	<0.000963	63.6	0.22	12.0	0.11	5.5	0.17	6.4	<0.000283	9358.1	14.30	0.4	0.43	0.9
S10	5		0.05	16.14	<0.000963	N/A	0.24	15.5	0.11	11.8	0.37	12.3	0.00	60.0	14.77	0.4	0.42	0.8
S11	5.5		0.08	26.00	<0.000963	12.8	0.21	5.6	0.10	4.9	0.20	15.6	0.01	48.9	14.13	0.3	0.39	1.6
S12	6.5		0.06	34.40	<0.000963	121.9	0.21	14.7	0.10	8.0	0.33	3.0	0.01	57.6	14.93	2.6	0.42	1.3
S13	7.5		0.05	15.67	<0.000963	N/A	0.18	4.2	0.10	11.1	0.37	13.7	<0.000283	113.3	14.97	1.4	0.46	1.4
S14	8.5	1.5	0.07	14.28	<0.000963	58.6	0.24	24.2	0.08	3.9	0.33	5.9	0.01	107.6	11.03	3.2	0.30	3.4
S15	9.5	2.5	0.11	27.05	<0.000963	87.2	0.22	9.7	0.08	11.8	0.33	6.9	0.02	73.9	11.22	0.8	0.31	2.0
S16	10.5	3.5	0.46	26.10	<0.000963	815.6	0.22	10.7	0.06	12.9	0.36	8.1	0.02	47.1	10.68	1.6	0.30	0.7
S17	11.5	4.5	0.37	23.19	<0.000963	252.9	0.20	8.7	0.07	4.0	0.30	3.4	0.02	120.9	10.86	2.5	0.31	1.1
S18	12.5	5.5	0.41	18.04	<0.000963	N/A	0.18	7.2	0.07	4.2	0.32	10.1	<0.000283	103.3	9.88	0.7	0.28	1.8
S19	13.5	6.5	0.63	4.48	<0.000963	65.0	0.19	5.4	0.06	9.1	0.26	15.5	0.03	62.7	9.02	2.3	0.26	2.1
S20	14.5	7.5	0.49	4.45	<0.000963	441.8	0.18	10.5	0.06	10.7	0.25	3.2	<0.000283	256.5	8.91	2.9	0.26	1.6
S21	15.5	8.5	0.49	15.08	<0.000963	N/A	0.16	13.8	0.06	9.2	0.29	8.0	0.01	36.2	8.93	2.1	0.26	1.0
S22	16.5	9.5	0.53	7.44	<0.000963	425.4	0.15	13.1	0.06	17.4	0.33	7.4	0.01	74.9	9.50	1.4	0.28	1.5
S23	17.5	10.5	0.47	3.27	<0.000963	68.7	0.19	16.6	0.06	8.2	0.37	6.9	0.01	130.0	9.51	1.2	0.28	1.3
S24	18.5	11.5	0.45	11.53	<0.000963	260.1	0.20	9.1	0.08	5.5	0.38	14.8	0.03	48.3	10.78	1.5	0.32	1.5

Layer	Depth (incl. external input)	Depth (excl. external input)	Mo		Ru		Pd		In		Sn		Sb		Cs		Ba	
	[cm]	[cm]	[µg/g]	RSD [%]	[µg/g]	RSD [%]	[µg/g]	RSD [%]	[µg/g]	RSD [%]	[µg/g]	RSD [%]	[µg/g]	RSD [%]	[µg/g]	RSD [%]	[mg/g]	RSD [%]
S25	19.5	12.5	0.68	11.47	<0.000963	2175.2	0.20	11.3	0.06	20.5	0.33	4.5	<0.000283	154.5	9.99	1.4	0.30	1.3
S26	20.5	13.5	0.87	12.91	<0.000963	121.2	0.21	24.2	0.07	6.8	0.27	8.8	0.01	200.9	9.93	0.2	0.30	1.1
S27	21.5	14.5	0.75	4.88	<0.000963	218.0	0.22	5.1	0.06	4.0	0.29	13.3	0.03	30.2	10.12	4.1	0.30	2.0
S28	22.5	15.5	1.00	3.34	<0.000963	242.9	0.18	11.7	0.07	11.1	0.35	4.0	0.02	17.5	10.42	3.8	0.31	2.4
S29	24	16.5	0.74	14.41	<0.000963	33.3	0.19	21.9	0.07	18.9	0.26	8.0	0.04	38.8	10.63	1.2	0.31	1.9
S30	25	18.0	0.60	16.33	<0.000963	447.2	0.25	14.6	0.07	7.1	0.36	15.9	0.02	83.0	11.14	0.8	0.33	0.6
S31	26	19.0	0.61	11.36	<0.000963	70.5	0.23	11.4	0.08	4.0	0.41	0.8	0.03	18.6	11.15	6.5	0.33	5.6
S32	27	20.0	0.20	10.28	<0.000963	252.2	0.17	8.8	0.07	9.1	0.19	11.7	0.02	107.5	9.86	1.4	0.28	1.5
S33	28	21.0	0.25	13.41	<0.000963	145.2	0.22	14.8	0.06	7.6	0.18	16.1	<0.000283	5635.1	9.29	3.4	0.27	2.3
S34	29	22.0	0.15	29.53	<0.000963	N/A	0.20	6.2	0.06	6.1	0.18	9.0	<0.000283	2.6	9.74	2.6	0.28	2.5
S35	30	23.0	0.52	11.54	<0.000963	N/A	0.16	1.5	0.07	2.4	0.32	2.0	0.01	102.9	9.22	1.8	0.27	2.5
S36	31	24.0	0.31	22.03	<0.000963	385.6	0.22	0.9	0.06	7.7	0.26	6.7	<0.000283	166.4	9.87	2.2	0.30	3.2
S37	32	25.0	0.57	3.36	<0.000963	36.4	0.22	14.2	0.06	18.4	0.34	11.8	0.04	57.6	9.23	1.3	0.27	2.2
S38	33	26.0	0.39	4.38	<0.000963	84.2	0.23	9.0	0.06	6.4	0.39	17.3	0.04	76.4	9.50	2.9	0.28	2.0
S39	34	27.0	0.41	8.56	<0.000963	N/A	0.18	11.2	0.06	21.9	0.35	4.4	<0.000283	147.1	9.72	2.1	0.28	2.7
S40	35	28.0	0.59	4.79	<0.000963	N/A	0.22	7.2	0.05	4.0	0.28	14.5	<0.000283	113.6	8.10	3.1	0.25	2.2
S41	36	29.0	0.44	18.88	<0.000963	N/A	0.18	8.2	0.07	13.2	0.38	4.7	<0.000283	42.1	10.38	2.2	0.29	2.9
S42	37	30.0	0.22	8.49	<0.000963	289.5	0.22	17.3	0.06	10.5	0.35	4.8	<0.000283	4805.1	9.89	3.2	0.29	3.0
S43	38		0.08	21.20	<0.000963	N/A	0.20	8.7	0.07	9.7	0.30	13.5	0.03	82.7	11.49	0.8	0.32	1.3
S44	39		0.08	58.97	<0.000963	33.1	0.21	19.2	0.06	5.9	0.26	9.5	<0.000283	166.4	8.93	2.8	0.25	2.7
S45	40	31.0	0.30	19.27	<0.000963	289.8	0.21	8.0	0.06	3.8	0.31	2.1	0.03	116.6	8.77	1.4	0.25	2.2
S46	41	32.0	0.40	10.80	<0.000963	1240.7	0.22	15.8	0.06	7.1	0.28	11.9	0.03	14.6	8.57	0.7	0.26	1.2

Layer	Depth (incl. external input)	Depth (excl. external input)	La		Ce		Pr		Nd		Sm		Eu		Gd		Tb		Dy	
	[cm]	[cm]	[µg/g]	RSD [%]	[µg/g]	RSD [%]	[µg/g]	RSD [%]	[µg/g]	RSD [%]	[µg/g]	RSD [%]	[µg/g]	RSD [%]	[µg/g]	RSD [%]	[µg/g]	RSD [%]	[µg/g]	RSD [%]
	0	0																		
S1	0.5	0.5	32.78	0.5	69.76	0.2	8.41	0.9	33.57	0.6	6.30	1.2	1.13	1.4	5.50	0.6	0.77	0.8	4.15	2.5
S2	1		31.89	0.5	69.48	0.3	8.24	0.3	32.86	0.5	6.30	1.6	1.19	0.7	5.53	1.9	0.76	1.6	4.24	0.8
S3	1.5		30.84	1.0	67.81	0.5	8.08	1.7	32.02	1.3	6.09	4.5	1.12	2.2	5.27	3.2	0.74	3.7	4.15	2.0
S4	2		32.29	0.8	71.10	0.6	8.42	1.0	33.32	0.8	6.35	1.1	1.22	3.3	5.55	4.0	0.78	3.7	4.39	1.4
S5	2.5		32.56	1.5	71.71	1.1	8.38	1.3	33.57	1.2	6.22	4.8	1.15	3.2	5.61	2.2	0.77	3.8	4.20	2.1
S6	3		34.66	0.6	76.47	0.3	8.99	1.6	35.48	1.6	6.55	1.6	1.19	4.0	5.82	2.7	0.78	2.5	4.36	2.3
S7	3.5		32.07	2.9	70.20	2.5	8.19	3.4	32.83	1.4	6.26	3.5	1.10	1.8	5.25	2.0	0.74	3.4	4.21	3.4
S8	4		32.77	0.8	72.44	0.6	8.48	0.6	33.62	1.5	6.38	1.2	1.18	1.5	5.39	0.7	0.79	4.5	4.21	0.7
S9	4.5		29.77	0.5	65.17	1.1	7.69	1.7	30.41	0.5	5.75	0.6	1.07	4.5	5.02	3.7	0.71	0.5	3.88	3.7
S10	5		32.40	1.0	69.09	0.6	8.33	1.6	33.02	1.5	6.18	2.4	1.12	1.9	5.38	3.4	0.74	0.9	4.10	1.6
S11	5.5		35.26	0.6	75.04	0.7	9.05	0.9	36.13	0.5	6.66	4.9	1.17	3.8	5.71	2.5	0.77	0.3	4.06	2.6
S12	6.5		32.76	2.0	69.18	1.9	8.45	1.7	33.85	3.0	6.24	3.3	1.15	2.5	5.31	1.3	0.73	1.0	4.01	3.3
S13	7.5		29.26	1.3	62.71	1.7	7.67	1.9	30.30	1.4	5.77	1.4	1.07	2.3	4.88	2.4	0.68	5.2	3.64	2.1
S14	8.5	1.5	36.30	2.5	74.93	2.0	9.36	1.7	36.66	2.9	7.01	5.2	1.16	3.0	5.79	2.1	0.78	5.3	3.95	4.4
S15	9.5	2.5	40.87	1.1	85.19	1.6	10.46	0.6	41.56	1.6	7.83	1.5	1.23	1.2	6.45	1.7	0.84	2.7	4.26	1.3
S16	10.5	3.5	41.24	1.0	86.67	0.7	10.64	0.3	42.45	0.6	7.92	2.8	1.21	2.1	6.56	0.8	0.86	1.7	4.27	2.3
S17	11.5	4.5	37.49	0.9	77.82	1.8	9.66	1.9	38.99	1.9	7.22	1.9	1.18	2.1	6.20	3.1	0.79	3.1	4.20	3.0
S18	12.5	5.5	32.13	2.4	66.32	2.1	8.30	2.4	32.93	1.8	6.12	3.0	1.05	4.2	5.30	3.2	0.70	1.4	3.62	3.1
S19	13.5	6.5	29.77	1.8	61.16	2.1	7.67	3.3	30.74	3.6	5.78	5.3	0.99	2.9	4.92	3.6	0.68	2.4	3.48	2.6
S20	14.5	7.5	31.47	0.9	65.92	1.8	8.14	2.0	31.82	1.8	6.14	4.0	0.97	4.8	5.23	3.3	0.66	1.8	3.51	1.1
S21	15.5	8.5	29.47	1.7	61.49	2.1	7.62	2.1	30.42	1.3	5.60	2.3	0.93	4.5	4.78	3.5	0.66	2.3	3.32	3.2
S22	16.5	9.5	32.79	1.7	68.37	1.6	8.43	2.4	33.21	2.4	6.31	1.6	1.06	3.0	5.31	5.1	0.70	4.4	3.64	2.0
S23	17.5	10.5	31.36	0.9	65.65	1.3	8.18	1.8	32.34	1.4	6.06	0.3	0.98	6.6	5.00	1.4	0.67	2.7	3.51	2.9
S24	18.5	11.5	36.75	2.3	77.76	2.5	9.57	2.6	37.68	1.4	7.05	2.6	1.12	5.4	5.88	2.8	0.80	0.3	4.08	1.9
S25	19.5	12.5	34.45	1.0	71.71	0.5	8.93	0.2	35.23	0.7	6.81	2.1	1.15	1.9	5.72	1.3	0.75	2.2	3.98	4.6

Layer	Depth (incl. external input)	Depth (excl. external input)	La		Ce		Pr		Nd		Sm		Eu		Gd		Tb		Dy	
	[cm]	[cm]	[µg/g]	RSD [%]	[µg/g]	RSD [%]	[µg/g]	RSD [%]	[µg/g]	RSD [%]	[µg/g]	RSD [%]	[µg/g]	RSD [%]	[µg/g]	RSD [%]	[µg/g]	RSD [%]	[µg/g]	RSD [%]
S26	20.5	13.5	34.34	1.4	71.76	1.5	8.90	1.0	35.85	1.4	6.70	0.5	1.10	2.2	5.79	2.5	0.78	0.9	3.91	2.9
S27	21.5	14.5	37.98	2.3	79.62	2.1	9.78	2.1	39.31	1.5	7.31	3.2	1.15	4.8	6.21	3.8	0.81	1.0	4.09	2.1
S28	22.5	15.5	37.02	2.7	77.84	3.6	9.58	2.8	38.47	2.8	7.21	3.1	1.14	5.6	5.97	5.5	0.79	4.8	4.14	2.9
S29	24	16.5	37.56	1.7	79.00	1.4	9.83	1.7	38.77	2.5	7.33	1.8	1.14	2.2	6.26	2.1	0.80	3.7	4.16	2.6
S30	25	18.0	36.37	1.6	76.70	1.1	9.64	2.1	38.36	1.9	7.11	1.6	1.18	6.8	6.19	3.1	0.83	0.9	4.23	0.1
S31	26	19.0	42.38	5.8	89.13	6.0	10.60	5.2	42.03	6.2	7.96	8.1	1.25	6.2	6.74	4.9	0.87	7.3	4.53	6.7
S32	27	20.0	34.78	1.5	73.50	2.2	9.05	2.2	36.06	0.9	6.68	0.6	1.08	2.1	5.67	5.9	0.76	3.3	3.81	3.0
S33	28	21.0	37.21	2.4	79.59	1.9	9.77	2.1	38.99	3.1	7.38	3.9	1.13	2.7	6.09	1.4	0.81	3.2	4.00	1.6
S34	29	22.0	37.05	2.4	78.69	2.0	9.48	2.1	37.86	2.2	7.18	3.2	1.07	3.1	5.82	2.7	0.77	6.2	3.83	2.1
S35	30	23.0	36.19	3.3	76.29	2.6	9.36	1.8	37.48	2.3	7.02	1.4	1.12	6.7	5.97	1.0	0.79	3.0	3.91	3.8
S36	31	24.0	40.54	3.0	86.71	3.0	10.54	2.6	42.06	4.1	7.87	4.5	1.20	3.7	6.70	4.9	0.86	6.5	4.51	2.3
S37	32	25.0	38.75	2.0	82.21	2.7	10.07	2.2	40.45	1.9	7.29	0.4	1.17	3.0	6.43	3.5	0.85	3.3	4.26	1.4
S38	33	26.0	40.65	1.9	86.50	2.8	10.53	1.7	41.83	0.9	7.73	3.8	1.19	2.0	6.54	4.5	0.86	1.9	4.25	3.0
S39	34	27.0	41.95	2.3	90.14	2.6	10.96	2.9	43.87	2.4	8.06	3.7	1.20	1.7	6.61	0.5	0.87	3.0	4.31	2.0
S40	35	28.0	39.04	2.2	82.76	2.4	10.14	2.5	40.43	2.5	7.52	2.4	1.14	2.5	6.31	3.5	0.81	3.3	4.13	2.5
S41	36	29.0	43.65	3.2	94.52	2.5	11.34	2.6	45.27	1.7	8.59	5.5	1.24	2.9	6.87	5.1	0.90	1.4	4.38	1.6
S42	37	30.0	48.29	2.4	104.33	2.1	12.54	3.3	49.43	3.0	9.13	1.9	1.24	6.3	7.44	4.1	0.97	2.1	4.57	3.3
S43	38		44.36	2.5	95.15	2.4	11.57	2.2	45.48	0.3	8.41	2.4	1.25	2.9	6.94	2.4	0.90	4.5	4.46	1.7
S44	39		53.04	1.9	114.47	2.0	13.60	2.9	53.95	3.0	10.04	3.7	1.26	1.3	7.92	4.2	1.00	1.0	4.56	5.6
S45	40	31.0	54.00	1.8	117.34	2.1	13.97	2.5	55.00	2.1	10.07	1.9	1.30	2.6	8.14	1.9	1.05	1.1	4.83	1.5
S46	41	32.0	46.28	1.7	100.03	1.1	12.04	0.8	47.52	0.6	8.95	1.4	1.21	4.3	7.35	1.9	0.95	0.7	4.62	2.3

Layer	Depth (incl. external input)	Depth (excl. external input)	Ho		Er		Tm		Yb		Lu		Hf		Ta		W	
	[cm]	[cm]	[µg/g]	RSD [%]	[µg/g]	RSD [%]	[µg/g]	RSD [%]	[µg/g]	RSD [%]	[µg/g]	RSD [%]	[µg/g]	RSD [%]	[µg/g]	RSD [%]	[µg/g]	RSD [%]
	0	0																
S1	0.5	0.5	0.74	0.9	1.97	2.9	0.27	1.1	1.71	4.0	0.24	4.9	0.28	6.9	<0.0	161.3	<0.000397	53.0
S2	1		0.78	2.5	2.10	2.0	0.28	1.6	1.86	2.0	0.25	5.2	0.21	3.8	<0.0	277.5	<0.000397	131.4
S3	1.5		0.79	2.1	2.07	2.4	0.29	0.4	1.89	2.0	0.24	3.2	0.20	8.5	<0.0	95.5	<0.000397	860.1
S4	2		0.83	1.3	2.21	1.0	0.31	1.8	1.96	4.8	0.27	5.5	0.20	8.2	<0.0	69.0	<0.000397	N/A
S5	2.5		0.79	1.6	2.11	1.0	0.30	1.6	1.79	4.6	0.25	5.8	0.21	8.5	<0.0	24.7	<0.000397	556.6
S6	3		0.81	2.5	2.14	2.8	0.29	2.9	1.84	0.4	0.26	3.2	0.22	5.2	<0.0	101.5	<0.000397	N/A
S7	3.5		0.78	2.4	2.09	2.0	0.29	6.5	1.81	5.1	0.25	5.9	0.23	4.9	<0.0	111.3	<0.000397	N/A
S8	4		0.79	3.6	2.15	0.6	0.30	3.6	1.83	2.1	0.25	15.5	0.20	16.8	<0.0	43.0	<0.000397	N/A
S9	4.5		0.72	4.9	1.92	2.6	0.26	5.2	1.70	3.2	0.22	5.0	0.20	5.6	<0.0	148.2	<0.000397	N/A
S10	5		0.73	3.4	1.93	1.6	0.25	5.8	1.62	4.6	0.23	6.5	0.24	21.3	<0.0	175.5	<0.000397	478.2
S11	5.5		0.73	2.3	1.85	2.8	0.26	7.3	1.54	3.6	0.20	1.1	0.22	11.3	<0.0	75.0	<0.000397	N/A
S12	6.5		0.71	2.0	1.81	2.8	0.24	1.1	1.55	5.5	0.20	11.7	0.22	2.4	<0.0	155.2	<0.000397	277.3
S13	7.5		0.68	2.0	1.73	4.8	0.24	1.5	1.56	6.1	0.20	4.5	0.22	14.8	<0.0	63.3	<0.000397	218.4
S14	8.5	1.5	0.69	4.6	1.77	3.5	0.21	2.8	1.39	2.2	0.17	11.0	0.28	12.6	<0.0	3991.7	<0.000397	75.8
S15	9.5	2.5	0.72	0.4	1.77	3.9	0.23	8.1	1.44	7.3	0.19	8.2	0.26	3.9	<0.0	147.8	<0.000397	106.7
S16	10.5	3.5	0.72	2.2	1.82	2.8	0.25	9.4	1.49	3.2	0.21	2.6	0.26	7.1	<0.0	133.3	<0.000397	18.4
S17	11.5	4.5	0.74	1.3	1.85	2.7	0.24	5.2	1.53	3.1	0.19	4.0	0.30	2.7	<0.0	280.0	<0.000397	123.8
S18	12.5	5.5	0.63	5.2	1.57	6.6	0.20	1.4	1.25	4.8	0.17	10.8	0.30	9.6	<0.0	242.0	<0.000397	230.3
S19	13.5	6.5	0.61	0.2	1.56	3.1	0.22	1.6	1.34	7.9	0.18	4.9	0.26	16.6	<0.0	1895.2	<0.000397	659.3
S20	14.5	7.5	0.64	3.6	1.49	3.7	0.20	3.7	1.23	4.4	0.18	6.9	0.26	8.3	<0.0	402.4	<0.000397	20.7
S21	15.5	8.5	0.56	2.1	1.46	3.0	0.20	4.4	1.22	3.5	0.16	9.7	0.24	20.0	<0.0	N/A	<0.000397	101.0
S22	16.5	9.5	0.63	3.3	1.58	3.1	0.20	1.3	1.29	4.2	0.18	16.2	0.30	8.6	<0.0	111.5	<0.000397	22.5
S23	17.5	10.5	0.60	1.0	1.61	2.1	0.21	0.4	1.27	5.2	0.18	8.5	0.26	25.3	<0.0	1.1	<0.000397	47.7
S24	18.5	11.5	0.70	2.2	1.76	4.7	0.25	4.7	1.36	2.5	0.19	7.0	0.26	7.4	<0.0	140.1	<0.000397	19.8
S25	19.5	12.5	0.69	2.1	1.73	1.1	0.23	4.4	1.40	5.5	0.19	3.7	0.31	11.3	<0.0	51.0	<0.000397	265.8

Layer	Depth (incl. external input)	Depth (excl. external input)	Ho		Er		Tm		Yb		Lu		Hf		Ta		W	
	[cm]	[cm]	[µg/g]	RSD [%]	[µg/g]	RSD [%]	[µg/g]	RSD [%]	[µg/g]	RSD [%]	[µg/g]	RSD [%]	[µg/g]	RSD [%]	[µg/g]	RSD [%]	[µg/g]	RSD [%]
S26	20.5	13.5	0.69	1.7	1.79	2.2	0.22	1.3	1.43	1.8	0.20	1.5	0.31	13.0	<0.0	1293.6	<0.000397	85.9
S27	21.5	14.5	0.70	3.1	1.73	5.2	0.22	5.9	1.42	7.5	0.19	4.7	0.31	8.1	<0.0	49.9	<0.000397	80.3
S28	22.5	15.5	0.71	1.3	1.73	4.2	0.22	6.4	1.47	0.8	0.20	9.5	0.34	9.7	<0.0	155.1	<0.000397	99.7
S29	24	16.5	0.70	3.0	1.75	3.2	0.24	3.1	1.46	6.5	0.19	10.9	0.29	19.8	<0.0	N/A	<0.000397	59.1
S30	25	18.0	0.75	2.4	1.83	0.6	0.24	8.2	1.55	4.7	0.21	9.7	0.28	3.0	<0.0	56.4	<0.000397	20.6
S31	26	19.0	0.78	5.6	2.04	2.6	0.26	6.4	1.56	4.6	0.22	5.9	0.37	6.0	<0.0	376.8	<0.000397	66.9
S32	27	20.0	0.64	1.2	1.64	4.7	0.22	11.1	1.37	9.3	0.17	10.1	0.19	3.9	<0.0	197.2	<0.000397	N/A
S33	28	21.0	0.68	4.9	1.70	2.3	0.23	5.8	1.33	4.6	0.17	5.6	0.19	22.7	<0.0	N/A	<0.000397	N/A
S34	29	22.0	0.65	3.3	1.62	5.7	0.21	4.1	1.22	4.5	0.16	7.1	0.16	8.2	<0.0	42.3	<0.000397	N/A
S35	30	23.0	0.67	2.4	1.75	1.9	0.22	3.1	1.45	7.0	0.20	17.4	0.30	5.0	<0.0	1116.2	<0.000397	61.8
S36	31	24.0	0.76	1.1	1.95	3.5	0.25	3.5	1.55	3.8	0.21	3.7	0.31	17.4	<0.0	150.1	<0.000397	260.1
S37	32	25.0	0.74	0.6	1.84	1.9	0.24	2.5	1.52	3.9	0.19	10.2	0.30	9.0	<0.0	843.1	<0.000397	698.0
S38	33	26.0	0.73	1.1	1.72	3.1	0.23	1.3	1.50	4.8	0.19	3.7	0.28	17.2	<0.0	137.6	<0.000397	186.4
S39	34	27.0	0.73	3.6	1.82	4.3	0.23	3.4	1.44	6.8	0.18	5.5	0.30	12.7	<0.0	220.0	<0.000397	146.8
S40	35	28.0	0.72	0.3	1.78	1.7	0.23	6.1	1.39	2.3	0.18	6.2	0.34	6.3	<0.0	536.1	<0.000397	69.1
S41	36	29.0	0.71	3.5	1.78	2.6	0.22	7.4	1.42	2.7	0.19	6.6	0.30	8.8	<0.0	56.6	<0.000397	9.1
S42	37	30.0	0.75	1.5	1.78	4.3	0.24	2.1	1.42	4.4	0.19	7.4	0.26	9.5	<0.0	2931.1	<0.000397	51.3
S43	38		0.80	2.5	1.85	2.9	0.24	4.0	1.43	6.1	0.20	8.2	0.25	10.0	<0.0	147.1	<0.000397	N/A
S44	39		0.74	3.9	1.70	3.3	0.21	0.4	1.29	2.8	0.19	5.7	0.27	18.6	<0.0	2316.9	<0.000397	N/A
S45	40	31.0	0.78	3.1	1.89	5.9	0.23	1.7	1.42	6.5	0.17	5.5	0.30	9.6	<0.0	365.7	<0.000397	266.1
S46	41	32.0	0.78	2.1	1.90	0.8	0.25	2.8	1.52	1.8	0.21	4.6	0.29	7.2	<0.0	130.4	<0.000397	344.5

Layer	Depth (incl. external input)	Depth (excl. external input)	Pt		Hg		Tl		Bi		Th		U	
	[cm]	[cm]	[µg/g]	RSD [%]	[µg/g]	RSD [%]	[µg/g]	RSD [%]	[µg/g]	RSD [%]	[µg/g]	RSD [%]	[µg/g]	RSD [%]
	0	0												
S1	0.5	0.5	<0.0	231.8	<0.004475	117.0	1.15	3.0	0.70	1.4	9.28	0.7	2.50	0.8
S2	1		<0.0	226.4	<0.004475	101.2	1.23	0.4	0.79	1.8	9.52	0.7	2.52	2.1
S3	1.5		<0.0	41.1	<0.004475	N/A	1.19	3.2	0.80	6.2	9.14	2.5	2.29	1.5
S4	2		<0.0	17.8	<0.004475	N/A	1.16	2.9	0.81	4.0	9.25	1.2	2.14	0.3
S5	2.5		<0.0	54.1	<0.004475	148.4	1.01	4.3	0.68	1.4	8.95	2.4	2.14	1.1
S6	3		<0.0	153.6	<0.004475	39.9	0.99	6.7	0.67	3.5	9.25	1.8	1.96	2.5
S7	3.5		<0.0	61.1	<0.004475	N/A	0.93	2.0	0.63	0.9	8.69	4.1	1.84	2.0
S8	4		<0.0	82.7	<0.004475	209.9	1.00	2.1	0.68	1.5	8.96	2.3	1.79	2.7
S9	4.5		<0.0	19.8	<0.004475	N/A	1.00	2.5	0.67	1.9	8.26	0.9	1.77	3.7
S10	5		<0.0	65.8	<0.004475	193.9	1.05	0.6	0.68	5.5	8.85	0.7	2.72	1.7
S11	5.5		<0.0	31.4	<0.004475	33.0	1.01	2.0	0.61	5.5	9.68	1.3	2.57	4.3
S12	6.5		<0.0	67.9	<0.004475	N/A	1.00	2.8	0.65	3.3	9.45	1.0	1.87	2.1
S13	7.5		<0.0	67.2	<0.004475	120.0	1.16	3.0	0.70	1.4	8.67	3.5	2.31	0.7
S14	8.5	1.5	<0.0	82.6	<0.004475	292.3	0.87	5.2	0.49	2.2	9.60	4.1	2.62	2.2
S15	9.5	2.5	<0.0	270.6	<0.004475	92.9	0.86	1.0	0.55	5.0	10.88	2.0	2.28	3.9
S16	10.5	3.5	<0.0	37.5	<0.004475	N/A	0.86	3.0	0.51	4.3	11.09	2.2	2.34	3.5
S17	11.5	4.5	<0.0	120.8	<0.004475	N/A	0.91	7.3	0.50	5.0	10.11	2.2	2.35	3.9
S18	12.5	5.5	<0.0	257.0	<0.004475	589.2	0.79	4.0	0.47	7.5	8.73	4.3	2.11	1.6
S19	13.5	6.5	<0.0	154.2	<0.004475	N/A	0.77	1.7	0.44	4.9	7.67	3.0	2.71	2.6
S20	14.5	7.5	<0.0	167.6	<0.004475	N/A	0.72	6.0	0.39	6.7	8.51	0.8	2.42	3.6
S21	15.5	8.5	<0.0	135.9	<0.004475	52.8	0.71	3.6	0.42	3.4	7.95	1.4	2.16	1.2
S22	16.5	9.5	<0.0	N/A	<0.004475	N/A	0.73	6.2	0.41	9.0	8.95	0.2	2.36	2.4
S23	17.5	10.5	<0.0	227.4	<0.004475	N/A	0.74	5.3	0.41	8.2	8.53	1.7	2.47	2.2
S24	18.5	11.5	<0.0	N/A	<0.004475	N/A	0.84	5.0	0.51	2.0	9.78	2.4	2.91	4.9
S25	19.5	12.5	<0.0	330.3	<0.004475	N/A	0.81	4.8	0.44	3.4	9.25	4.6	3.35	2.3

Layer	Depth (incl. external input)	Depth (excl. external input)	Pt		Hg		Tl		Bi		Th		U	
	[cm]	[cm]	[µg/g]	RSD [%]	[µg/g]	RSD [%]	[µg/g]	RSD [%]	[µg/g]	RSD [%]	[µg/g]	RSD [%]	[µg/g]	RSD [%]
S26	20.5	13.5	<0.0	66.5	<0.004475	848.2	0.88	1.4	0.51	0.4	9.32	2.0	3.32	2.8
S27	21.5	14.5	<0.0	164.5	<0.004475	96.9	0.84	1.4	0.51	2.9	10.47	2.7	3.03	3.0
S28	22.5	15.5	<0.0	218.4	<0.004475	N/A	0.85	8.1	0.50	5.9	10.16	3.9	2.66	1.6
S29	24	16.5	<0.0	36.0	<0.004475	N/A	0.84	4.7	0.54	7.4	10.33	2.1	2.68	1.9
S30	25	18.0	<0.0	N/A	<0.004475	192.1	0.83	2.8	0.50	1.1	10.37	2.8	2.69	4.9
S31	26	19.0	<0.0	180.6	<0.004475	N/A	0.78	5.1	0.43	6.7	10.83	4.5	2.79	3.2
S32	27	20.0	<0.0	73.0	<0.004475	N/A	0.75	1.5	0.40	4.4	9.53	1.8	2.73	2.0
S33	28	21.0	<0.0	206.9	<0.004475	N/A	0.75	3.0	0.41	1.9	10.08	4.6	2.97	0.2
S34	29	22.0	<0.0	106.8	<0.004475	N/A	0.77	3.0	0.43	3.2	10.20	0.8	2.36	3.0
S35	30	23.0	<0.0	88853	<0.004475	N/A	0.77	2.9	0.43	4.3	9.80	3.5	3.04	1.5
S36	31	24.0	<0.0	82.7	<0.004475	1064.0	0.82	3.7	0.46	8.2	11.11	1.7	2.76	1.0
S37	32	25.0	<0.0	146.6	<0.004475	213.0	0.75	3.7	0.43	4.9	10.36	3.9	3.02	1.7
S38	33	26.0	<0.0	122.0	<0.004475	258.7	0.77	3.4	0.44	6.2	11.30	4.1	2.97	0.9
S39	34	27.0	<0.0	170.7	<0.004475	N/A	0.77	7.3	0.45	9.3	11.67	2.1	3.07	1.9
S40	35	28.0	<0.0	169.5	<0.004475	26.9	0.70	1.0	0.36	4.3	10.70	4.4	3.65	0.8
S41	36	29.0	<0.0	151.9	<0.004475	N/A	0.88	6.8	0.50	3.7	11.97	3.2	3.03	1.5
S42	37	30.0	<0.0	64.8	<0.004475	2051.4	0.80	1.6	0.46	5.0	13.56	1.3	2.92	5.3
S43	38		<0.0	99.9	<0.004475	484.5	0.88	2.0	0.60	6.4	12.08	0.6	2.23	1.8
S44	39		<0.0	366.5	<0.004475	N/A	0.73	3.5	0.38	2.7	14.54	2.9	2.61	3.8
S45	40	31.0	<0.0	238.5	<0.004475	114.5	0.70	2.6	0.37	1.6	14.91	2.3	3.02	3.6
S46	41	32.0	<0.0	35.1	<0.004475	N/A	0.69	3.8	0.37	5.0	12.51	0.0	3.33	3.8

Appendix 2 Detection limits

Appx 2 Calculated Detection limits (DL), blanks and Background Equivalent Concentrations (BEC) for sediment samples in µg/L. Scan mode for all elements were MS/MS, and all elements had a correlation, R = 1.00.

Name	Tune Mode	Q1	Q2	Blank [µg/L]	DL [µg/L]	BEC [µg/L]
Al	H2	27	27	7.30E-04	4.10E-03	2.32E-02
As	O2	75	91	1.23E-06	5.17E-04	9.95E-05
B	H2	11	11	1.06E-03	1.79E-01	5.13E-01
B	O2	11	11	1.28E-03	4.53E-03	5.77E-01
Ba	O2	137	137	7.41E-05	2.37E-03	1.60E-03
Be	H2	9	9	0.00E+00	0.00E+00	0.00E+00
Bi	O2	209	209	3.34E-04	5.10E-04	1.16E-03
Br	O2	79	79	4.35E-04	2.93E-01	7.43E-01
Ca	H2	40	40	2.21E-02	2.15E-02	2.69E-01
Cd	O2	111	111	1.85E-06	3.34E-04	6.44E-05
Ce	O2	140	156	3.08E-05	2.16E-05	7.42E-05
Cl	O2	35	51	4.42E-03	9.57E+01	8.64E+02
Co	O2	59	59	5.09E-04	1.14E-03	3.72E-03
Cr	O2	52	52	2.03E-03	1.80E-03	2.04E-02
Cs	O2	133	133	2.86E-04	4.86E-04	7.41E-04
Cu	O2	63	63	2.21E-03	3.60E-03	3.29E-02
Dy	O2	163	179	5.45E-06	1.06E-04	3.53E-05
Er	O2	166	182	1.81E-06	4.63E-05	8.91E-06
Eu	O2	153	153	1.85E-06	3.68E-05	7.08E-06
Fe	H2	56	56	1.91E-02	6.25E-03	1.53E-01
Ga	H2	71	71	3.33E-05	3.91E-04	4.32E-04
Gd	O2	157	173	1.87E-06	1.12E-04	2.15E-05
Hf	O2	178	194	1.81E-06	9.69E-05	1.87E-05
Hg	O2	202	202	5.76E-04	7.86E-03	2.42E-02
Ho	O2	165	181	1.87E-06	1.59E-05	3.06E-06
In	O2	115	115	1.27E-05	9.63E-05	2.96E-05
K	O2	39	39	5.63E-02	6.19E-02	6.98E-01
La	O2	139	155	9.30E-06	2.16E-05	2.07E-05
Li	No Gas	7	7	1.60E-03	4.31E-03	1.20E-02
Lu	O2	175	191	5.44E-06	4.55E-05	8.75E-06
Mg	O2	24	24	1.91E-03	4.03E-03	4.44E-02
Mn	O2	55	55	1.58E-03	1.52E-03	1.03E-02
Mo	O2	95	127	3.81E-05	1.30E-03	8.34E-04
Na	O2	23	23	1.08E-01	1.05E-01	1.85E+00
Nb	O2	93	125	1.49E-05	6.95E-05	5.28E-05
Nd	O2	146	162	3.04E-06	1.27E-04	3.27E-05
Ni	O2	60	60	1.58E-04	7.26E-04	5.46E-03
P	O2	31	47	1.20E-04	1.32E-02	4.66E-02
Pb	O2	208	208	9.76E-04	1.98E-04	2.72E-03
Pd	O2	105	105	1.51E-04	6.91E-04	1.37E-03
Pr	O2	141	157	5.56E-06	3.11E-05	1.03E-05
Pt	O2	195	195	4.89E-05	9.92E-04	5.74E-04
Rb	O2	85	85	5.37E-04	5.80E-04	3.46E-03

Name	Tune Mode	Q1	Q2	Blank [µg/L]	DL [µg/L]	BEC [µg/L]
Ru	O2	101	101	1.02E-04	1.71E-03	1.75E-03
S	O2	32	48	7.82E-03	1.38E-01	1.47E+00
Sb	O2	121	137	1.81E-06	4.51E-04	8.68E-05
Sc	O2	45	61	2.71E-04	2.54E-03	2.48E-03
Se	H2	78	78	3.66E-06	7.38E-03	1.42E-03
Si	O2	28	44	1.02E-02	1.39E-01	1.23E+00
Sm	O2	147	163	1.85E-06	1.15E-04	2.21E-05
Sn	O2	118	118	1.78E-04	5.39E-04	1.70E-03
Sr	H2	88	88	9.34E-04	1.49E-03	4.26E-03
Ta	O2	181	213	7.23E-06	4.50E-05	1.31E-05
Tb	O2	159	175	5.46E-06	2.78E-05	9.26E-06
Th	O2	232	248	4.45E-05	8.46E-04	3.45E-04
Ti	O2	47	63	1.35E-05	2.84E-03	1.67E-03
Tl	O2	205	205	5.83E-04	3.08E-04	1.96E-03
Tm	O2	169	185	3.71E-06	3.59E-05	6.91E-06
U	H2	238	238	8.09E-06	1.57E-04	3.01E-05
V	O2	51	67	9.44E-05	9.67E-04	8.18E-04
W	O2	182	214	6.34E-05	6.99E-04	5.38E-04
Y	O2	89	105	3.08E-05	9.65E-05	8.74E-05
Yb	O2	172	172	1.80E-06	8.03E-05	1.54E-05
Zn	H2	66	66	1.77E-04	1.03E-02	1.39E-02
Zr	O2	90	106	6.70E-05	3.77E-04	5.05E-04

Appendix 3: Example of calculation of pigment concentration

This example is based on the results from the first sample of Fucoxanthin (S1).

Areal peak of Fucoxanthin in S1 = 4.855 mAU

Extracted sediments = 0.11 g

Amount of extracted acetone = 1 mL

Concentration in Fucoxanthin standard = 1.188 µg/mL

Areal peak standard = 2.0275 mAU

Areal of pure intern standard = 0.808 mAU

Areal of intern standard in the sample = 0.823 mAU

Dilution factor (20% water) = 1.25

1. Calculation of Fucoxanthin concentration in sample extract

$$\frac{1.188\ \mu g/mL}{2.0275\ mAU} * 4.855\ mAU = 2.84\ \mu g/mL$$

2. Calculation of the total amount of Fucoxanthin in the sample

$$(2.84\ \mu g/mL) * 1\ mL = 2.84\ \mu g$$

Since extracted with 1 mL acetone, the total amount of Fucoxanthin did not change

3. Calculation of the amount of Fucoxanthin per gram sediment

$$\frac{2.84\ \mu g}{0.11\ g} = 25.8\ \mu g/g$$

4. Correction with intern standard

$$\frac{0.808\ mAU}{0.823\ mAU} * 25.8\ \mu g/g = 25.3\ \mu g/g$$

5. The concentration of Fucoxanthin including the dilution factor

$$25.3\ \mu g/g * 1.25 = 31.6\ \mu g/g$$

Appendix 4: Indirect dating of sediment core

Tabell 1 Modified table of ^{210}Pb chronology of Sarsvatnet sediment core SBAC1, retrieved in 1995 by Appleby (2004). The sedimentation rate was used in calculations of chronology in sediment core obtained August 2021.

Depth [cm]	Chronology [Date AD]	Sedimentation rate [cm y-1]	± [%]
0.00	1995	-	-
0.50	1986	0.027	-
1.00	1971	0.027	-
1.50	1951	0.027	28
2.00	1926	0.027	-
2.50	1909	-	-
3.00	1907	0.210	-
4.00	1901	0.210	-
5.00	1897	0.210	37
6.00	1892	0.210	-
6.50	1889	-	-
7.00	1867	0.022	-
8.00	1831	0.020	-
9.00	1776	0.017	-
10.00	1724	0.025	-
11.00	1689	0.028	-
12.00	1653	0.028	-
13.00	1618	0.030	-
14.00	1586	0.037	-
15.00	1566	0.059	-
16.00	1549	0.054	-
17.00	1529	0.049	-
18.00	1510	0.055	-
19.00	1488	0.033	-
20.00	1450	0.025	-
21.00	1413	0.032	-
22.00	1386	0.035	-
23.00	1352	0.027	-
24.00	1313	0.026	-
25.00	1281	0.040	-
26.00	1258	0.042	-

For sample S14 (retrieved August 2021), with a sediment layer thickness of 1.0 cm, the chronology is calculated to 1843:

$$Current\ year = 1889 - \frac{1.0\ cm}{0.022\ cm\ y^{-1}} = 1843$$

Appendix 5: Contributing parameters of PC1 and PC2

Appx 3 The 6 highest loaded parameters in PC1 and PC2.

Parameter	PC1	Parameter	PC2
K	-0.292	S	-0.4889
Mg	-0.2907	As	-0.4438
Cr	-0.2906	LOI	-0.3672
Pb	-0.2873	Cd	-0.3397
Fe	-0.2861	Chlorophyll *a*	-0.3049
Na	-0.2853	Ca	-0.3023

Appendix 6: Mann-Kendall Trend Test and Sen's Slope

Appx 4 Mann-Kendall Trend Test (Z, p) and Sen's Slope (Q). p-value determines whether the Z-value, indicating positive or negative trend, is statistically significance. Sen's slope is applied for parameters with a significant trend

Parameter	Z	p-value	Sen's slope, Q
Fe	-0.63244	0.5271	
Mn	-3.2595	0.0011	-0.00360907
As	-3.2595	0.09486	
Cd	-1.4108	0.1583	
Cr	-1.5406	0.1234	
Cu	-0.56758	0.5703	
Ni	-0.63244	0.5271	
Pb	-2.5136	0.01195	-0.08219477
Zn	-0.92434	0.3553	
V	-1.4108	0.1583	
Ca	-0.92434	0.3553	
K	-2.3514	0.0187	-0.0691459
Mg	-1.2487	0.2118	
Na	-1.8	0.07186	
P	-2.7081	0.006766	-0.00255969
S	-0.8919	0.3724	
Ti	0.37298	0.7092	
Chlorophyll *a*	-1.2811	0.2002	
LOI	-2.0461	0.04075	-0.08284314

Appendix 7 Principal Component Analysis

Appx 5 Summary of PCA values.

```
Importance of components:
                          PC1    PC2     PC3     PC4     PC5     PC6    PC7     PC8     PC9    PC10
Standard deviation     3.3298 1.8711 1.14353 1.03908 0.76915 0.66979 0.5549 0.46778 0.42608 0.28540
Proportion of Variance 0.5836 0.1843 0.06882 0.05683 0.03114 0.02361 0.0162 0.01152 0.00955 0.00429
Cumulative Proportion  0.5836 0.7678 0.83666 0.89348 0.92462 0.94823 0.9644 0.97595 0.98551 0.98979
                          PC11    PC12    PC13    PC14    PC15    PC16    PC17   PC18    PC19
Standard deviation     0.22889 0.22544 0.17659 0.16005 0.12269 0.09781 0.07981 0.0442 0.03128
Proportion of Variance 0.00276 0.00267 0.00164 0.00135 0.00079 0.00050 0.00034 0.0001 0.00005
Cumulative Proportion  0.99255 0.99523 0.99687 0.99821 0.99901 0.99951 0.99985 1.0000 1.00000
```

Norges miljø- og biovitenskapelige universitet
Noregs miljø- og biovitskapelege universitet
Norwegian University of Life Sciences

Postboks 5003
NO-1432 Ås
Norway